



**The Production and use of cyclohexanone
monooxygenase for Baeyer-Villiger biotransformations**

Scott Sinclair Barclay, BSc

**A thesis submitted for the degree of
Doctor of Philosophy to the University of London**

Supervisor - Dr. J. M. Woodley
Industrial Supervisor - Dr. P. L. Spargo

The Advanced Centre for Biochemical Engineering
Department of Biochemical Engineering
University College London
Torrington Place, London
WC1E 7JE, UK

ProQuest Number: 10609398

All rights reserved

INFORMATION TO ALL USERS

The quality of this reproduction is dependent upon the quality of the copy submitted.

In the unlikely event that the author did not send a complete manuscript and there are missing pages, these will be noted. Also, if material had to be removed, a note will indicate the deletion.



ProQuest 10609398

Published by ProQuest LLC (2017). Copyright of the Dissertation is held by the Author.

All rights reserved.

This work is protected against unauthorized copying under Title 17, United States Code
Microform Edition © ProQuest LLC.

ProQuest LLC.
789 East Eisenhower Parkway
P.O. Box 1346
Ann Arbor, MI 48106 – 1346

ABSTRACT

Traditional chemical catalytic routes to optically pure materials are often inadequate, expensive and in some cases unknown. Optically pure lactones can form the starting material for a large number of drug classes. The Baeyer-Villiger reaction can be used to produce lactones from cyclic ketones. Using a biological catalyst (cyclohexanone monooxygenase) a more efficient, stereoselective and environmentally friendly route may be found.

This thesis examines the production and use of the biocatalyst cyclohexanone monooxygenase from both the wild type organism *A. calcoaceticus* (a known class II pathogen) and a recombinant *Escherichia coli* strain expressing the protein. The protocols have been developed to maximise the productivity of the fermentations of both organisms. Novel feeding strategies were developed for producing enzyme from *A. calcoaceticus* with an order of magnitude increase in productivity over the published methods.

This research has shown that the production of cyclohexanone monooxygenase in both the wild type organism, *A. calcoaceticus*, and a recombinant *E. coli* is dependent on the feeding and induction strategy. In *E. coli* the productivity of the fermentation is greatly influenced by the growth rate at the time of induction while in *A. calcoaceticus* inducing growth substrate is required at the beginning of the fermentation if the enzyme is to be induced by a later substrate switch.

The use of whole cells and crude homogenate from both organisms have been evaluated. Only whole cells from *A. calcoaceticus* were found to be of use due to the inability of *E. coli* cells to facilitate the reaction. The homogenate from *E. coli* was found to be most useful as a biocatalyst due to the overmetabolism of the lactone by *A. calcoaceticus*.

ACKNOWLEDGEMENTS

I would like to take this opportunity to thank the people who have assisted me during the course of this PhD project. Firstly my love and appreciation to Alan and Liz without whose support and understanding I would never have been given the chance to even begin.

To my supervisors Malcolm Lilly and John Woodley for all their advice and encouragement. Malcolm is greatly missed by many, both personally and professionally; his contribution to Biochemical engineering and enzyme technology continues to be an inspiration.

I am grateful to all the members of the Baeyer-Villiger group both at UCL and Exeter for all their help, especially Matt Hogan and Rachel Stones for their work with *E. coli* biotransformations. Thanks also to Dr. Sejal Patel for producing the recombinant *E. coli*.

I acknowledge the support of the Biotechnology and Biological Sciences Research Council and Pfizer Pharmaceuticals especially Dr. Peter Spargo and Alan Pettman for all their assistance with organic chemistry (see I managed not to burn down the labs after all!).

A special thanks for Dr. Kate Large for providing love and much needed encouragement without whom this may never have been completed.

ABSTRACT	2
ACKNOWLEDGEMENTS	3
TABLE OF CONTENTS	4
LIST OF TABLES	8
LIST OF FIGURES	9
ABBREVIATIONS	15
NOMENCLATURE	16
1 INTRODUCTION	17
1.1 BIOTRANSFORMATION	17
1.1.2 <i>Enzyme biotransformation</i>	18
1.2 THE BAEYER-VILLIGER OXIDATION	18
1.2.1 <i>General</i>	18
1.2.2 <i>Mechanism</i>	19
1.2.2 <i>Chemical methods</i>	20
1.2.3 <i>Biological methods</i>	20
1.3 BAEYER-VILLIGER CATALYSTS	21
1.3.1 <i>Range of organisms</i>	21
1.3.2 <i>Baeyer-Villiger reactions using Pseudomonas putida</i>	23
1.3.3 <i>Baeyer-Villiger reactions using Acinetobacter calcoaceticus NCIMB9871</i>	27
1.3.4 <i>Mechanism</i>	30
2 PROJECT RATIONALE	32
2.1 CHOICE OF ORGANISM	32
2.2 CHOICE OF SUBSTRATE	33
3 MATERIALS AND METHODS	37
3.1 ANALYTICAL METHODS	37
3.1.1 <i>Cell growth analysis</i>	37
3.1.2 <i>Cyclohexanone monooxygenase activity assay</i>	37
3.1.3 <i>Protein assay</i>	41
3.1.4 <i>GC assay for reactants and products</i>	41
3.2 EQUIPMENT	41
3.2.1 <i>Chromatographic apparatus</i>	41
3.2.2 <i>Spectroscopic apparatus</i>	42

3.2.3	<i>Fermentation equipment and analysis</i>	42
3.2.4	<i>Downstream processing equipment</i>	43
3.3	RECOMBINANT <i>E. COLI</i>	43
3.4	FERMENTATION MEDIA	44
3.5	MICROORGANISMS	45
3.5.1	<i>Maintenance of organisms</i>	45
3.5.2	<i>Solid culture media</i>	45
3.6	GROWTH OF <i>ACINETOBACTER CALCOACETICUS</i>	45
3.6.1	<i>Media</i>	45
3.6.2	<i>Shake flask growth</i>	46
3.6.3	<i>Batch fermentation</i>	47
3.7	GROWTH OF JM107/PQR210	47
3.7.1	<i>Media</i>	47
3.7.2	<i>Shake flask growth</i>	49
3.7.3	<i>Batch fermentation</i>	49
3.7.4	<i>Fed-batch fermentation</i>	50
3.7.5	<i>Plasmid stability</i>	51
3.8	DOWNSTREAM PROCESSING METHODS	51
3.8.1	<i>Preparation of crude extract by sonication</i>	51
3.8.2	<i>Preparation of crude extract by Lab 40 homogenisation</i>	52
3.8.3	<i>Storage and stability of cells</i>	52
3.8.4	<i>Storage and stability of homogenate</i>	52
3.9	BIOTRANSFORMATIONS	53
3.9.1	<i>Whole cell biotransformations</i>	53
3.9.2	<i>Homogenate biotransformations</i>	53
3.10	CHEMICAL SYNTHESSES	54
3.10.1	<i>Literature Method</i>	54
3.10.2	<i>Developed method</i>	55
4	RESULTS	58
4.1	CYCLOHEXANONE MONOOXYGENASE ASSAY	58
4.2	GROWTH OF <i>ACINETOBACTER CALCOACETICUS</i>	61
4.2.1	<i>Growth on cyclohexanol</i>	61
4.2.2	<i>Production of biomass on sodium succinate</i>	65
4.2.3	<i>Production of biomass on monosodium glutamate</i>	65
4.2.4	<i>Diauxic growth investigation</i>	70
4.2.5	<i>Production of CHMO</i>	70
4.3	GROWTH OF <i>ESCHERICHIA COLI</i> JM107/PQR210	77
4.3.1	<i>Carbon source investigation</i>	77

4.3.2	<i>IPTG concentration investigation</i>	77
4.3.3	<i>Plasmid retention during shake flask fermentations</i>	80
4.3.4	<i>Growth on complex medium</i>	80
4.3.5	<i>Growth on defined medium</i>	87
4.4	INDUCTION OF CYCLOHEXANONE MONOOXYGENASE.....	91
4.4.1	<i>Batch fermentation</i>	91
4.4.2	<i>Batch fermentation with supplementation</i>	91
4.4.3	<i>Fed batch exponential feeding</i>	101
4.4.4	<i>Fed batch linear feeding</i>	108
4.5	STABILITY OF STORED CATALYSTS.....	115
4.5.1	<i>Whole cells</i>	115
4.5.2	<i>Homogenate</i>	115
4.6	BIOTRANSFORMATIONS - WHOLE CELL <i>ACINETOBACTER CALCOACETICUS</i>	119
4.6.2	<i>Biotransformation of 2-ethyl cyclopentanone</i>	119
4.6.3	<i>Biotransformation of 4-methyl cyclohexanone</i>	120
4.7	BIOTRANSFORMATION - <i>ACINETOBACTER CALCOACETICUS</i> HOMOGENATE.....	127
4.7.1	<i>Biotransformations of 4-methyl cyclohexanone</i>	127
4.7.2	<i>Biotransformation of 2-methyl cyclohexanone</i>	131
4.8	BIOTRANSFORMATIONS - WHOLE CELL <i>ESCHERICHIA COLI</i>	131
4.9	BIOTRANSFORMATIONS - <i>ESCHERICHIA. COLI</i> HOMOGENATE.....	131
5	DISCUSSION	139
5.1	BIOCATALYST PRODUCTION IN <i>ACINETOBACTER CALCOACETICUS</i>	139
5.1.1	<i>Carbon source investigation</i>	139
5.1.2	<i>CHMO production</i>	141
5.2	BIOCATALYST PRODUCTION IN <i>ESCHERICHIA COLI</i>	144
5.2.1	<i>Over expression of CHMO in an Escherichia coli construct</i>	144
5.2.2	<i>Plasmid stability</i>	145
5.2.3	<i>IPTG concentration</i>	145
5.2.4	<i>Growth and production of CHMO on complex media</i>	146
5.2.5	<i>Initial study of growth and production of CHMO on defined media</i>	147
5.2.6	<i>Development of fed-batch fermentation</i>	150
5.2.7	<i>Constant growth rate</i>	151
5.2.8	<i>Constant feed rate</i>	153
5.3	STABILITY OF STORED CATALYSTS.....	155
5.3.1	<i>Whole cells</i>	155
5.3.2	<i>Homogenate</i>	156
5.4	BIOTRANSFORMATION - <i>A. CALCOACETICUS</i> WHOLE CELLS.....	157
5.4.1	<i>Stability of CHMO activity during biotransformations</i>	157

5.4.2	<i>Cyclohexanone</i>	158
5.4.3	<i>2-ethyl cyclopentanone</i>	158
5.4.4	<i>4-methyl cyclohexanone</i>	159
5.5	BIOTRANSFORMATION - <i>E. COLI</i> WHOLE CELL.....	160
5.6	BIOTRANSFORMATION - <i>A. CALCOACETICUS</i> HOMOGENATE.....	161
5.7	BIOTRANSFORMATION - <i>E. COLI</i> HOMOGENATE.....	163
5.8	SUMMARY.....	164
6	CONCLUSIONS AND FURTHER WORK.....	169
6.1	CONCLUSION.....	169
6.2	FURTHER WORK.....	171
7	APPENDICES.....	173
	APPENDIX I.....	173
	APPENDIX II.....	181
	APPENDIX III.....	184
8	REFERENCES.....	186

LIST OF TABLES

Table 3.1	Suppliers of the fermentation media and the grade used.	44
Table 3.2	Mineral media constituents for <i>A. calcoaceticus</i> fermentation	46
Table 3.3	Composition of culture media for JM107/pQR210.	48
Table 3.4	Composition of feed solutions 1-4 used in fed-batch fermentations of JM107/pQR210.	49
Table 4.1	Summary of growth of <i>Acinetobacter</i> in shake flasks	62
Table 4.2	Effect of cyclohexanol as co-growth substrate on CHMO production.	70
Table 4.3	Plasmid stability of <i>E. coli</i> JM107/pQR210 in shake flasks.	80
Table 5.1	Summary of carbon source investigation	142
Table 5.2	Summary of biocatalyst production	164

LIST OF FIGURES

Figure 1.1	The Baeyer-Villiger reaction	19
Figure 1.2	Mechanism of the Baeyer-Villiger reaction	19
Figure 1.3	The Baeyer-Villiger oxidation of sulphides	23
Figure 1.4	Baeyer-Villiger oxidation of 4-thiocyclohexanone	23
Figure 1.5	Biooxidation of norbanone	25
Figure 1.6	Recycle of NADPH by linkage to alcohol dehydrogenase	26
Figure 1.7	Recycle of NADPH by linkage to G-6-P dehydrogenase	26
Figure 1.8	Metabolic pathway of cyclohexanol in <i>Acinetobacter calcoaceticus</i>	27
Figure 1.9	Biooxidation of fenchone	28
Figure 1.10	Baeyer-Villiger oxidation of bicyclo[3.2.0]hept-2-en-6-one	29
Figure 1.11	Proposed mechanism of action of cyclohexanone monooxygenase	31
Figure 2.1	Baeyer-Villiger oxidation of 2-(2',4',7'-trioxaoctyl) cyclopentanone	34
Figure 2.2	Methyl 1,4-dioxaspiro[4.4]nonane-6-carboxylate	35
Figure 3.1	Correlation between optical density and dry cell weight for <i>A. calcoaceticus</i>	38
Figure 3.2	Correlation between optical density and dry cell weight for <i>E. Coli</i> JM107/pQR210	39
Figure 3.3	Methyl 1,4-dioxaspiro[4.4]nonane-6-carboxylate	54
Figure 3.4	2-hydroxymethyl cyclopentanone	55

Figure 3.5	Synthesis of 2-(2',4',7'-trioxaoctyl)cyclopentanone	56
Figure 3.6	Synthesis of 6-(2',4',7'-trioxaoctyl)tetrahydropyran-2-one	57
Figure 4.1	Errors at low volume handling of enzyme preparation	59
Figure 4.2	Initial rate of background NADPH oxidation in CHMO activity assay.	60
Figure 4.3	Biomass production in 2L fed batch fermentation of <i>A. calcoaceticus</i> on cyclohexanol.	63
Figure 4.4	Biomass production in 2L fed batch fermentation of <i>A. calcoaceticus</i> on cyclohexanol.	64
Figure 4.5	Biomass production in 2L batch fermentation of <i>A. calcoaceticus</i> on succinate.	66
Figure 4.6	Biomass production in 2L batch fermentation of <i>A. calcoaceticus</i> on succinate	67
Figure 4.7	Biomass production in 2L batch fermentation of <i>A. calcoaceticus</i> on glutamate.	68
Figure 4.8	Biomass production in 2L batch fermentation of <i>A. calcoaceticus</i> on glutamate	69
Figure 4.9	Fermentation profile for 7 L batch fermentation of <i>A. calcoaceticus</i> .	72
Figure 4.10	Productivity of 7L batch fermentation of <i>A. calcoaceticus</i> .	73
Figure 4.11	Fermentation profile for 7 L batch fermentation of <i>A. calcoaceticus</i> .	74

Figure 4.12	Productivity of 7 L batch fermentation of <i>Acinetobacter calcoaceticus</i> .	75
Figure 4.13	Productivity of 7 L batch fermentation of <i>Acinetobacter calcoaceticus</i>	76
Figure 4.14	Expression of CHMO in recombinant <i>E. coli</i> in shake flasks.	78
Figure 4.15	Effect of IPTG concentration on CHMO induction in shake flasks.	79
Figure 4.16	Fermentation profile for 7 L batch fermentation of JM107/pQR210 on complex medium.	82
Figure 4.17	Productivity of 7 L batch fermentation of JM107/pQR210.	83
Figure 4.18	Productivity of 7 L batch fermentation of JM107/pQR210	84
Figure 4.19	Fermentation profile for 7 L batch fermentation of JM107/pQR210 with oxygen limitation.	85
Figure 4.20	Productivity of 7 L batch fermentation of JM107/pQR210 with oxygen limitation.	86
Figure 4.21	Fermentation profile for 7 L batch fermentation of JM107/pQR210 on defined medium.	88
Figure 4.22	Biomass production in 7 L batch fermentation of JM107/pQR210 on defined medium.	89
Figure 4.23	Biomass production in 7 L batch fermentation of JM107/pQR210 on defined medium	90
Figure 4.24	Fermentation profile for 7 L batch fermentation of JM107/pQR210 on defined medium with induction of CHMO.	91

Figure 4.25	Productivity of batch fermentation of JM107/pQR210 on defined medium with induction of CHMO.	93
Figure 4.26	Biomass production in batch fermentation of JM107/pQR210 on defined medium with induction of CHMO	94
Figure 4.27	Fermentation profile for 7 L batch fermentation of JM107/pQR210 on defined medium with induction of CHMO.	95
Figure 4.28	Productivity of batch fermentation of JM107/pQR210 on defined medium with induction of CHMO.	96
Figure 4.29	Biomass production in batch fermentation of JM107/pQR210 on defined medium with induction of CHMO	97
Figure 4.30	Fermentation profile for 7 L batch fermentation of JM107/pQR210 on defined medium with media supplementation.	98
Figure 4.31	Productivity of 7 L batch fermentation of JM107/pQR210 on defined medium with supplementation.	99
Figure 4.32	Biomass production in 7 L batch fermentation of JM107/pQR210 on defined medium with supplementation	100
Figure 4.33	Fermentation profile for 7 L fed batch fermentation of JM107/pQR210.	102
Figure 4.34	Productivity of 7 L fed batch fermentation of JM107/pQR210.	103
Figure 4.35	Biomass production in 7 L fed batch fermentation of JM107/pQR210	104
Figure 4.36	Fermentation profile for 7 L fed batch fermentation of JM107/pQR210.	105

Figure 4.37	Productivity of 7 L fed batch fermentation of JM107/pQR210.	106
Figure 4.38	Biomass production in 7 L fed batch fermentation of JM107/pQR210	107
Figure 4.39	Fermentation profile for 7 L exponential then linear fed batch fermentation of JM107/pQR210	109
Figure 4.40	Productivity of 7 L fed batch fermentation of JM107/pQR210.	110
Figure 4.41	Biomass production in 7 L fed batch fermentation of JM107/pQR210	111
Figure 4.42	Fermentation profile for 7 L linear fed batch fermentation of JM107/pQR210.	112
Figure 4.43	Productivity of 7 L fed batch fermentation of JM107/pQR210.	113
Figure 4.44	Biomass production in 7 L fed batch fermentation of JM107/pQR210	114
Figure 4.45	Stability of CHMO activity in <i>Acinetobacter</i> cells stored at -18 °C.	116
Figure 4.46	Stability of CHMO activity in <i>E. coli</i> cells stored at -18 °C.	117
Figure 4.47	Stability of CHMO activity in clarified homogenate of <i>Escherichia coli</i> .	118
Figure 4.48	Biotransformation of cyclohexanone by whole cell <i>A. calcoaceticus</i> .	121
Figure 4.49	Specific activity of cyclohexanone monooxygenase during a cyclohexanone biotransformation.	122
Figure 4.50	Biotransformation of 2-ethyl cyclopentanone by whole cell <i>A. calcoaceticus</i> .	123

Figure 4.51	Specific activity of cyclohexanone monooxygenase during a 20 mM 2-ethyl cyclopentanone biotransformation.	124
Figure 4.52	Biotransformation of 20 mM 4-methyl cyclohexanone, with cyclohexanol co-substrate, by whole cell <i>A. calcoaceticus</i> .	125
Figure 4.53	Biotransformation of 20 mM 4-methyl cyclohexanone, with cyclohexanol co-substrate, by whole cell <i>A. calcoaceticus</i> .	126
Figure 4.54	Biotransformation of 4-methyl cyclohexanone by <i>A. calcoaceticus</i> homogenate.	128
Figure 4.55	Biotransformation of 20 mM 4-methyl cyclohexanone by <i>A. calcoaceticus</i> homogenate with cyclohexanol cosubstrate.	129
Figure 4.56	Stability of CHMO in <i>A. calcoaceticus</i> homogenate.	130
Figure 4.57	Biotransformation of 20 mM 2-methyl cyclohexanone by <i>A. calcoaceticus</i> homogenate with isatoic anhydride.	133
Figure 4.58	Biotransformation of 20 mM 2-ethyl cyclopentanone by whole cell <i>E. coli</i> .	134
Figure 4.59	Biotransformation of 20 mM 2-methyl cyclohexanone by <i>E. coli</i> homogenate	135
Figure 4.60	Biotransformation of 20 mM 2-methyl cyclohexanone by <i>E. coli</i> homogenate	136
Figure 4.61	Comparison between <i>A. calcoaceticus</i> and <i>E. coli</i> homogenate biotransformation of 2-methyl cyclohexanone.	137
Figure 4.62	Comparison between <i>A. calcoaceticus</i> and <i>E. coli</i> homogenate biotransformation of 2-methyl cyclohexanone	138
Figure 5.1	Carbon sources for <i>A. calcoaceticus</i>	142

ABBREVIATIONS

NAD	Nicotinamide adenine dinucleotide
R & S	Absolute conformation of isomers
e.e.	Enantiomeric excess
NADH	Nicotinamide adenine dinucleotide (reduced form)
NADPH	Nicotinamide adenine dinucleotide phosphate (reduced form)
FMN	Flavin mononucleotide
G	Glucose
P	Phosphate
FAD	Flavin adenine dinucleotide
TEPP	Tetraethyl pyrophosphate
m	Multiplet
s	Singlet
t	Triplet
d	Doublet
dd	Double doublet
br	Broad peak
Me	Methyl
THF	Tetrahydrofuran
°C	Degrees centigrade
HCl	Hydrochloric acid
R _f	Relative retention time
DCM	Dichloromethane
mmHg	millimetres of mercury
GC	Gas chromatography
TLC	Thin layer chromatography
UV	Ultra violet
(¹ H)	designates proton NMR
<i>E coli</i>	<i>Escherichia coli</i>
AnalR	Analytical reagent
GLR	General laboratory reagent
M	molar concentration
SOP	Standard operating procedure
PID	Proportional Integral Derivative
PPG	Polypropylene glycol
mol	Moles
CHMO	Cyclohexanone monooxygenase
IPTG	Isopropyl-β-D-thiogalactopyranoside
Tris	Tris(hydroxymethyl)aminomethane
BSA	Bovine serum albumin
l	Light path
OD	Optical density
gdc	Grams of dry cells
lac	Lactose operon
tac	hybrid lactose and tryptophan operon

NOMENCLATURE

OUR	Oxygen uptake rate	mmole L ⁻¹ min ⁻¹
CER	Carbon evolution rate	mmole L ⁻¹ min ⁻¹
RQ	Respiratory quotient	CER / OUR
DOT	Dissolved oxygen tension	% saturation
μ	Specific growth rate	h ⁻¹
F	Feed rate	g h ⁻¹
Y_{gly}	Yield on glycerol	g g ⁻¹
x	Dry biomass concentration	g L ⁻¹
V	Fermenter volume	L
s_f	Glycerol concentration	g L ⁻¹
λ	Wavelength	nm
U	Units of enzyme activity	$\mu\text{mol min}^{-1}$
ΔA	Change in absorbance	
ϵ	Extinction coefficient	
rpm	Revolutions per minute	
dcw	Dry cell weight	g L ⁻¹

1 INTRODUCTION

1.1 Biotransformation

1.1.1 Whole cell biotransformation

Biotransformation is the chemical modification of a compound using a biological catalyst, which may be an enzyme or whole cell, to facilitate the reaction. In the case of an enzyme this might be a highly purified protein or simply a cell extract, while the whole cell may be actively growing or 'resting' in buffered solution.

The use of biotransformation is becoming increasingly recognised as an important tool in organic synthesis for a wide range of reactions (Jones, 1986; Davies *et al.*, 1990; Faber, 1992). The specific nature of bio-reactions means that biotransformations can be used as an alternative to traditional methods and to facilitate reactions not currently possible through chemistry (Roberts and Turner, 1992).

Developments in protein and genetic engineering allow manipulation of catalysts to improve both activity and stability of the catalyst. Protein engineering can be used to increase catalytic activity and stability, while genetic engineering can achieve greater expression of the enzyme or produce overexpression in a recombinant organism that is more convenient to handle, often *E. coli* (Hanna, 1987, Prentis, 1984).

Whole cells are probably the most commonly used biocatalysts because of their more robust nature and the lack of purification required prior to use (Lilly, 1977). There can however be some significant problems associated with this.

One of the major problems is the possibility of further metabolism of the product caused by the required enzyme being part of a pathway. The product of the required reaction may in turn be a substrate for the next enzyme in the pathway (Faber, 1992). In some cases this can be catastrophic for product yield and in others merely introduce by-products that must be removed, often with difficulty, in downstream processing.

1.1.2 Enzyme biotransformation

Pure or practically pure enzymes may be used to catalyse reactions with very good specificity and high yields. The formation of by-products can be kept to a minimum and product recovery therefore simple. Problems with the stability of the enzyme during the reaction may be encountered (Faber, 1992) and if the presence of cofactors are required in stoichiometric quantities they may become prohibitively expensive (Roberts and Willetts, 1993).

Cofactor recycling systems have been used successfully but this adds to the complexity of a multi-enzyme system.

1.2 The Baeyer-Villiger oxidation

1.2.1 General

The Baeyer-Villiger reaction can be described as the transformation of a ketone to an ester, or a cyclic ketone to a lactone using an oxidant such as a peroxy acid (Figure 1.1) (Baeyer and Villiger, 1899). This reaction is very important in organic synthesis and has been much studied (Krow, 1981).

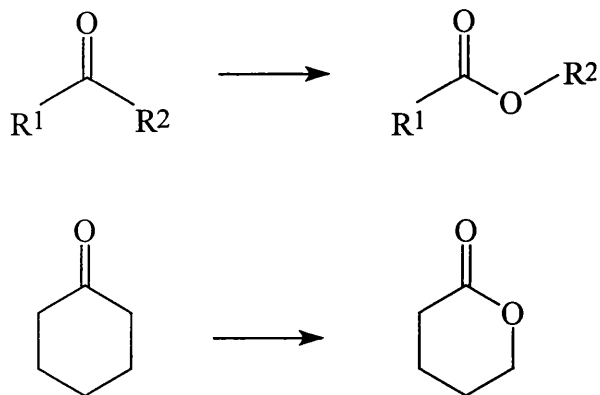


Figure 1.1 The Baeyer-Villiger reaction

1.2.2 Mechanism

The mechanism is accepted as being a two step oxidation with the formation of an unstable intermediate (Figure 1.2) (Criegee, 1948).

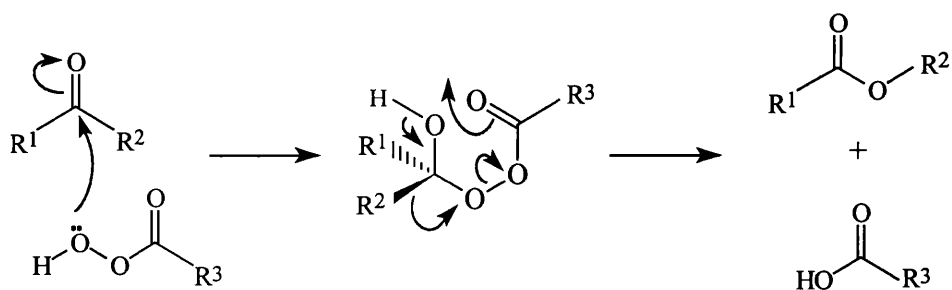


Figure 1.2 Mechanism of the Baeyer-Villiger reaction

Peroxyacid attacks the carbonyl group of the ketone creating a tetrahedral intermediate that rearranges to the corresponding ester or lactone. The substituent that can better accommodate a partial positive charge is the one that migrates to the incoming oxygen atom. In the case of the substituents being very similar, i.e. R¹ = R² in figure 1.2, both regioisomers are formed (Krow, 1981).

1.2.2 Chemical methods

There are many oxidants that can be used for the reaction, the most popular are *meta*-chlorobenzoic acid, trifluoroperoxyacetic acid, peroxybenzoic acid and hydrogen peroxide. These chemicals are very hazardous and often unstable which makes their use dangerous and scaling up a difficult process.

Some more stable oxidants have been used such as bis(trimethylsilyl) peroxide (Suzuki, 1992) and more recently molecular oxygen when used with a metal catalyst (Bolm, 1994).

1.2.3 Biological methods

Enzyme catalysed Baeyer-Villiger reactions have been known since the late 1950's (Bradshaw *et al.*, 1959). These bio-oxidations can be done by whole cell or purified enzyme systems. There are three main advantages to using a biochemical rather than a traditional chemical route: mild conditions, i.e. of temperature, pH and pressure, enzymes are chiral catalysts and can produce optically active products, and due to the specificity of enzymes they can perform reactions that are difficult to perform chemically (Roberts & Turner, 1992).

The enzymes found to catalyse these reactions are members of the class of enzymes known as monooxygenases. These enzymes have been found in a large number of organisms from both bacteria and fungi and a wide range of substrates have been used.

Monooxygenases are a set of enzymes that transfer one atom of molecular oxygen to a co-substrate, and usually require a cofactor for their function. A major class is the flavoprotein monooxygenases that typically require NAD usually in the reduced form as a cofactor. This group includes phenolic α -hydroxylases that convert phenols to catechols, bacterial luciferases that convert aliphatic aldehydes to aliphatic carboxylic acids (emitting light), and cyclic ketone oxygenases that produce cyclic lactones.

1.3 Baeyer-Villiger catalysts

1.3.1 Range of organisms

Many organisms that have been used for Baeyer-Villiger type reactions are *Xanthobacter autotrophicus* NCIMB 10811 and other species (Magor *et al.*, 1976) and it has been found that although the enzymes catalyse the same reaction, i.e. the insertion of molecular oxygen into the carbon ring, there are marked differences in both regioselectivity and enantiospecificity depending on the catalyst used (Wright *et al.*, 1994).

There has also been work by groups exploring the use of actinomycete species notably *Corynebacterium* that have been found to be diastereo-selective and enantioselective in the oxidation of β methyl secondary alcohols. This organism has also been used to produce the cortisone derivative prednisolone (Ohta *et al.*, 1986).

During the 1980's many researchers began to screen large numbers of organisms for transformation ability including a large number of fungi. *Cylindrocarpon radicumicola* was found to produce enzymes that acted on a number of steroids to produce the corresponding lactones (Itagaki, 1986). Other work with *Cylindrocarpon radicumicola* has shown that this organism is capable of producing Baeyer-Villiger reactions with bicyclic ketones (Konigsberger *et al.*, 1990). These workers discovered problems with volatility of products that made yields very difficult to ascertain.

Other problems that they encountered were caused by the presence of other enzymes, mainly hydrolases, that resulted in acid production. Enantioselectivity was not reported for the majority of the substrates tested and was only limited on others when compared to later work with *A. calcoaceticus* using similar substrates.

Carnell and Willetts (1990) undertook a screening programme, after work by Ouazzani-Chahdi (1987) showed that the fungus *Curvularia lunata* could give enantioselective degradation of racemic (R,S)-2,2,5,5-tetramethyl-1,4-hydroxycyclohexanone to produce optically pure (R)-ketone and (S)-lactone, to find other fungi with similar properties. The rationale was that filamentous fungi would make downstream processing far simpler. Twenty nine organisms from thirteen genera were tested. They were all grown on complex media and racemic bicyclo[3.2.0]hept-2-en-6-

one added directly, i.e. no special induction mechanism was used. Most later work with *Acinetobacter calcoaceticus* and *Pseudomonas putida* involved growth on substrates with an enzyme inducing carbon source and then the addition of the reaction substrate.

Carnell and Willetts (1990) found that certain fungi, especially *C. lunata*, would produce both regioisomers in equal amounts both in enantiomeric excesses of approximately 70%, when the substrate was fully utilised, and both regioisomers in the ratio of 5:1 after 70% conversion. These results showed that the isomers were produced at different rates although no reasons were postulated at this time.

In a later paper (Carnell and Willetts, 1992) they showed that a variation in products is possible from a racemic starting material when different species of *Curvularia* were used. These experiments showed that one enantiomer of each regioisomer was produced in greater quantity and this was most often the (-)-3-oxa and (-)-2-oxa lactones from bicyclo[3.2.0]hept-2-en-6-one. One example however gave an e.e. of 68% for the (-)-3-oxa lactone but produced racemic 2-oxa-lactone, highlighting the difference the organism can make to the selectivity of the biotransformation of optically active chemicals.

Much interest has been shown by a number of workers in the use of cyclohexanone monooxygenase to produce sulphoxides (Figure 1.3) (Ryerson *et al.*, 1982; Pasta *et al.*, 1995). High enantiomeric excesses have been reported, with the structure of the sulphide being a determining factor in the enantioselectivity with products reported to range from e.e. 99% (R) to e.e. 93% (S) when using the same enzyme (Carrea *et al.*, 1992; Pasta *et al.*, 1995; Secundo *et al.*, 1993).

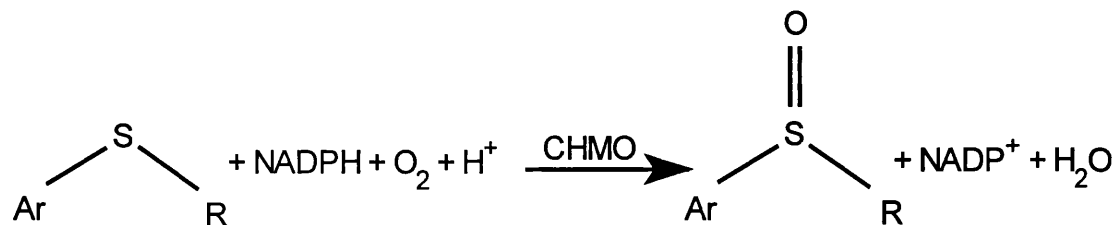


Figure 1.3 The Baeyer-Villiger oxidation of sulphides

Pasta *et al.* (1995) found that in general the introduction of substituents in the aromatic ring or increasing the size of the alkyl chain had (S) directing effects. Although the mechanism is different and no insertion into the ring was reported, this information may be useful in terms of the effects of functional substituents on enantioselectivity.

It is interesting to note that when confronted with 4-thiocyclohexanone, the reaction proceeds in favour of ring expansion by oxygen insertion with no apparent sulphur oxidation at all (Figure 1.4) (Latham and Walsh, 1987).

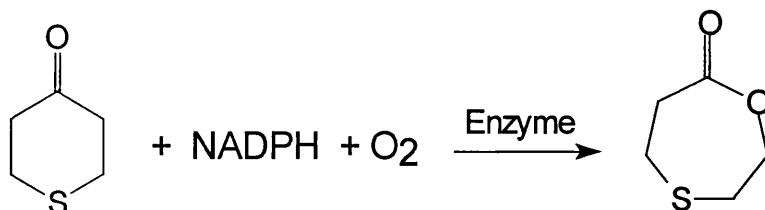


Figure 1.4 Baeyer-Villiger oxidation of 4-thiocyclohexanone

1.3.2 Baeyer-Villiger reactions using *Pseudomonas putida*

The enzymes from two organisms, namely *Pseudomonas putida* and *Acinetobacter calcoaceticus*, have been well characterised and used for biotransformations by many workers (Ryerson *et al.*, 1982; Alphand *et al.*, 1990; Shipston *et al.*, 1992).

Two different enzymes from *Pseudomonas putida* have been identified and are both believed to be involved in the catabolism of the substrate camphor. A NADH requiring enzyme was found that could oxidise bicyclic ketones and was found to be composed of two dissimilar polypeptides which interact through a FMN bound to one of them (Taylor *et al.*, 1982). Later work showed that it was in fact a pair of isoenzymes, 2,5-diketocamphane 1,2-monooxygenase and 3,6-diketocamphane monooxygenase, that have been purified independently (Jones *et al.*, 1993).

A NADPH dependent enzyme has also been identified as cyclopentanone monooxygenase (Ougham *et al.*, 1983) that shows greater activity towards monocyclic ketones. Both the cyclopentanone and diketocamphane monooxygenases have been found to have some activity with both ketone types (Grogan *et al.*, 1993; Gagnon *et al.*, 1994).

P. putida has been widely used to transform a number of substrates to products of industrial importance including the building blocks for prostaglandins and much work has been directed to producing analogues with enhanced pharmacological action. The enzyme has a major advantage over the chemical synthesis because it is selective for the correct active isomer. Problems of further metabolism are however an important consideration: in this case the production of a lactone hydrolase that causes the production of the associated hydroxy acid.

The correct bridgehead lactone was produced in the ratio 38:1, compared to the 9:1 ratio for the chemical reaction (Sandey & Willetts, 1989). In this paper the biotransformation of norbanone to the bridgehead lactone by a washed cell suspension of cyclopentanone fed *P. putida* is described. (Figure 1.5). They report the possibility that the native lactone cleaving hydrolase enzyme present in the cells does not have such broad substrate specificity as the monooxygenase, since they found no degradation of the products (lactones). This is an interesting idea that has not been explored in subsequent literature and could possibly allow the biotransformation to proceed without the necessity for a dehydrogenase inhibiting chemical.

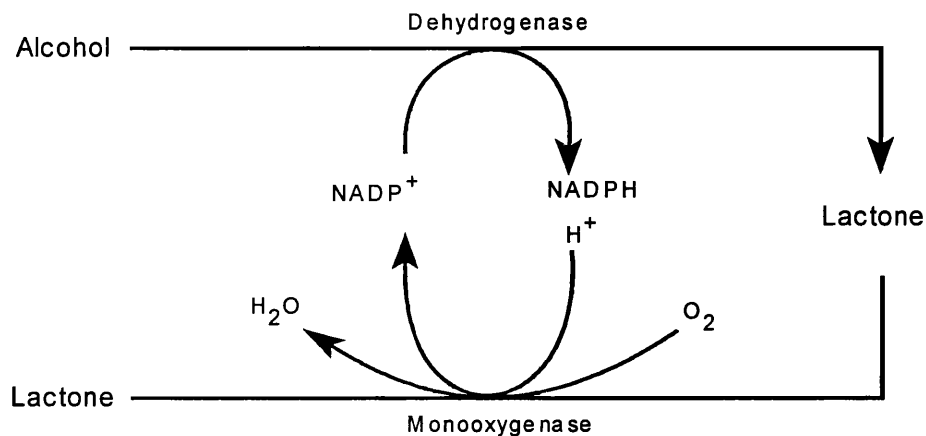


Figure 1.6 Recycle of NADPH by linkage to alcohol dehydrogenase

Recycling systems for NADPH, which is approximately ten times the cost of NADH, have also been described (Schwab *et al.*, 1983) with successful results (Figure 1.7). Glucose-6-phosphate dehydrogenase was used to reduce the oxidised NADP and although successful the dehydrogenase enzyme is relatively expensive.

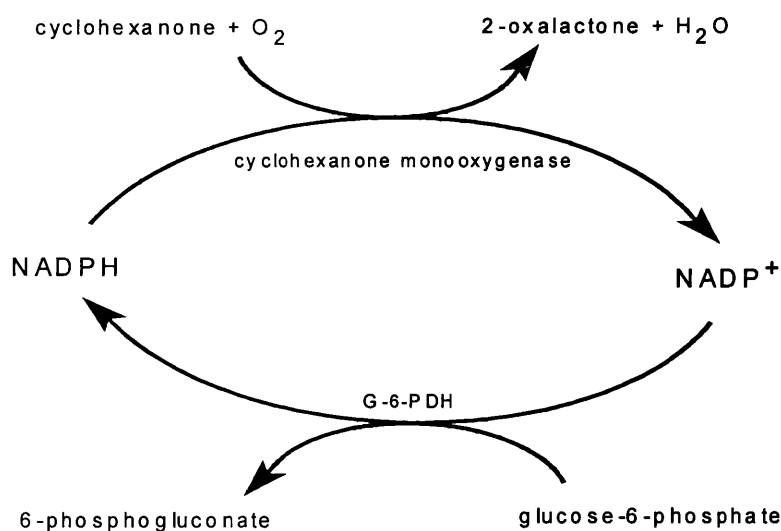


Figure 1.7 Recycle of NADPH by linkage to G-6-P dehydrogenase

1.3.3 Baeyer-Villiger reactions using *Acinetobacter calcoaceticus* NCIMB9871

The enzyme from *A. calcoaceticus* has a molecular weight of approximately 59,000 and is a single polypeptide chain with one molecule of FAD bound to it firmly enough to insure that it does not dissociate during purification (Donoghue *et al.*, 1976). It is described as cyclohexanone monooxygenase and is believed to be part of the metabolic pathway in the biodegradation of cyclohexane present in fossil fuels. This part of the pathway gives the biodegradation of cyclohexanol to lactone then subsequent hydrolysis to 6-hydroxyhexanoate, followed by oxidation to adipate (Donoghue and Trudgill, 1975) and β -oxidation to acetyl coenzyme A and succinyl coenzyme A (Figure 1.8) (Chapman & Duggleby, 1967).

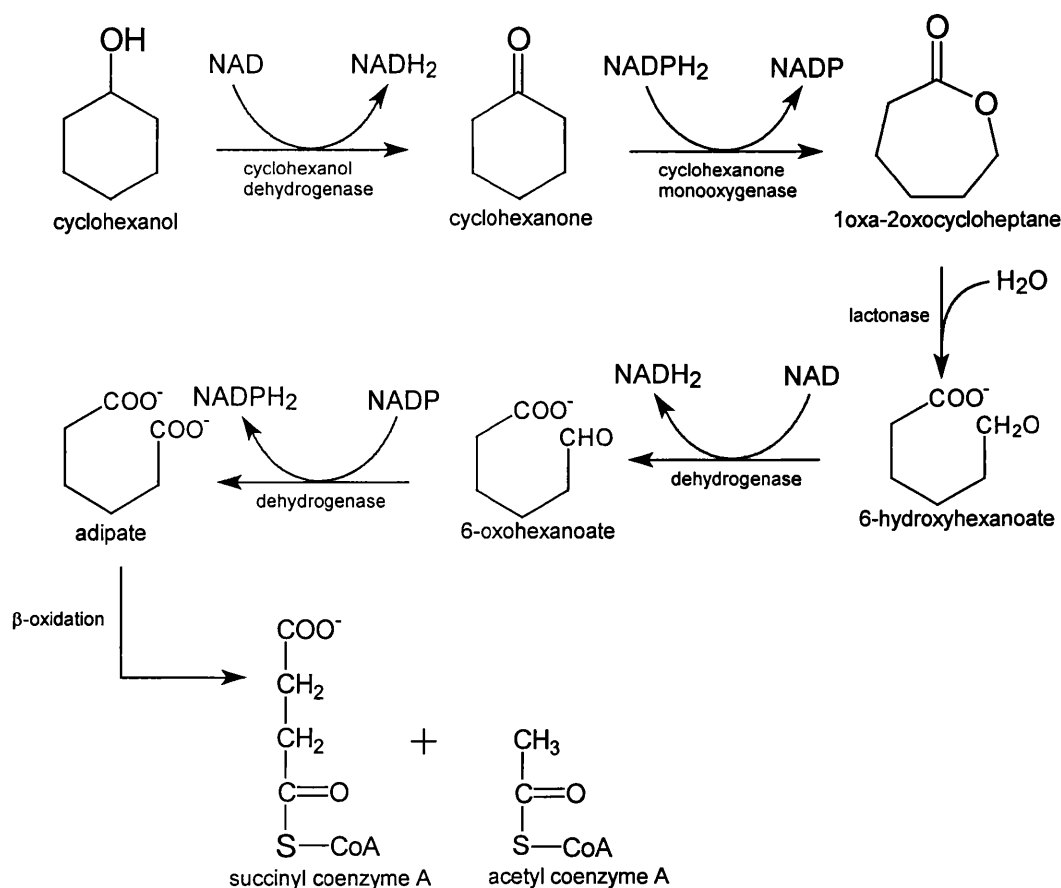


Figure 1.8 Metabolic pathway of cyclohexanol in *Acinetobacter calcoaceticus*. Reproduced from Donoghue and Trudgill, 1975 and Chapman & Duggleby, 1967.

The regioselectivity and enantioselectivity of the cyclohexanone monooxygenase from *Acinetobacter calcoaceticus* NCIB9871 have been shown by many workers. Taschner and Black (1988) transformed a number of substituted cyclohexanones including non chiral para substituted compounds to form chiral products. Abril and co-workers (1989) found a number of substrates that were transformed by enzyme preparations with some regioselectivity a good example being fenchone which was transformed to 1,2-fencholide and 2,3-fencholide in an 8:1 ratio (Figure 1.9), although this shows good regioselectivity they concluded that no advantage is to be gained over the chemical route in terms of enantioselectivity.

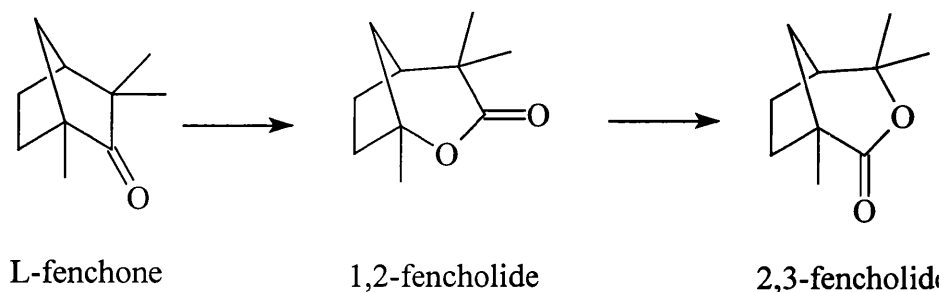


Figure 1.9 Biooxidation of fenchone

It has been shown that the enzyme system using whole washed cells of *A. calcoaceticus* can achieve a reaction equivalent to the chemical one and offer significant regioselective advantage, in this case however no information is given on enantioselectivity (Levitt *et al.*, 1990).

Alphand *et al.* (1990) used whole cells to produce the enantiopure pheromone 5-hexadecanolide. They found that the lactone product reached a maximum yield of 10% and then was found to disappear. The action of a lactone hydrolase as previously reported known to have 27 times the activity of the monooxygenase (Donoghue *et al.*, 1975; Schwab *et al.* 1983) was proposed as the cause and investigated. Using TEPP (tetraethyl pyrophosphate) to block the action of dehydrogenase they found that the product reached a yield of 40%. They discovered that only one regioisomer was formed as expected by the normal rules of the reaction, i.e. the oxygen atom is inserted into the

ring between the ketyl and the most substituted carbon atom. Only one enantiomer was transformed to produce the (+) lactone while ketone of the (-) form was recovered with 95% e.e.

Selectivity was further explored by Shipston *et al.* (1992) where racemic bicyclo[3.2.0]hept-2-en-6-one (Figure 1.10) was transformed and the production of the four possible products monitored. It was discovered that yields were lower i.e. lactone yield dropped from 98% to 67% when whole cells rather than enzyme preparations were used as has been reported in earlier work where the presence of a lactone dehydrogenase causes break down of the lactone product (Schwab *et al.*, 1983). However the relative amounts of each lactone were found to be very similar indicating that the lactone dehydrogenase is most likely not stereo or regio selective. In both cases the regioisomers were produced in approximately equal amounts with the (-)2-oxa and (-)3-oxa lactones produced in high (94%) e.e. which is markedly different from the results achieved with *P.putida* where the (+)2 and (+)3-oxa lactones were produced in high e.e., and the relative amounts of the two regioisomers were different.

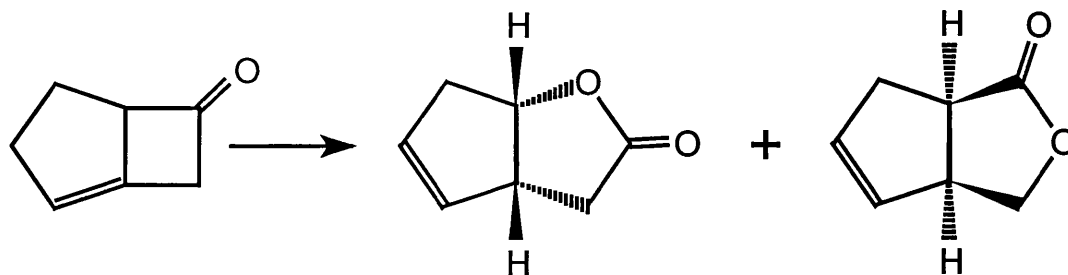


Figure 1.10 Baeyer-Villiger oxidation of bicyclo[3.2.0]hept-2-en-6-one

The biotransformation was repeated using individual enantiomers of the starting ketone and it was shown that the (+)ketone was transformed to (-)2-oxa lactone (99.8% e.e.) whilst (-) ketone was transformed more slowly to (-)3-oxa lactone (100% e.e.) (Shipston *et al.*, 1992). These results show a very high stereoselectivity but no regioselectivity from racemic starting material. Earlier work by Alphand *et al.* (1989) show similar results while other workers have shown that from essentially the same conditions the reaction proceeds with a good degree of regioselectivity to produce the

(-)-2-oxa and (-)-3-oxa regioisomers in a 9:1 ratio. There is no evidence to explain these differences in the biotransformation although differences in the time of harvesting the cells prior to the biotransformation may have an effect due to the presence of lactase and dehydrogenase enzymes.

Many of these workers showed that, in the case of bicyclic ketones at least, the substitutions affect both regio and enantioselectivity. Carnell *et al.* (1991) showed that depending on the substitution good regio with poor enantio, good regio and enantio or poor regio and good enantioselectivity could be observed. These results show that the starting material could be manipulated to produce the required selectivity.

1.3.4 Mechanism

Work by Ryerson *et al.* (1982) on cyclohexanone monooxygenase from *A. calcoaceticus* showed that NADPH was consumed at the same rate as oxygen and this together with other experimental evidence is given as proof that NADPH oxidation was fully coupled to substrate oxygenation. They describe the mechanism as one where a 4 α -peroxyflavin complex is formed as this would explain the capability of the enzyme to deliver both electrophilic and nucleophilic oxygen.

Braunchaud and Walsh (1985) showed from a wide range of substrates that the enzyme was capable of delivering nucleophilic oxygen to substrates such as cyclohexanone and butyraldehyde and electrophilic oxygen to a wide range of sulphides. These studies also show the similarity between the action of the enzyme and that of the classical model based on peroxide chemistry.

Alphand and Furstoss (1992) proposed a model representing the active site as a cube with stereoselectivity imposed by a forbidden zone within the cube. Tashner's model (Taschner *et al.*, 1992) is based on a similar theory with the formation of a hydroperoxyflavin complex. Neither of these models allow for the wide range of substrates that have been observed especially the sulphide oxidation. This lack of flexibility in the model led Ottolina *et al.* (1995) to propose a variation where the spatial arrangement of active sites allows not only for the insertion of oxygen into a

wide variety of cyclic and bicyclic ketones and the observation that each enantiomer tends to produce one regioisomer but also the oxidation of sulphides.

There is at present no structural data available on the enzyme to allow models to be further elucidated, although it is widely believed that the oxygen transfer takes place through a substrate-4 α -hydroperoxy flavoenzyme complex (Figure 1.11) (Ryerson *et al.*, 1982).

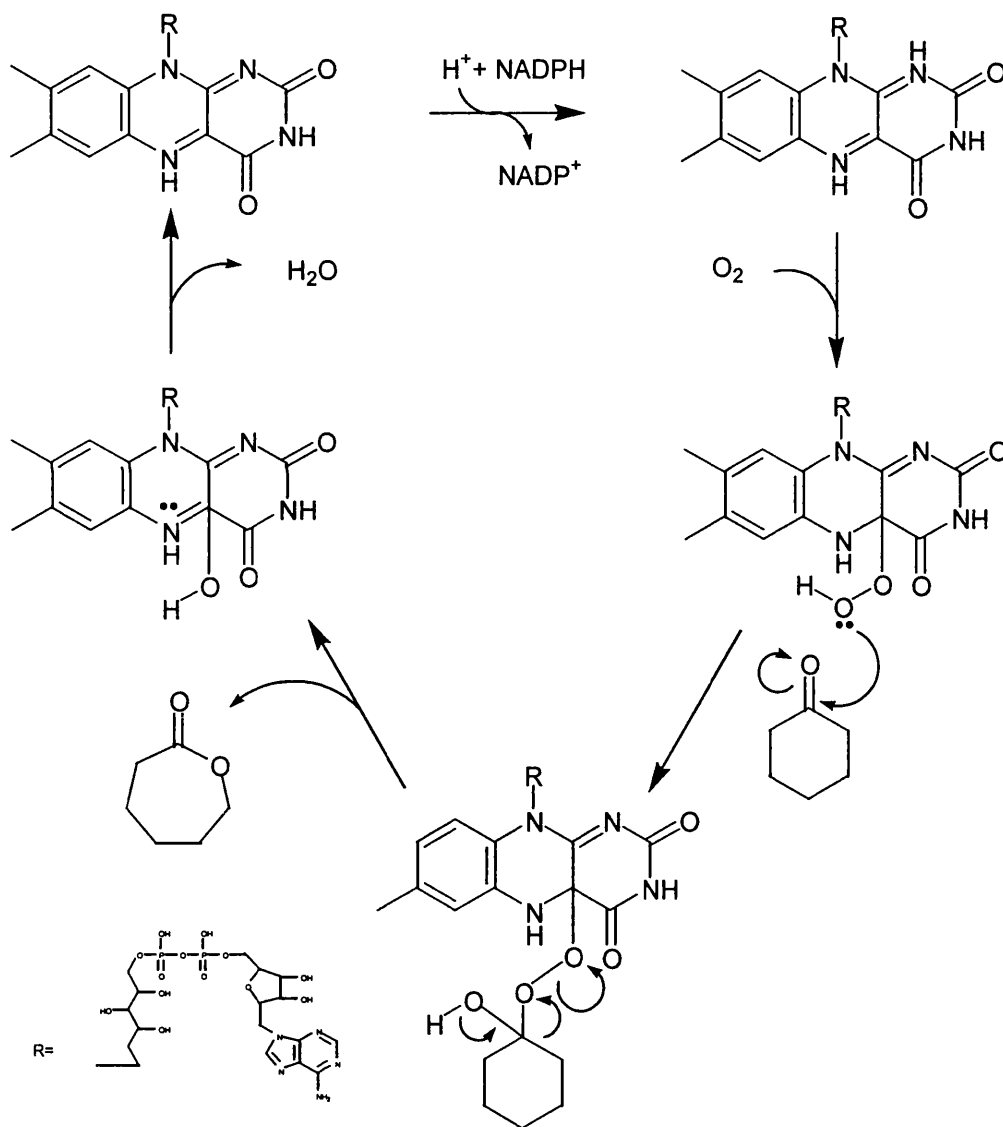


Figure 1.11 Proposed mechanism of action of cyclohexanone monooxygenase

2 Project rationale

2.1 Choice of organism

This research was carried out in order to investigate the production of a biocatalyst in the wild type organism and a recombinant *E. coli* expressing the biocatalyst. This thesis aims to identify the important factors in the production of the biocatalyst from the wild type and the recombinant organisms and to produce rules for biocatalyst production that have wider applicability.

While the use of both whole cells and enzyme preparations have been used for Baeyer-Villiger oxidations there is little data concerning direct comparisons. Data from whole cell and homogenate biotransformations will also be gathered. The process of biocatalyst production and use will be examined as a whole, and the factors identified which allow an informed choice of route.

This project is concerned with the production of biocatalyst for use in the transformation of cyclic ketones into lactones. The Baeyer-Villiger monooxygenase from *Acinetobacter calcoaceticus* has been produced in both the wild type organism and in a recombinant *E. coli* expressing the protein..

Despite the fact that the enzyme from *A. calcoaceticus* requires an expensive cofactor (NADPH) and is known to be a class two pathogen it was decided that this should be the organism and enzyme for study for two main reasons

The enzyme has been well studied and many successful biotransformations have been recorded. As mentioned earlier the enzyme from *A. calcoaceticus* is a single polypeptide sequence which made subsequent cloning and overexpression in *E. coli* easier to achieve. A recombinant should eliminate the possibility of product degradation

by lactone dehydrogenase as the host organism is unlikely to have enzymes capable of utilising these compounds as substrates. This method also allows for the use of an inducing agent specified by the promoter cloned with the CHMO gene. This would allow the cells to be grown on a nutrient media to achieve good growth. The gene encoding for CHMO could then be induced by chemical addition and not by growth on cyclohexanol which gives poor growth.

The second factor that influenced the choice is the future possibility of immobilising the enzyme. Immobilising an enzyme that requires a coenzyme can create many problems on its own without the added complication of having a multi subunit enzyme such as the monooxygenase from *P. putida*.

2.2 Choice of substrate

As can be seen from the literature the majority of work with this enzyme concerning regio and enantioselectivity has been carried out using various bicyclic ketones, the diversity of which is wide (Taschner and Peddada, 1992). A simple molecule that would give the same selectivity was considered to be required if the reaction was to be performed on a larger scale. Taschner *et al.* (1993) describe the production of optically active lactones from a range of asymmetrically substituted cyclohexanones with most showing a high degree of enantioselectivity typically above 98%. However they do not report the relative amounts of the regioisomers produced or any regioselectivity

Far less work has been reported on cyclopentanones, however the biotransformation of various 2 substituted cyclopentanones has been described (Alphand *et al.*, 1990). They discovered that as the length of aliphatic chain increased and the molecule became more hydrophobic, the yield of lactone increased. Alphand *et al.* (1990) also found that the addition of 1,2-cyclohexanediol increased yields of the shorter chain substituted lactones but decreased yields of the longer ones. They propose that the 1,2-cyclohexanediol acts as a substrate for a separate metabolic pathway and hence competes with the ketone increasing yields of lactone. Enantiomeric excess however behaves in the opposite manner, decreasing as chain length increases. They

expected that e.e. would fall after 50% conversion as the other enantiomer was used but this was not observed, and postulate that the second metabolic pathway uses up the ketone that is not used for lactone production while neither forming nor consuming lactone.

The biotransformation of the compound initially selected for this project, 2-(2',4',7'-trioxaoctyl) cyclopentanone, (Figure 2.1) is known to occur with good yield (97%), total regioselectivity, as can be predicted from the structure following the normal rules for Baeyer-Villiger reactions, and with a good deal of enantioselectivity (90% ee for both lactone and recovered ketone) (Adger *et al.* 1995).

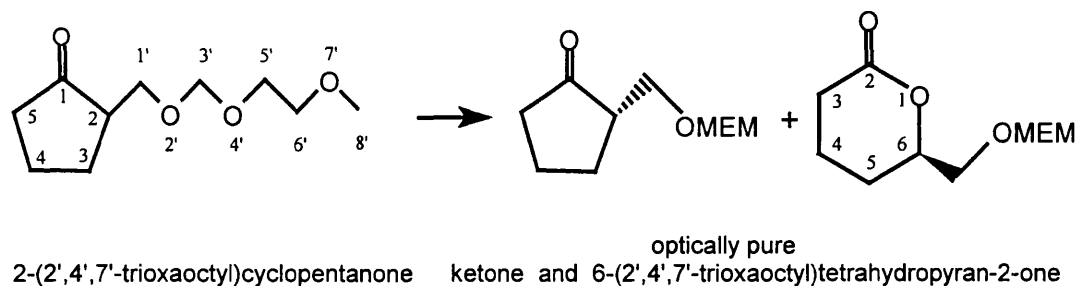


Figure 2.1 Baeyer-Villiger oxidation of 2-(2',4',7'-trioxaoctyl)cyclopentanone

Both ketone (2-(2',4',7'-trioxaoctyl)cyclopentanone) and lactone (6-(2',4',7'-trioxaoctyl) tetrahydropyran-2-one) are known to be relatively water soluble thus removing the need for a two phase system of biotransformation (Adger *et al.*, 1995).

This compound was not available commercially and so a method for its production had to be found. The method from literature was used to produce sufficient quantities for use as a standard marker for analysis but the reagents involved are not suitable for larger scale (multigram) production.

After the initial production of this compound it was found that scaling up the reaction would prove to be problematic. It was decided that the production of similar compounds would prove to be equally difficult because of the reagents involved, the cost and the amount of time it would take to manufacture.

A substrate would have to be found that was available commercially. Although the substrates available were not as substituted and hence would not show the same level of selectivity, 4-methyl cyclohexanone and 2-ethyl cyclopentanone (Figure 2.5) were chosen.

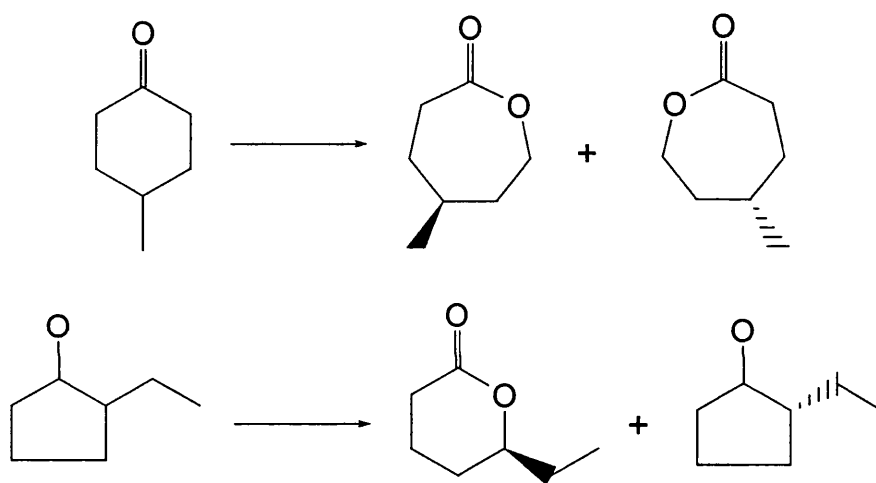


Figure 2.2 Proposed biotransformation of 4-methyl cyclohexanone and 2-ethylcyclopentanone

These compounds were chosen as substrates because they illustrate the two important types of reaction catalysed by cyclohexanone monooxygenase. The biotransformation of 4-methyl cyclohexanone is an example of the introduction of a chiral centre to a prochiral starting material, while the conversion of 2-ethyl cyclopentanone is a chiral resolution.

After performing biotransformations using these substrates it was found that the chiral GC column could not discriminate between the enantiomers of substituted cyclopentanones. This meant that the selectivity could not be measured. The column was however capable of separating the enantiomers of substituted cyclohexanones. For this reason 2-methyl cyclohexanone (which was available commercially) was substituted for 2-ethyl cyclopentanone in later biotransformations.

3 MATERIALS AND METHODS

3.1 Analytical methods

3.1.1 Cell growth analysis

All optical densities of growing cultures reported were measured at $\lambda = 670$ nm. A correlation was produced by measuring the cell mass in a known volume of culture passed through a pre-dried nitro-cellulose membrane (0.2 μm) and kept in an oven at 100 °C until a constant mass was recorded. Figure 3.1 illustrates this correlation between optical density and dry cell weight for *A. calcoaceticus* and Figure 3.2 for *E. Coli* JM107/pQR210.

3.1.2 Cyclohexanone monooxygenase activity assay

The CHMO assay used for all quantitative determinations of CHMO was based on a method described by Donoghue *et al.* (1976). This involves the cyclohexanone stimulated oxidation of NADPH to NADP⁺. The assay was therefore followed spectrophotometrically at 340 nm. The rate of oxidation of NADPH (indicated by a decrease in absorbance at 340 nm) was directly proportional to the concentration of CHMO in the assay.

In a final volume of 1 mL the following reagents, expressed in their final concentrations were added to a spectroscopic cuvette: Tris-HCL buffer , 50 mM; pH 9.0

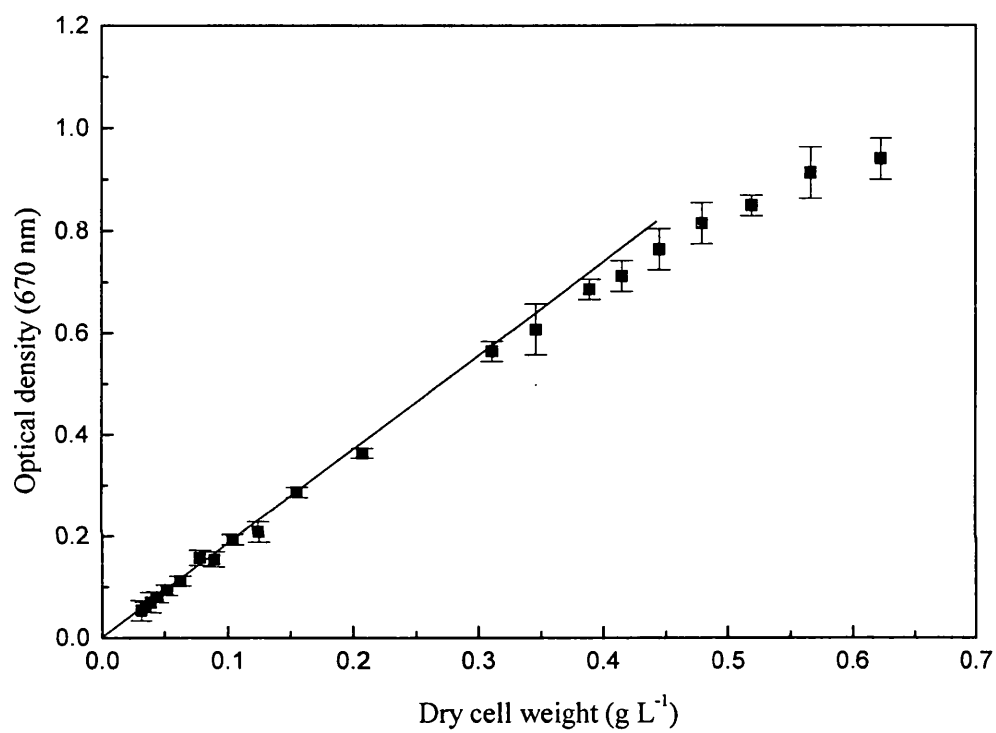


Figure 3.1: This figure illustrates the correlation between optical density and dry cell weight for *A. calcoaceticus*

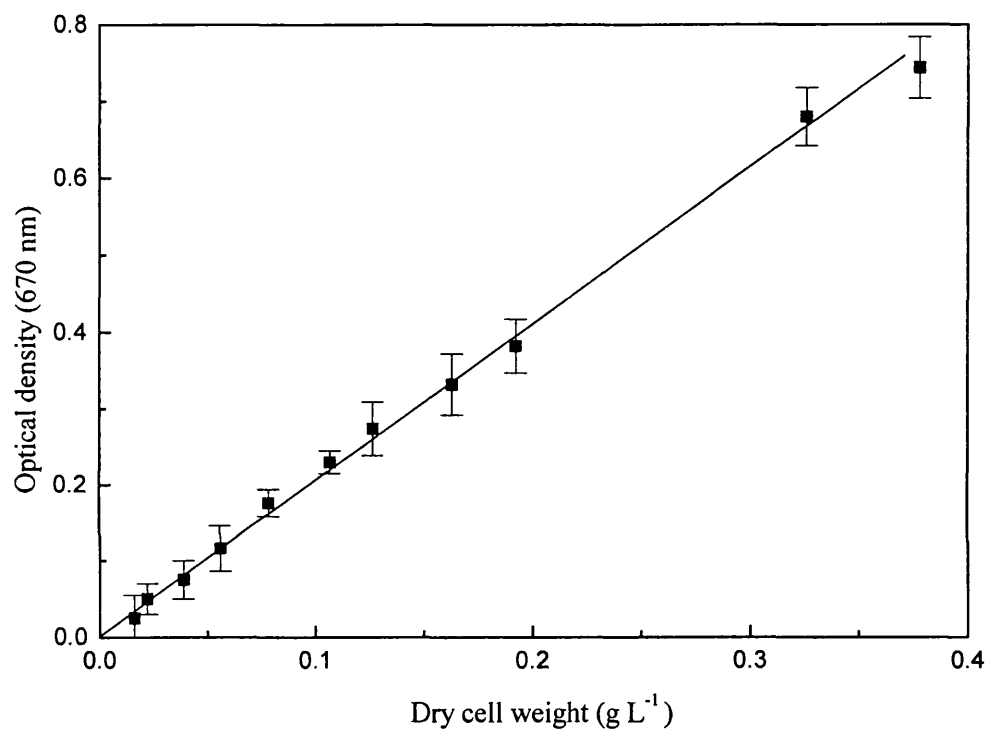


Figure 3.2: This figure illustrates the correlation between optical density and dry cell weight for *E. Coli* JM107/pQR210

bovine serum albumen, 5 mg mL⁻¹; NADPH, 0.180 mM, CHMO source, 0.1-0.15 U; cyclohexanone, 2 mM. The cyclohexanone was added last and the decrease in absorbance measured with time. After a brief lag phase a linear decline in absorbance is observed and this rate is used to determine the CHMO activity.

The relationship between rate of oxidation of NADPH ($\Delta A/\Delta t$) and CHMO activity and its derivitisation is given below.

The extinction coefficient for NADPH: $\epsilon_{\text{NADPH}} = 6200 \text{ L (mol.cm)}^{-1}$
 With a 1 cm light path at 340 nm $= 6.2 \text{ mL } \mu\text{mol}^{-1}$

$$\begin{aligned} \Rightarrow [\text{CHMO}] \text{ in assay} &= \frac{\text{rate of oxidation of NADPH (min}^{-1}\text{)}}{\epsilon_{\text{NADPH}} \text{ (mL } \mu\text{mol}^{-1}\text{)}} \\ &= (\mu\text{mol mL}^{-1}) \text{ min}^{-1} \\ &= \text{U mL}^{-1} \end{aligned}$$

since the total volume is 1 mL:

$$\text{Units of CHMO in assay} = (\text{rate of oxidation of NADPH}) \times 0.161$$

The result from this calculation can easily be related to the CHMO in the test sample by taking into account the dilution in the assay, and any dilutions in the preparation of the extract.

3.1.3 Protein assay

Protein concentrations were routinely determined using Coomassie Plus Protein Reagent. The assay reagent (950 μL) was added to the protein solution or crude cell extract (50 μL), left to stand at room temperature for 5 minutes and the absorbance read at 595 nm. Samples to be assayed were diluted so as to give a protein concentration of between 0.05 and 0.5 mg mL^{-1} . The protein concentration was standardised using bovine serum albumin solutions of known concentration (0.025 to 0.6 mg mL^{-1}). A standard curve was produced for each set of assays (Appendix III).

3.1.4 GC assay for reactants and products

Samples containing biotransformation reactants and products were analysed using a lipodex chiral GC capillary column (section 3.1.1). Samples were prepared for analysis by deproteination with an equal volume of ice cold 2-propanol, standing on ice for 5 min and centrifugation (5 min at 15000 rpm). This technique was found to adequately remove protein to avoid build up of organic matter in the injector of the gas chromatograph. The supernatant (1 mL) was then analysed by injection onto the column by autosampler. Standard solutions containing both reactants and products (where available), prepared in cell homogenate and treated in the same manner, were used to establish retention times and to calibrate the peak area to component concentration.

3.2 Equipment

3.2.1 Chromatographic apparatus

Thin layer chromatography (TLC) was performed on pre-coated silica glass plates (Merck gel 60F 254) and were visualised using a 1% solution of bismuth oxynitrate ($4\text{BiNO}_3(\text{OH})_2$) in acetic acid and 1% potassium permanganate (KMnO_4) solution in ethanol.

Flash chromatography was performed on silica (Merck Kieselgel 60) and the mass of silica was approximately ten fold greater than the mass of sample.

3.2.2 Spectroscopic apparatus

UV spectra, spectrophotometric assays and optical density readings were recorded on a Kontron Instruments, Uvikon 922 Spectrophotometer (Kontron Instruments Ltd, Watford, Herts., UK). Microtitre plates were read by Dynatech MR7000 microtitre plate reader (Dynatech, Guernsey, Channel Islands, UK).

Gas chromatography was performed on a Lipodex C chiral capillary column (0.25 $\mu\text{m} \times 30 \text{ m}$). A Perkin Elmer Gas Chromatograph (Perkin Elmer, Norwalk, CT, USA) was used with flame ionisation detection. The injection volume was 1 μL with a split ratio of 1:100. The carrier gas was helium at a pressure of 5 psi for a run time of 5 min at 80 $^{\circ}\text{C}$ followed by a 2 $^{\circ}\text{C min}^{-1}$ ramp to 140 $^{\circ}\text{C}$.

Nuclear magnetic resonance (NMR) spectra (^1H) were recorded on a Bruker AM300 (Bruker UK LTD, Coventry, UK) 300 MHz ^1H spectrometer, with samples made up in CDCl_3 . All chemical shifts (δ) are reported in parts per million (ppm) and the results are given as :

δ (number of protons, multiplicity, assignment)

where the multiplicity is denoted as:

s = singlet, d = doublet, dd = double doublet, br = broad, m = multiplet.

I am grateful to Alan Pettman (Pfizer) for his help in NMR spectrogram analysis.

3.2.3 Fermentation equipment and analysis

Inocula flasks were incubated on a ISF-1-V orbital shaker at 200 rpm (Adolf Kühner, Schmeiz, Switzerland) with a throw diameter of 0.1 m. Fermentations were performed in an LH Inceltech Series 210 2L glass fermenter (Inceltech/LH Fermentation Ltd., Reading, Berks., UK). For larger scale fermentations a 7 L stainless steel

fermenter (FT Applikon Series 230, Applikon Dependable Instruments BV, Schiedam, The Netherlands) with a height to diameter ratio of 2.2, fitted with three six bladed turbine impellers (diameter 0.06 m). Analysis of fermentation exit gases was achieved with a VG Prima mass spectrometer controlled by a VG gas analysis microprocessor (MM8-80F, VG Gas Analysis, Winsford, Cheshire, UK). The analysis produces O₂, CO₂, N₂ and Ar percentage composition. Control and logging of the fermentation parameters and logging of the gas analysis data was achieved with BioXpert software which was used to calculate the values of oxygen uptake rate (OUR), carbon dioxide evolution rate (CER) and the respiratory quotient (RQ). The information was logged every minute during the fermentation.

Fed batch fermentations were controlled with a LabView software program designed by M. Gregory (1993) run via a personal computer.

3.2.4 Downstream processing equipment

Disruption of cells by sonication was performed using a Sanyo, MSE Soniprep 150 (Sanyo Gallenkamp PLC, Loughborough, UK). Centrifugation of fermentation broth and debris post disruption was performed using either a Heraeus Sepatech Megafuge 1.0R (Heraeus Instruments GmbH, Hanau, Germany) with an HFA 15.2 rotor for small scale samples, or a Beckman J2MI (Beckman Instruments Inc., Beaconsfield, UK) with a JA10 rotor for larger volumes.

An APV Lab 40 (APV Ltd, Crawley, UK) Manton Gaulin homogeniser was used for larger scale cell disruption.

3.3 Recombinant *E. coli*

The recombinant *E. Coli* stain JM107/pQR210 expressing cyclohexanone monooxygenase was prepared by Dr. Sejal Patel of the Department of Biochemistry and Molecular Biology, UCL.

3.4 Fermentation media

Reagent	Supplier	Grade
Ammonia (0.880)	BDH	AnalR
Ampicillin	Sigma	AnalR
Antifoam (PPG)	BDH	2000
Boric acid	Sigma	AnalR
CaCl ₂	Sigma	GLR
CaCO ₃	Sigma	GLR
Citric acid	Sigma	AnalR
CoCl ₂	Sigma	AnalR
CuSO ₄ .5H ₂ O	Sigma	AnalR
Fe(NH ₄) ₂ (SO ₄) ₂ .7H ₂ O	Sigma	AnalR
FeSO ₄ .7H ₂ O	Sigma	AnalR
Glycerol	BDH	AnalR
HCl	Sigma	GLR
KH ₂ PO ₄	Sigma	AnalR
K ₂ SO ₄	Sigma	AnalR
MgSO ₄ .7H ₂ O	Sigma	AnalR
MnCl ₂ .4H ₂ O	Sigma	AnalR
MnSO ₄ .4H ₂ O	Sigma	AnalR
NaCl	Sigma	GLR
Na ₂ HPO ₄	Sigma	AnalR
NH ₄ Cl	Sigma	GLR
Tryptone	Oxoid	-
(NH ₄) ₂ SO ₄	Sigma	AnalR
Yeast Extract	Oxoid	-
ZnSO ₄ .7H ₂ O	Sigma	AnalR
Cyclohexanol	Sigma	AnalR

Table 3.1 Suppliers of the fermentation media and the grade used.

Aldrich Chemical Company, New Rd, Gillingham, Dorset, SP8 4JL, UK.

BDH, Merck Ltd, Merck House, Poole, Dorset, BH15 1TD, UK.

Oxoid Chemical Company Ltd, Wade Rd, Basingstoke, Hampshire, RG24 0PW, UK.

Sigma Chemical Company, Fancy Rd, Poole, Dorset, BH17 7BR, UK.

3.5 Microorganisms

3.5.1 Maintenance of organisms

The cyclohexanol oxidising strain of *A. calcoaceticus* NCIMB 9872 was kindly supplied by Dr. Ewald Schroder of Exeter University, Exeter, UK. The *Escherichia coli* construct JM107/pQR210 was obtained from Dr. Sejal Patel (UCL) on agar plates.

Stock cultures of both organisms were routinely prepared by suspending freshly grown culture from a shake flask in a sterile (50:50) glycerol/phosphate buffer solution and stored as 1 mL aliquots at -70 °C. The phosphate buffer was prepared by dissolving Na₂HPO₄ (4 g L⁻¹) and KH₂PO₄ (2 g L⁻¹) in demineralised water and adjusting to pH7 with phosphoric acid (phosphate buffer). These stock cultures were reactivated by streaking onto sterile agar plates (section 3.5.2).

3.5.2 Solid culture media

The medium used for solid culture was as table 3.2 for *A. calcoaceticus* with the addition of glutamate and technical agar (15 g L⁻¹). For the JM107 *E. coli* strain nutrient agar was used. When selective pressure was required ampicillin (500 mg L⁻¹) was added by filtration through 0.2 µm nitrocellulose membrane filters when the medium had cooled to approximately 50 °C.

3.6 Growth of *Acinetobacter calcoaceticus*

3.6.1 Media

A defined aqueous salts media, pH 7, was used for both shake flask and fermenter growth. For composition see Table 3.2.

Succinic acid or monosodium glutamate, both neutralised with sodium hydroxide, or cyclohexanol was then added. In the case of succinic acid and monosodium glutamate this was added prior to sterilisation by autoclaving, while cyclohexanol was added by direct injection after sterilisation. The amount of ammonium sulphate was increased for some fermentations so as to maintain a concentration that was 20 % by weight of the concentration of the carbon source.

Anhydrous constituent	g L⁻¹
Sodium hydrogen phosphate (Na ₂ HPO ₄)	4
Potassium dihydrogen phosphate (KH ₂ PO ₄)	2
Ammonium sulphate ((NH ₄) ₂ SO ₄)	2
Trace element solution (4 mL)	g L⁻¹
Magnesium sulphate (MgSO ₄ .7H ₂ O)	19.6
Iron sulphate (FeSO ₄ .7H ₂ O)	5.6
Calcium carbonate (CaCO ₃)	2
Zinc sulphate (ZnSO ₄ .7H ₂ O)	1.4
Manganese chloride (MnCl ₂ .4H ₂ O)	1.1
Cobalt chloride (CoCl ₂)	0.28
Copper sulphate (CuSO ₄)	0.25
Boric acid	0.06
Hydrochloric acid	53 mL

Table 3.2 Mineral media constituents for *A. calcoaceticus* fermentation

3.6.2 Shake flask growth

Stored cultures (3.5.1) were used to inoculate an agar plate from which two or three colonies were used to inoculate the above media (200 mL) in a shake flask (2 L) with either succinic acid, monosodium glutamate, cyclohexanol or a combination of carbon sources. The flasks were then incubated at 28 °C in a LH Mk X Incubator Shaker at 200 rpm for 16 to 24 hours.

3.6.3 Batch fermentation

The media (1.3 L or 4.5 L) with the addition of antifoam (0.2 mL L^{-1}) was sterilised *in situ* by heating with steam to $121 \text{ }^{\circ}\text{C}$ and held for 20 minutes before cooling. The pH was adjusted to 7.0 with NaOH solution (3M) and orthophosphoric acid (3 M) and the temperature maintained at $28 \text{ }^{\circ}\text{C}$. The trace element solution and cyclohexanol were added by filter sterilisation ($0.2 \text{ }\mu\text{m}$) prior to inoculation.

The inoculum (100 mL or 200 mL; section 3.6.2) was aseptically transferred to the fermentation and growth allowed to proceed. Standard Operating Procedures (SOP) were written and followed to ensure that the fermentations were carried out so as to minimise the release of the organism and operator exposure because of the pathogenicity of the organism (see appendix I).

Temperature and pH were controlled via PID to the set points indicated above. Air flow rate into the fermenter was set at 1 fermenter volume per minute and the agitation rate altered manually so as to maintain the dissolved oxygen tension (DOT) to a value greater than 20 % air saturation until the maximum stirrer speed of the vessel (1500 rpm) was reached. Sterile antifoam (20 % PPG) was added manually as required.

3.7 Growth of *E. coli* JM107/pQR210

3.7.1 Media

E. coli JM107/pQR210 was grown either on a complex media or a defined salts medium. In each case the inocula were made up in the same media as the fermenter (Table 3.3). Fed-batch fermentations used feed solutions as detailed in table 3.4.

Constituent	Medium					
	1	2	3	4	5	6
Glycerol	3	30	5	1	10	15
Tryptone	10	30				
Yeast extract	10	30				
NaCl	10	10				
K ₂ SO ₄			6.62	6.62	6.62	6.62
KH ₂ PO ₄			3.96	3.96	3.96	3.96
NaHPO ₄			2.1	2.1	2.1	2.1
NH ₄ Cl	1	6	1.32	1.32	2	3
MgSO ₄ .7H ₂ O			0.66*	0.66*	0.66*	0.66*
Citric acid			0.66*	0.66*	0.66*	0.66*
Fe(NH ₄) ₂ (SO ₄) 2			0.60*	0.60*	0.60*	0.60*
CaCl ₂			0.33*	0.33*	0.33*	0.33*
ZnSO.7H ₂ O			0.0032*	0.0032*	0.0032*	0.0032*
MnCl ₂ .4H ₂ O			0.00056*	0.00056*	0.00056*	0.00056*
CuSO ₄ .5H ₂ O			0.00033*	0.00033*	0.00033*	0.00033*
Ampicillin			0.05*	0.05*	0.05*	0.05*
Thiamine			0.001*	0.001*	0.001*	0.001*

Table 3.3 Composition of culture media for JM107/pQR210. All figures are given in g L⁻¹, where * denotes sterilised by filtration (0.2µm) and added after the rest of the media had been sterilised and prior to inoculation.

Constituent	Feed Solution			
	1	2	3	4
Glycerol	210	246	210	355
MgSO ₄ .7H ₂ O	15	15	15	15
Ampicillin*	0.05	0.05	0.05	0.05

Table 3.4 Composition of feed solutions 1-4 used in fed-batch fermentations of JM107/pQR210. All figures are given in g L⁻¹, where * denotes sterilised by filtration (0.2 µm) and added after the rest of the media had been sterilised by autoclave.

3.7.2 Shake flask growth

Stored cultures were used to aseptically inoculate an agar plate from which two or three colonies were used to inoculate complex media 1 (100 mL) in a shake flask (1 L) which was incubated at 37 °C in an LH Mk X Incubator Shaker at 200 rpm for 16 hours. A 10 mL aliquot was then transferred to another shake flask (2 L) containing sterile defined medium 3 (200 mL) and incubated as before.

3.7.3 Batch fermentation

Media 2 or 6 (4.8 L) with the addition of antifoam (0.2 mL L⁻¹) was sterilised *in situ* by heating with steam to 121 °C and held for twenty minutes before cooling. The pH was adjusted to 6.8 with ammonia solution (1:1, 0.880 ammonia: water) and the temperature maintained at 37 °C. The selective antibiotic ampicillin (0.05 g L⁻¹) was sterilised by passing it through a 0.2 µm membrane filter and added to the medium prior to inoculation.

The inoculum (200 mL) was aseptically transferred to the fermentation and growth allowed to proceed. Temperature and pH were controlled via PID to the set points indicated above. Air flow was set to 1 fermenter volume per minute and the

agitation rate altered manually so as to maintain the dissolved oxygen tension (DOT) to a value greater than 20 % air saturation until the maximum stirrer speed of the vessel was reached. Sterile antifoam (20 % PPG) was added manually as required.

3.7.4 Fed-batch fermentation

Media 3, 4 or 5 (3.8 L or 4.3 L) were prepared, with sufficient glycerol and other nutrients for a final volume of 5 L and 5.5 L respectively. The fermenter was then sterilised and prepared for inoculation as for the batch fermentations (section 3.6.3).

The fermenter was inoculated as for the batch process and growth allowed to continue until the carbon source was depleted. This was indicated by a rapid increase in the DOT and subsequent fall in both the OUR and CER. At this point the feed was started either by the initiation of a computer controlled fed batch procedure (Gregory & Turner, 1993) or by a constant rate pump. The feeding of sterile feed solution (1,2,3 or 4, section 4.1.1) was controlled to give a constant growth rate, μ , of 0.15 h^{-1} . In some fermentations the feed was then set to a constant rate to maintain a maximum OUR that was less than $70 \text{ mmol L}^{-1} \text{ h}^{-1}$.

The feed solution was controlled by the LabView software program (Gregory and Turner 1993) using the following control algorithms:-

$$F = (\mu/Y_{\text{gly}}).x(t).V(t)$$

$$x(t) = x(t-\Delta t).exp(\mu\Delta t)$$

$$V(t) = V(t-\Delta t) + (F\Delta t/s_f)$$

where F is the glycerol feed rate (g h^{-1}), μ is the specific growth rate (h^{-1}), Y_{gly} is the yield on glycerol (g g^{-1}), x is the dry biomass concentration (g L^{-1}), V is the fermenter volume (L), s_f is the glycerol concentration of the feed (g L^{-1}).

Using these equations, values for Y_{gly} determined from batch fermentations (section 4.3.5), the glycerol concentration in the feed and the biomass when feeding begins, the computer program calculates the required feed rate for any required growth rate. This is translated to a pump speed using the calibration curves for the variable

speed peristaltic pumps used and thus the software is able to maintain a constant growth rate.

At varying times the production of CHMO was then induced by the addition of IPTG and the broth was harvested if required.

3.7.5 Plasmid stability

Plasmid stability of the *E. coli* JM107/pQR210 recombinant was determined from the ratio of number of colonies from selective agar plates (with ampicillin) to that from non-selective plates. Sterile culture taken at intervals was diluted in sterile phosphate buffer to give approximately 100 colonies per plate in a 50 μ L aliquot and spread aseptically. Plates were incubated at 37 °C for 12-16 hours and the colonies counted.

3.8 Downstream processing methods

3.8.1 Preparation of crude extract by sonication

Sonication was used as a method of cell disruption in samples of shake flasks or to monitor the production of CHMO after induction of a fermentation.

Cells were removed from the broth sample (1-3 mL depending on the dry cell weight) by centrifugation (2 min, 15000 rpm) and resuspended in phosphate buffer (section 3.5.1). The cells were then removed again by centrifugation and resuspended in phosphate buffer (1 mL). The crude extract was then prepared by sonication: For *A. calcoaceticus* cells, 3 \times 30 sec separated by 1 min on ice, and for *E. coli* JM107/pQR210, 4 \times 10 sec separated by 10 sec on ice (Appendix II), followed by centrifugation to remove cell debris (5 min, 15000 rpm).

3.8.2 Preparation of crude extract by Lab 40 homogenisation

A Lab40 homogeniser was used to disrupt cells when a larger volume was required for analysis or to harvest the cyclohexanone monooxygenase. Cells were removed from the broth by centrifugation (15 min, 10000 rpm) and resuspended in phosphate buffer (section 3.5.1). Crude extracts from *E. coli* and *A. calcoaceticus* were prepared by high pressure homogenisation, 2 and 4 passes at 900 bar respectively, followed by centrifugation to remove cell debris (45 min, 10000 rpm).

3.8.3 Storage and stability of cells

Cells were removed from culture medium by centrifugation (15 min, 10000 rpm) and resuspended in phosphate buffer (section 3.5.1). The resulting suspension was then either stored at 4 °C, -18 °C or mixed with an equal volume of sterile glycerol. The suspension was then aliquoted and stored at -18 °C. When required the suspension was centrifuged (15 min, 15000 rpm) and resuspended in buffer. Crude extracts were routinely tested for CHMO activity by disrupting the cells (section 3.8.1) and assaying the crude extract (3.1.2).

3.8.4 Storage and stability of homogenate

Homogenate (section 4.4.2) was either stored at 4 °C, -18 °C or mixed with an equal volume of glycerol and stored at -18 °C. It was routinely tested for CHMO activity.

3.9 Biotransformations

3.9.1 Whole cell biotransformations

Whole cell biotransformations were carried out using freshly grown cells that had been harvested by centrifugation from the fermentation medium and resuspended in 100 mL phosphate buffer. The cells were centrifuged again and resuspended in a further 100 mL of the same buffer in 1 L shake flasks. This avoided the problems associated with handling small volumes of liquid accurately. Cyclohexanol (0.5 g L^{-1}) in the case of *A. calcoaceticus* or glycerol (0.5 g L^{-1}) in the case of *E. coli* was added to the flasks and they were incubated at $30 \text{ }^{\circ}\text{C}$ and 250 rpm. Biotransformations were initiated by the addition of substrate and samples taken at intervals and prepared for analysis (section 3.1.4). Samples were also prepared for CHMO activity analysis.

3.9.2 Homogenate biotransformations

Crude homogenate was prepared and biotransformations were carried out as section 4.6.1 without the addition of cyclohexanol or glycerol as a carbon feed source. When enantiomers could be resolved the enantiomeric excess of one enantiomer over the other was calculated as follows:

$$\text{ee.} = \frac{100 \times ([\text{R}] - [\text{S}])}{[\text{R}] + [\text{S}]}$$

where [R] and [S] are the concentrations of the two enantiomers.

3.10 Chemical Syntheses

3.10.1 Literature Method (Adger *et al.*)

Under a nitrogen atmosphere, ethylene glycol (280 g) and para-toluene sulphonic acid (0.910 g) were added to a solution of methyl 2-oxocyclopentane carboxylate (64 g) in toluene (400 mL). The mixture was heated to reflux for 5 hours and allowed to cool to room temperature. The organic phase was separated from the aqueous phase which was then extracted with toluene (2 × 100 mL). The combined organic phase was then dried over magnesium sulphate. The solvent was evaporated under reduced pressure to give the crude product which was purified by vacuum distillation to give methyl-1,4-dioxaspiro[4,4]nonane-6-carboxylate (28 g, 44%) (Figure 2.2) as a faintly coloured oil. δ_{H} (300 MHz, CDCl_3) 4.06-3.84 (4 H, m, H-2 and H-3), 3.69 (3 H, s, CH_3O), 2.91 (1 H, t, H-6), 2.20-1.55 (6H, m, H-7, H-8 and H-9).

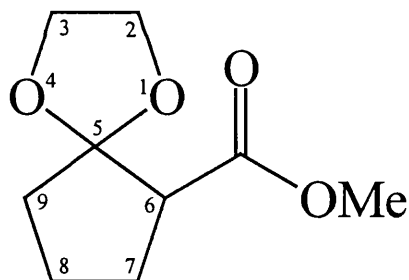


Figure 3.3 Methyl 1,4-dioxaspiro[4.4]nonane-6-carboxylate

Under a nitrogen atmosphere a solution of methyl-1,4-dioxaspiro[4.4]nonane-6-carboxylate (500 mg) in THF (5 mL) was added dropwise to a stirred suspension of lithium aluminium hydride (205 mg) in THF (15 mL) at $^{\circ}\text{C}$. The mixture was stirred at room temperature for 2 h, cooled to 0°C and quenched with 2 M HCl (20 mL) added dropwise. After stirring for 30 minutes, 25 mL of ethanol was added. The mixture was stirred at room temperature. After 30 minutes the mixture was extracted with

dichloromethane (4 × 50 mL). The combined organic extracts were washed with saturated sodium bicarbonate solution (50 mL) and saturated sodium chloride solution (50 mL) then finally dried over magnesium sulphate. The solvent was evaporated under reduced pressure to give the crude produce which was purified by flash column chromatography, with hexane-ethyl acetate (7:5) to give 2-hydroxymethyl cyclopentanone (Figure 2.3) as a nearly colourless oil (100 mg, 20% yield) $R_f = 0.13$

δ_H (300 MHz, $CDCl_3$) 3.8 (1H, dd, H-1'), 3.7 (1H, dd, H-1'), 2.5 (1H, br s, OH), 2.4-2.2 (2H, m, H-2 and H-5), 2.2-2 (3H, m, H-5 and H-3), 2-1.6 (2H, m, H-4).

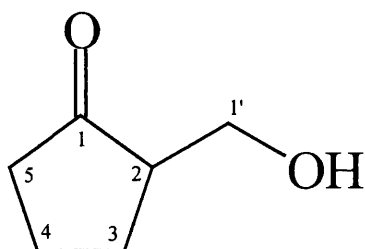


Figure 3.4 2-hydroxymethyl cyclopentanone

3.10.2 Developed method

This method was not suitable for scaling up so a new route had to be found. A literature search of similar compounds and reactions produced few alternatives that involved more basic chemistry and less reactive reagents. From discussions with organic chemists at Pfizer, notable Alan Pettman, the following method was developed.

Cyclopentanone (500 g) was added to a stirred solution of potassium carbonate (82.15 g) in water (2 L). Aqueous formaldehyde (40%) was added in 100 mL volumes with cooling of the mixture in an ice bath between additions. The mixture was stirred at room temperature for three hours. The mixture was washed with hexane (1.5 L) and the aqueous phase separated. The aqueous phase was then saturated with sodium chloride and extracted with DCM (3 × 500 mL). The combined organic extracts were dried over magnesium sulphate and the solvent evaporated under reduced pressure to give the

crude product which was purified by vacuum distillation (0.5 mm Hg, vapour temperature 80 °C) to give 2-(hydroxymethyl) cyclopentanone (70 g, yield 14%) (Figure 3.4).

δ_{H} (300 MHz, CDCl_3) 3.8 (1H, dd, H-1') 3.7 (1H, dd, H-1'), 2.5 (1H, br s, OH), 2.4-2.2 (2H, m, H-2 and H-5), 2.2-2 (3H, m, H-5 and H-3), 2-1.6 (2H, m, H-4).

An alternative method for producing the final stage could not be found and so the original literature method was followed including the use of methoxyethoxymethyl chloride which is known to contain a carcinogenic impurity.

To a stirred solution of 2-(hydroxymethyl) cyclopentanone (21.2 g) in dichloromethane (200 mL), diisopropylethylamine (36.1 g) was added. Methoxyethoxymethyl chloride (35 g) was added dropwise. The mixture was stirred for 16 hours at room temperature and then quenched with water (150 mL) and stirred for a further 15 minutes. The organic phase was separated from the aqueous phase which was extracted with DCM (200 mL). The combined organic phase was dried over magnesium sulphate and the solvent evaporated under reduced pressure to give the crude product, which was purified by flash column chromatography with toluene-ethyl acetate (3:1) to give 2-(2', 4', 7'-trioxaoctyl) cyclopentanone (27 g, 72% yield) as a faintly coloured oil $R_f = 0.31$

δ_{H} (300 MHz, CDCl_3) 4.65 (2H, s, H-3'), 3.75 (1H, dd, H-1'), 3.7 (1H, dd, H-1'), 3.69-3.6 (2H, m, CH₂O), 3.59-3.45 (2H, m, CH₂O), 3.35 (3H, s, H-8'), 2.35-1.7 (7H, m, H-2, H-3, H-4, H-5).

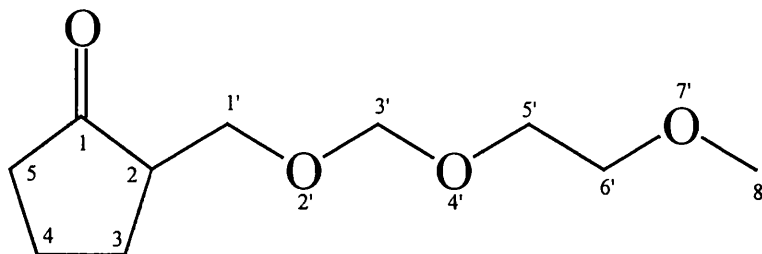


Figure 3.5 Synthesis of 2-(2',4',7'-trioxaoctyl)cyclopentanone

The lactone product of a Baeyer-Villiger reaction was also produced for use as a marker in future experiments.

Under a nitrogen atmosphere sodium bicarbonate (630 mg) and metachloroperoxybenzoic acid (1.72 g) were added to a stirred solution of 2-(2', 4', 7'-trioxaoctyl) cyclopentanone (1 g) in dichloromethane (25 mL) at room temperature. After 16 hours the mixture was washed sequentially with sodium sulphite solution (2 × 25 mL), distilled water (2 × 25 mL) and saturated sodium chloride solution (2 × 25 mL). The organic phase dried over magnesium sulphate and the solvent evaporated under reduced pressure to give the crude product which was purified by flash column chromatography with ethyl acetate to give 6-(2', 4', 7'-trioxaoctyl) tetrahydropyran-2-one as a colourless oil (Figure 3.6).

δ H (300 MHz, CDCl₃) 4.7 (2H, s, H-3'), 4.4 (1H, m, H-6), 3.75-3.65 (4H, m, 2 × CH₂O), 3.6-3.5 (2H, m, CH₂O), 3.4 (3H, s, H-8'), 2.65-2.4 (2H, m, H-3), 2.05-1.6 (4H, m, H-4 and H-5).

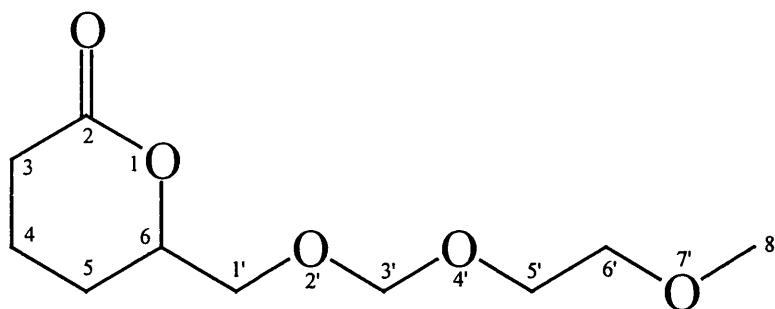


Figure 3.6 Synthesis of 6-(2',4',7'-trioxaoctyl)tetrahydropyran-2-one

4 RESULTS

4.1 Cyclohexanone monooxygenase assay

The spectrophotometric assay used to measure CHMO activity was based on the literature method of Donoghue *et al.* (1976). The process was slightly modified by the addition of BSA (5 mg mL⁻¹) to the reaction mixture before the addition of the crude preparation to avoid CHMO binding to the walls of the cuvette. The procedure was also modified to remove errors present at low enzyme activities. The quoted linear range in the reference (Donoghue 1976) was found to result in a lower specific activity due to errors in the handling of small volumes when samples with high CHMO activities were assayed and the subsequent high factor multiplication. The method was therefore modified to use a minimum of 20 µL addition of enzyme preparation which was found to eliminate this error (Figure 4.1). This could have been caused by protein adhering to the pipette tips and the proportionally larger contribution of the background oxidation of NADPH.

The method was further modified to take into account an initial rapid oxidation of some of the NADPH. It was found that upon addition of the enzyme to the assay mix the initial rate of background NADPH oxidation slowed to a steady state (Figure 4.2). The original Donoghue method detailed determinations of background and CHMO stimulated NADPH oxidation from separate assays. Allowing the background oxidation to stabilise before the addition of cyclohexanone allowed a more reproducible and accurate background measurement.

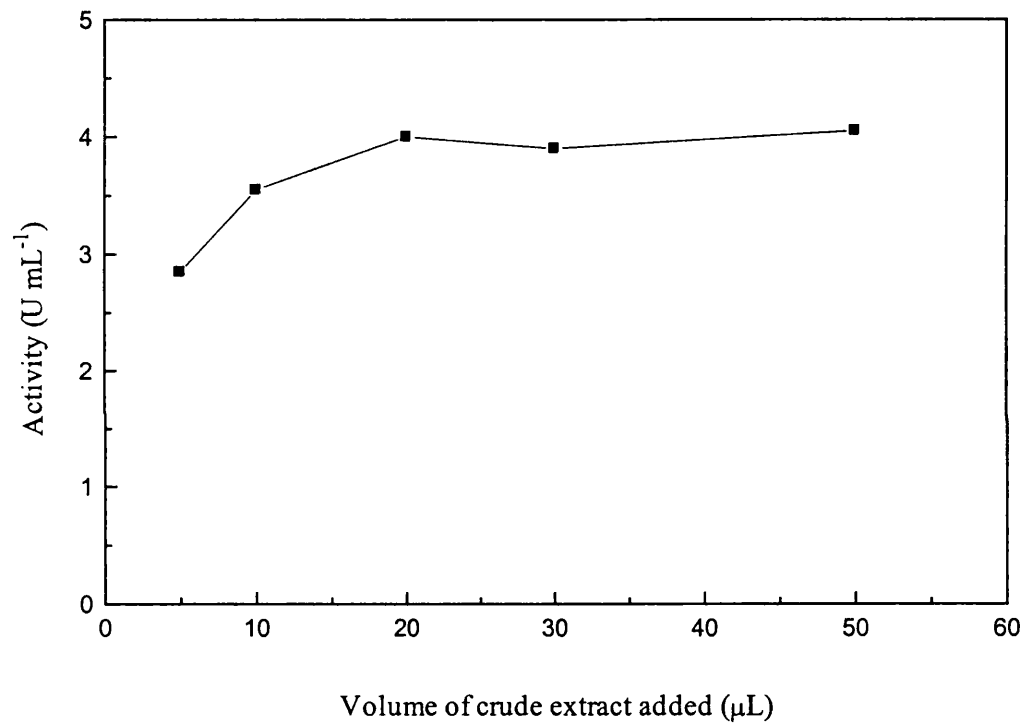


Figure 4.1: Errors at low volume handling of enzyme preparation. This figure illustrates how the activity of crude extract appeared lower when smaller volumes were added.

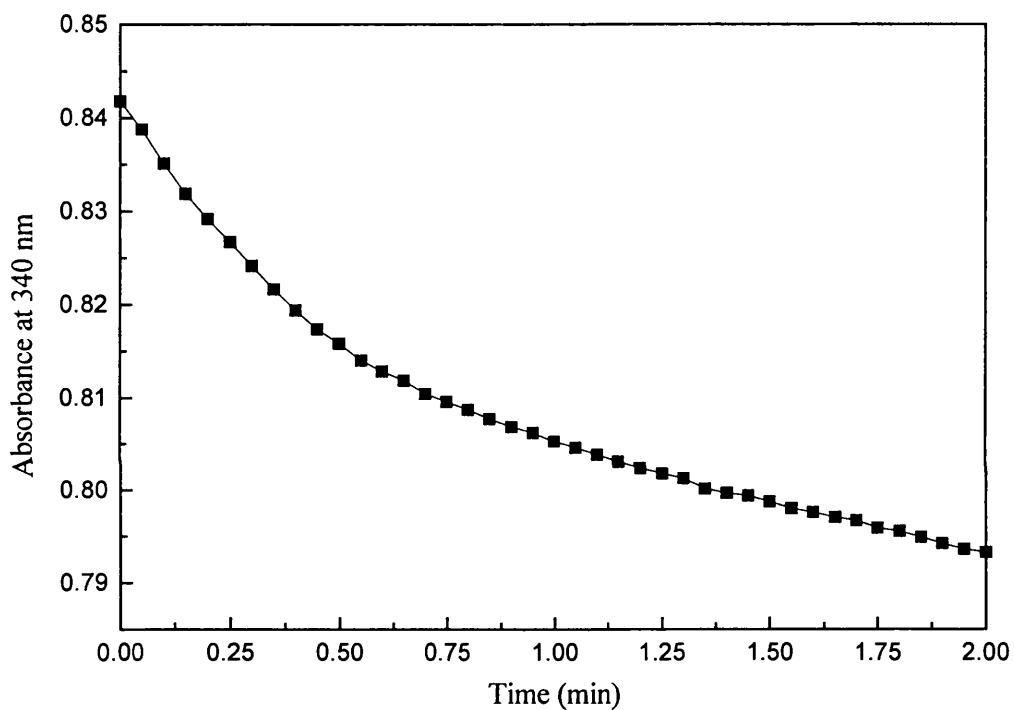


Figure 4.2: Initial rate of background NADPH oxidation in CHMO activity assay. This graph illustrates the rapid initial oxidation of NADPH (0-0.75 min), and the subsequent steady background rate. Background oxidation was therefore measured between one and two minutes, and the assay subsequently started by the addition of CHMO.

It was demonstrated that this assay allowed quantitative measurement of CHMO activity between 0.01 U and 0.2 U. Below 0.01 U the background oxidation became significant and above 0.2 U the rate of NADPH oxidation was too rapid to follow accurately.

4.2 Growth of *Acinetobacter calcoaceticus*

4.2.1 Growth on cyclohexanol

The *Neisseriaceae* family of bacteria are known to grow poorly if at all with hexose sugars as their sole carbon source but do grow well on acetate or pyruvate (Lautrop 1974).

Previous work on biotransformation using this organism describes the use of mainly washed cell suspensions (Carnell *et al.*, 1991; Alphand and Furstoss, 1990; Levitt *et al.*, 1990). This involves the growth of the organism in a minimal salts medium and the addition of cyclohexanol as the sole carbon source which causes the induction of the enzyme to facilitate growth.

When grown in a batch mode with an initial cyclohexanol concentration of 1 mL L⁻¹, the growth was poor producing an optical density of only about 2 absorbance units at 500 nm. The specific enzyme activity throughout the period of growth showed that the activity was greater at the late log stage of growth (Sandey, 1991). This means that unless the cells are harvested at the correct time i.e. 0.8 OD the productivity is low.

Cyclohexanol is known to be toxic to the organism (Sandey, 1991) so the concentration can not be increased above 1 mL L⁻¹. This leads to the possibility of a fed batch production where the concentration is maintained at a level to keep the growth in the log phase for a greater period. This should provide more cells and hence greater productivity from the fermentation.

Growth of *A. calcoaceticus* in shake flasks on minimal medium (section 3.5) with cyclohexanol (1 g L⁻¹) as the sole carbon and energy source was found to be very slow, typically taking 26 hours to reach an optical density of 0.9 at 670 nm (Table 4.1). This represents a dry cell weight concentration of 0.5 g L⁻¹ and a yield on cyclohexanol of 0.5 gdc g⁻¹.

Fermentation	OD	Dry cell weight
Shake flask 1	0.92	0.54
Shake flask 2	0.86	0.50
Shake flask 3	1.01	0.59

Table 4.1: Summary of growth of *A. calcoaceticus* in shake flasks. This table shows the results of three shake flask fermentations carried out under the same conditions.

A. calcoaceticus was then grown on the same minimal medium in a 2 L fermenter with regular additions of cyclohexanol to increase the biomass and hence the productivity of the fermentation (Figure 4.3). Due to the pathogenic nature of this organism SOP (standard operating procedures) were written to cover the safe handling of cultures (Appendix I). Growth was found to be similar to that in shake flasks ($\mu = 0.16 \text{ h}^{-1}$), with slightly lower optical density for the same addition of cyclohexanol. Due to the losses of the volatile cyclohexanol in the off gas (which was obvious from the distinctive odour) estimating yields is very difficult. The maximum OD achieved was ~ 5.5 after 55 h and a total addition of 10.5 g of cyclohexanol.

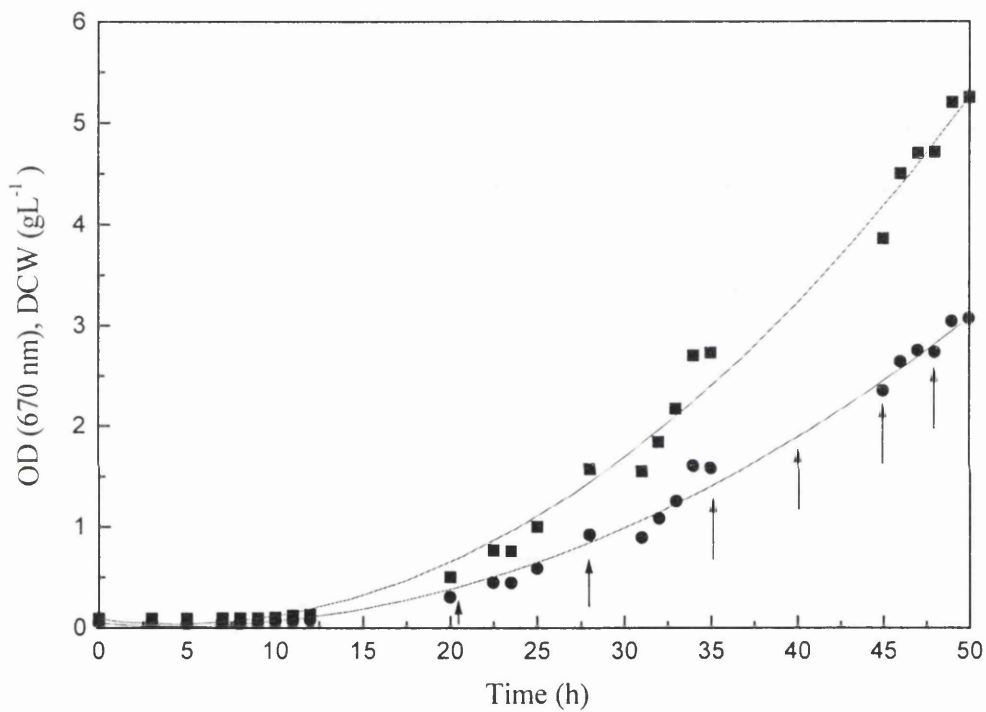


Figure 4.3: Biomass production in 2 L fed batch fermentation of *A. calcoaceticus* on cyclohexanol. This figure illustrates the growth of *A. calcoaceticus* under conditions as detailed in section 3.6.3 and shows optical density (■), dry cell weight (●), and the addition of 1.5 g cyclohexanol (↑).

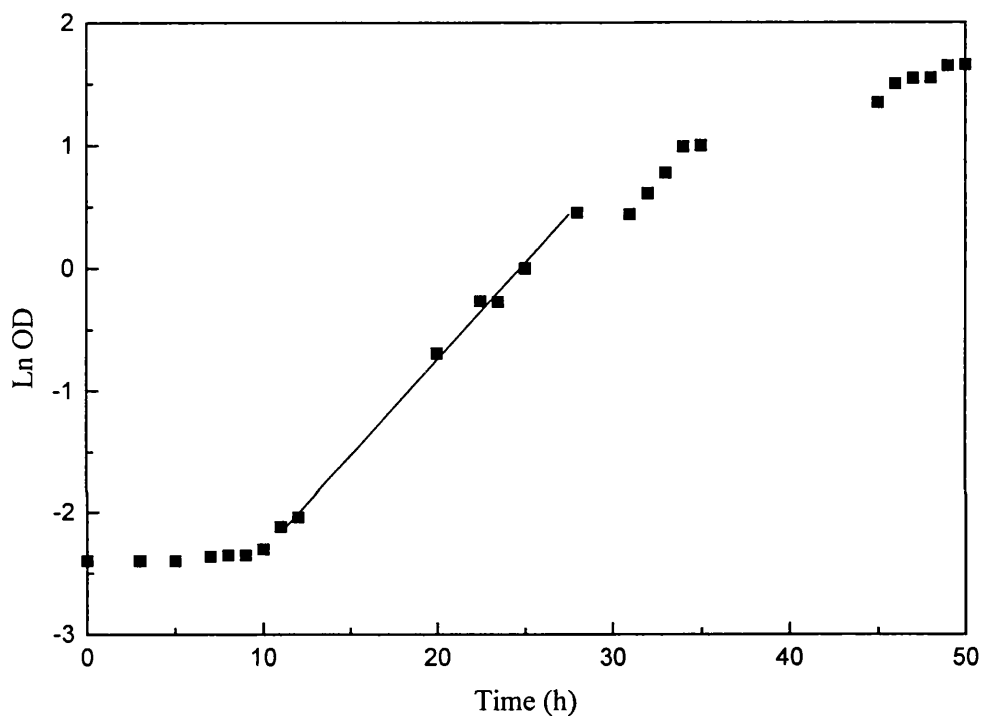


Figure 4.4 Biomass production in 2 L fed batch fermentation of *A. calcoaceticus* on cyclohexanol. This figure illustrates the growth of *A. calcoaceticus* under conditions as detailed in section 3.6.3 and shows the growth rate during exponential phase (gradient = 0.16 h^{-1}) calculated from ln OD (■).

4.2.2 Production of biomass on sodium succinate

Growth of *A. calcoaceticus* on cyclohexanol was slow, required regular feeding and produced only 3 g L⁻¹ dry cell weight. It was therefore decided to separate the production of the biocatalyst into two distinct operations; biomass production and induction of the required enzyme.

It was known that *A. calcoaceticus* could utilise succinate (Sandey 1991) as a carbon source but that the cells would not produce monooxygenase. Succinate was therefore chosen as a growth substrate for the biomass production. Figures 4.5 and 4.6 show a typical batch fermentation with 10 g L⁻¹ sodium succinate. The growth rate was increased to approximately 0.22 h⁻¹ (this figure requires significant interpolation due to missing data) and the 9 hour lag at the beginning of the fermentation was removed.

There was little improvement in the maximum achievable biomass due to problems with excessive foaming when sufficient succinate was added to give greater than 4 g L⁻¹ biomass. Succinate was therefore abandoned as a carbon source and monosodium glutamate was investigated.

4.2.3 Production of biomass on glutamate

Shake flask experiments showed that glutamate was a good substrate for growth and a batch fermentation to determine the maximum biomass achievable was performed. Figures 4.7 and 4.8 show a typical fermentation with 30 g L⁻¹ glutamate. *A. calcoaceticus* grew on glutamate with a maximum growth rate of 0.44 h⁻¹, which was approximately double the growth rate on succinate and therefore an important advantage to process time and therefore cost. A maximum biomass concentration of 14 g L⁻¹ was achieved which gives a yield on glutamate of 0.47 gdc g⁻¹.

Production of CHMO was then attempted by the addition of cyclohexanol to the fermentation when the glutamate was exhausted as shown by the decrease in growth rate. While this was not proven by chemical analysis but the level of nutrients and nitrogen in the medium had been shown to support greater biomass. No activity could be detected up to 5 hours after the addition of the cyclohexanol.

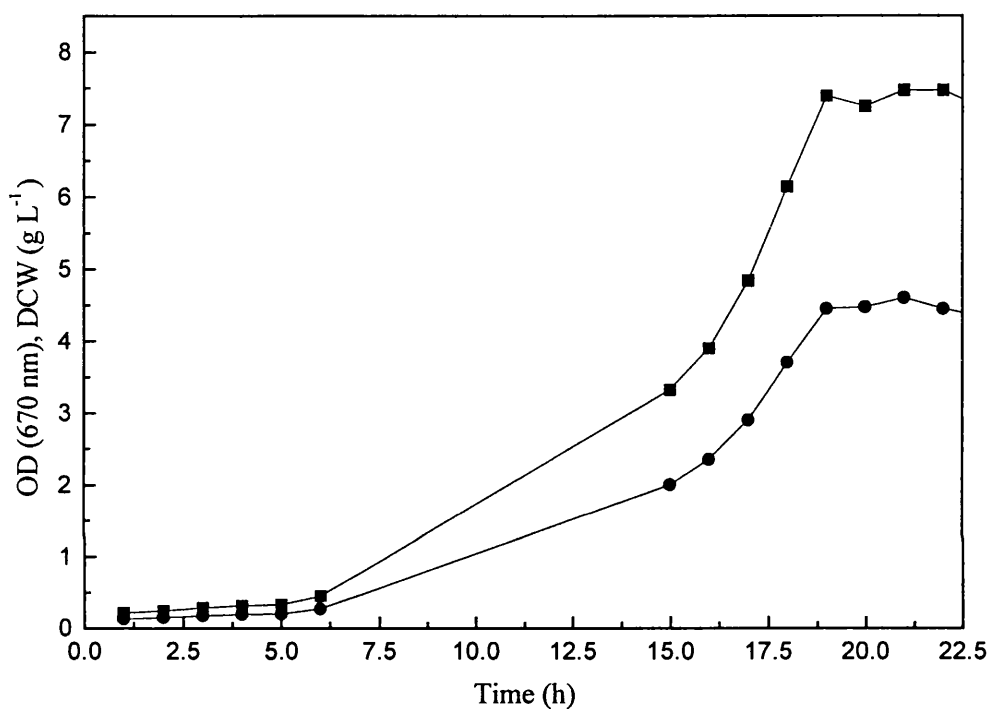


Figure 4.5: Biomass production in 2 L batch fermentation of *A. calcoaceticus* on succinate. This figure illustrates the growth of *A. calcoaceticus* under conditions as detailed in section 3.6.3 and illustrates optical density (■) and dry cell weight (●) measured as detailed in section 3.1.1.

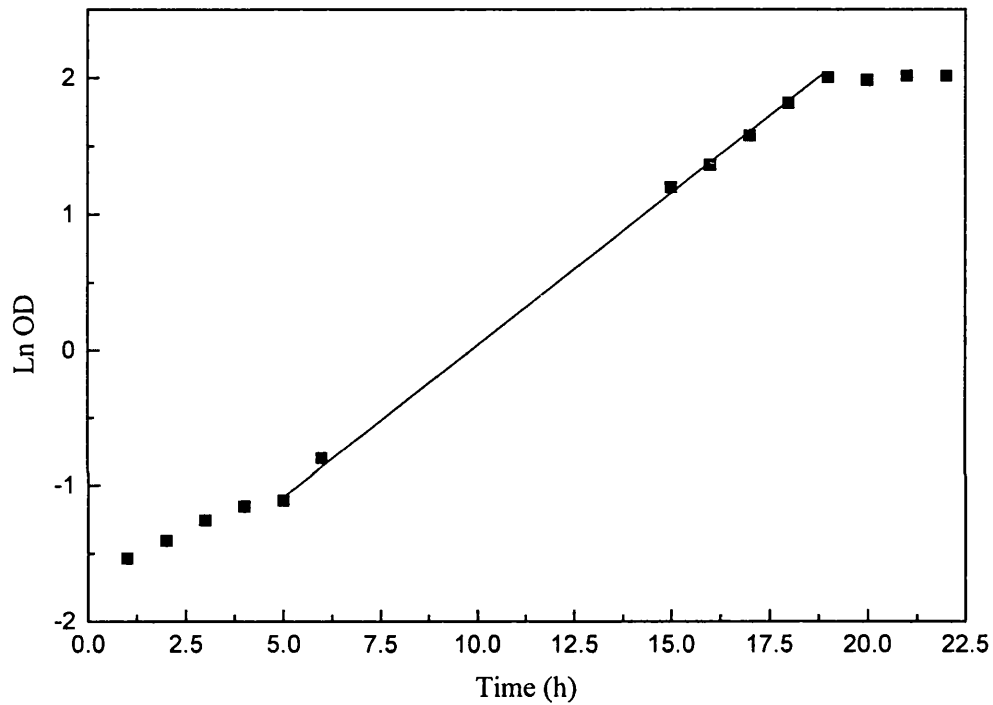


Figure 4.6 Biomass production in 2 L batch fermentation of *A. calcoaceticus* on succinate. This figure illustrates the growth of *A. calcoaceticus* under conditions as detailed in section 3.6.3 and shows the growth rate during exponential phase (gradient = 0.22 h^{-1}) calculated from Ln OD (■)..

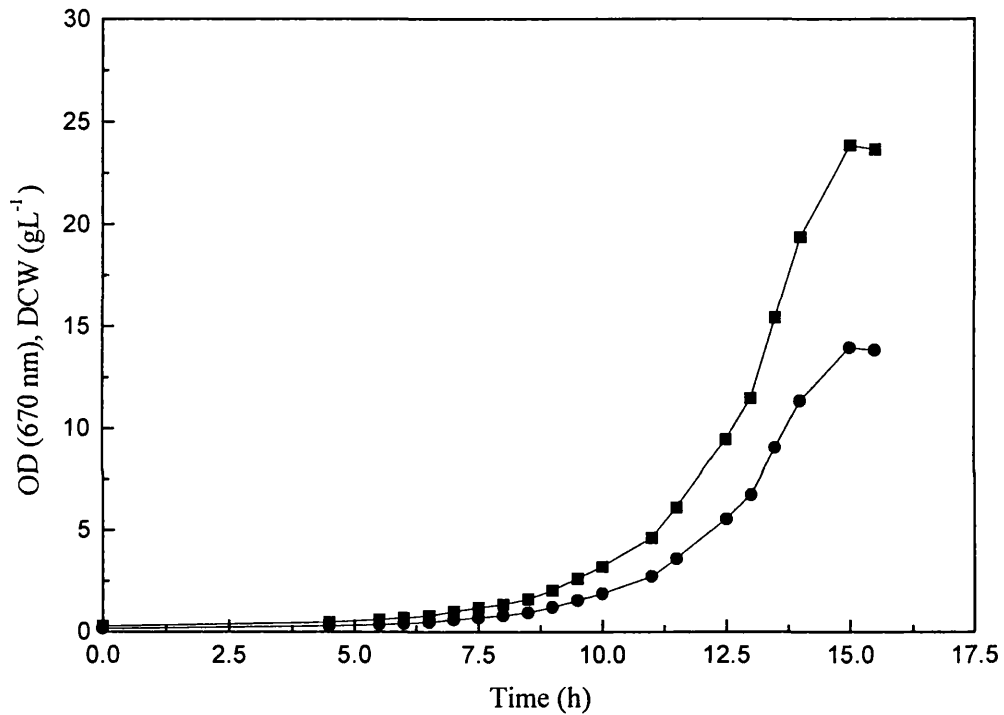


Figure 4.7: Biomass production in 2L batch fermentation of *A. calcoaceticus* on glutamate. This figure illustrates the growth of *A. calcoaceticus* under conditions as detailed in section 3.6.3 and illustrates optical density (■) and dry cell weight (●) measured as detailed in section 3.1.1.

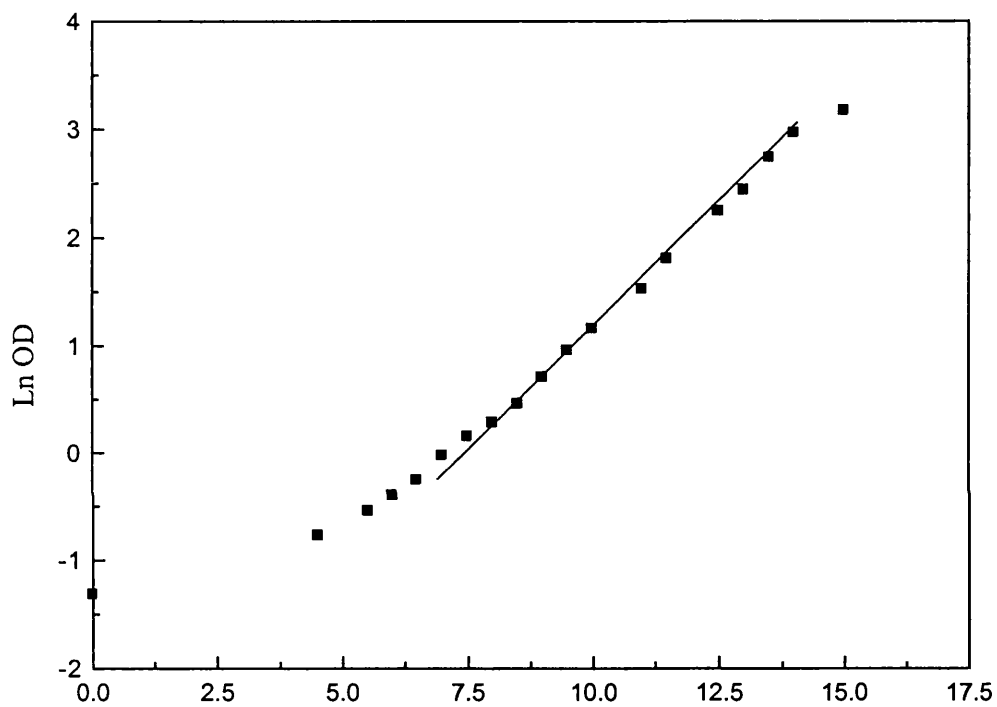


Figure 4.8: Biomass production in 2L batch fermentation of *A. calcoaceticus* on glutamate. This figure illustrates the growth of *A. calcoaceticus* under conditions as detailed in section 3.6.3 and shows the growth rate during exponential phase (\blacktriangle gradient = 0.44 h^{-1}), calculated from ln OD (\blacksquare).

4.2.4 Diauxic growth investigation

The lack of activity when cyclohexanol was added to the glutamate fermentation (4.2.3) was not expected. The effect of cyclohexanol present as a co-substrate from the beginning of the fermentation was investigated. It was discovered that cells grown exclusively on glutamate did not produce CHMO when cyclohexanol was added. Table 4.2 shows that CHMO activity can only be induced when the cells have been grown with cyclohexanol present at the start of the fermentation. Cells grown on glutamate alone appear to lose the ability to later produce CHMO when the inducing substrate, cyclohexanol, is added at a later stage. For further fermentations cyclohexanol was therefore added (1 g L^{-1}) from the beginning of the fermentation.

Carbon source	Specific Activity (U gdc^{-1})	Biomass (gdc L^{-1})
Cyclohexanol	25	1
Glutamate	0	2.5
Glutamate + Cyclohexanol	17	2.1

Table 4.2: Effect of cyclohexanol as co-growth substrate on CHMO production.

4.2.5 Production of CHMO

This development led to the addition of 1 g L^{-1} cyclohexanol to the fermentation medium. There was distinct evidence of diauxic growth as shown by Figures 4.9 and 4.11, with the cyclohexanol being used in preference to the glutamate. At the end of growth on cyclohexanol, metabolism is switched over to glutamate, clearly indicated by the change in RQ from 0.6 to 1.3 and back to 0.6. The two fermentations showed good agreement. In both cases the oxygen demand exceeded the maximum that the vessel could supply (DOT reaches 0) for the last 45 min of growth on glutamate each fermentation. The growth rate on glutamate is 0.42 h^{-1} as expected from previous

experiments when calculated from OD measurements. The yields on glutamate were both 0.5 gdc g^{-1} .

When the glutamate is exhausted production of CHMO is induced by switching the metabolism back to the cyclohexanol pathway by the addition of sufficient cyclohexanol to give a concentration of 1 g L^{-1} in the case of Figure 4.9 and 2 g L^{-1} in Figure 4.11. The difference in the metabolism can be seen by the difference in area under the OUR and CER curves for the two fermentations. When the greater amount cyclohexanol was added, the level of CHMO was slightly lower.

The activity profiles for each fermentation (Figures 4.10 and 4.12) show the rapid production of monooxygenase and then the equally rapid decline once the cyclohexanol substrate is exhausted. When further additions of cyclohexanol were added after the cyclohexanol was consumed and DOT began to rise the decline in activity was not evident. The level of activity was however never increased above the first maximum.

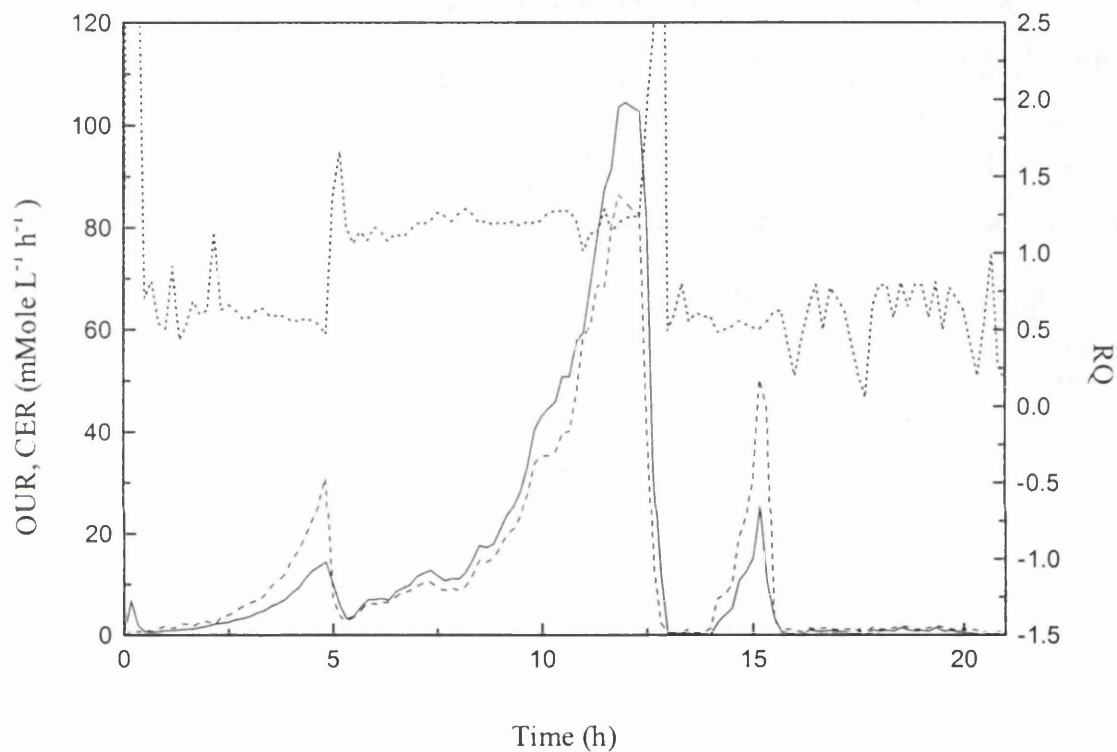


Figure 4.9: Fermentation profile for 7 L batch fermentation of *A. calcoaceticus*. This figure shows the growth of *A. calcoaceticus* under conditions as detailed in section 3.6.3 and illustrates the change in carbon source utilisation from cyclohexanol to glutamate (5 h) and back again (12.5 h) as shown by the changes in OUR (---), CER (—), and RQ (.....).

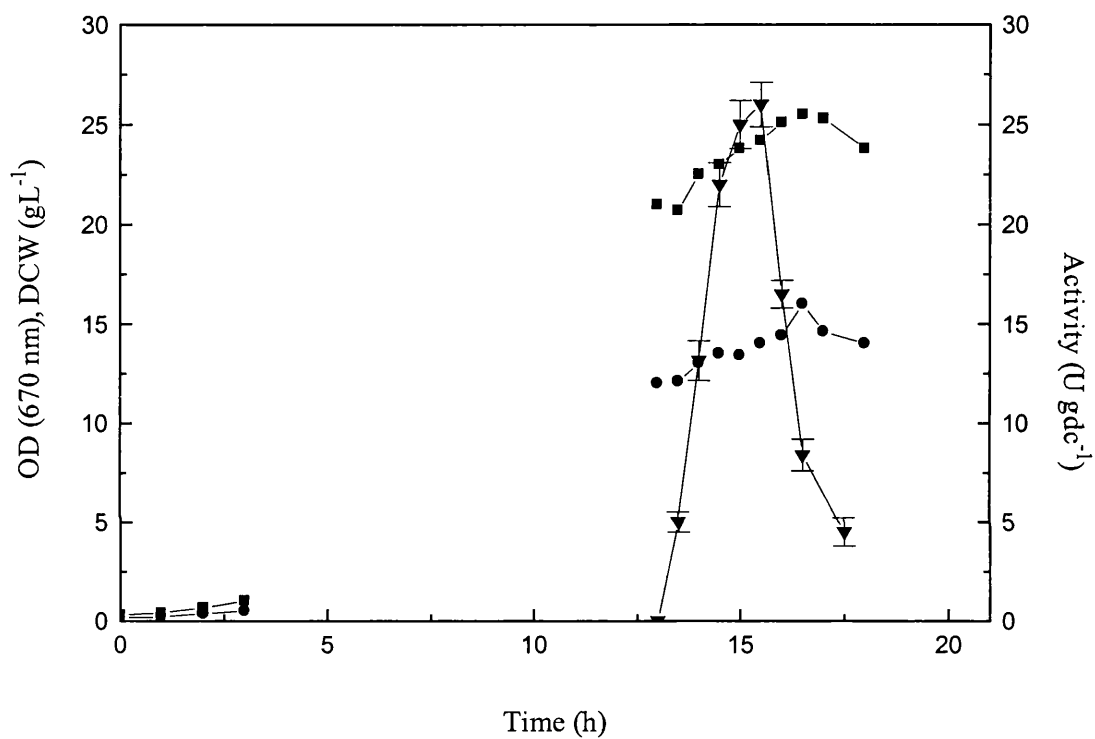


Figure 4.10: Productivity of 7L batch fermentation of *A. calcoaceticus*. This figure illustrates the production of active CHMO for the fermentation described by figure 4.9. The rise and fall in the specific CHMO activity (▼) of crude cell homogenate is closely correlated to the metabolim of cyclohexanol. The growth is shown by OD (■) and dry cell weight (●).

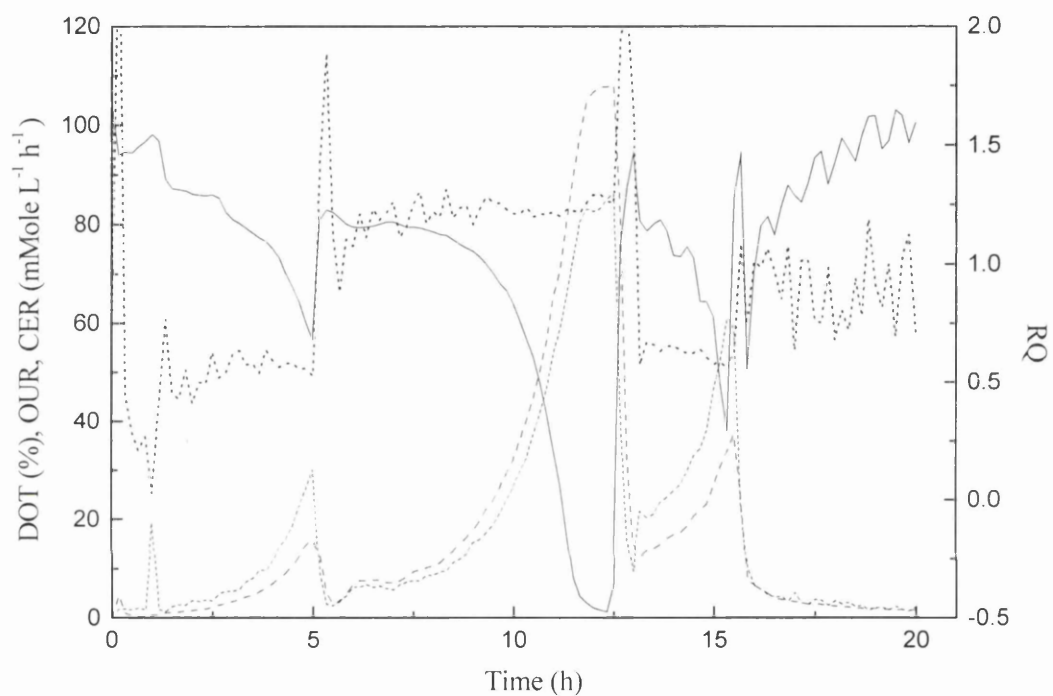


Figure 4.11: Fermentation profile for 7 L batch fermentation of *A. calcoaceticus*. This figure shows the growth of *A. calcoaceticus* under conditions as detailed in section 3.6.3 and illustrates the change in carbon source utilisation from cyclohexanol to glutamate (6 h) and back again (13 h) as shown by the changes in OUR (---), CER (—), and RQ (.....).

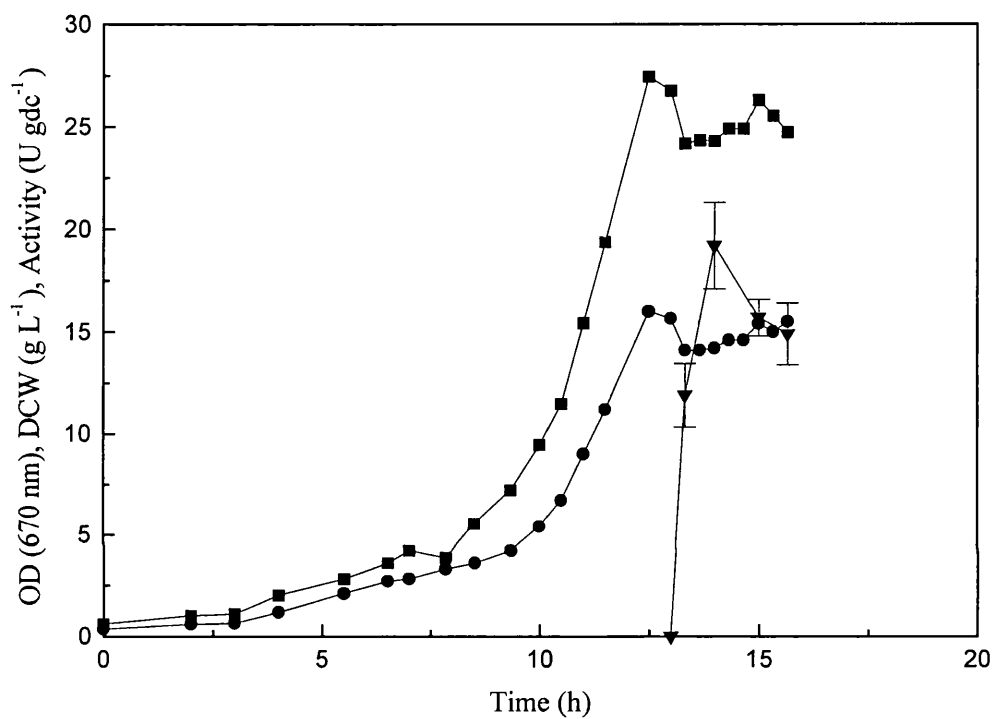


Figure 4.12: Productivity of 7L batch fermentation of *A. calcoaceticus*. This figure illustrates the production of active CHMO for the fermentation described by figure 4.11. The rise and fall in the specific CHMO activity (▼) of crude cell homogenate is closely correlated to the metabolim of cyclohexanol. The growth is shown by OD (■) and dry cell weight (●).

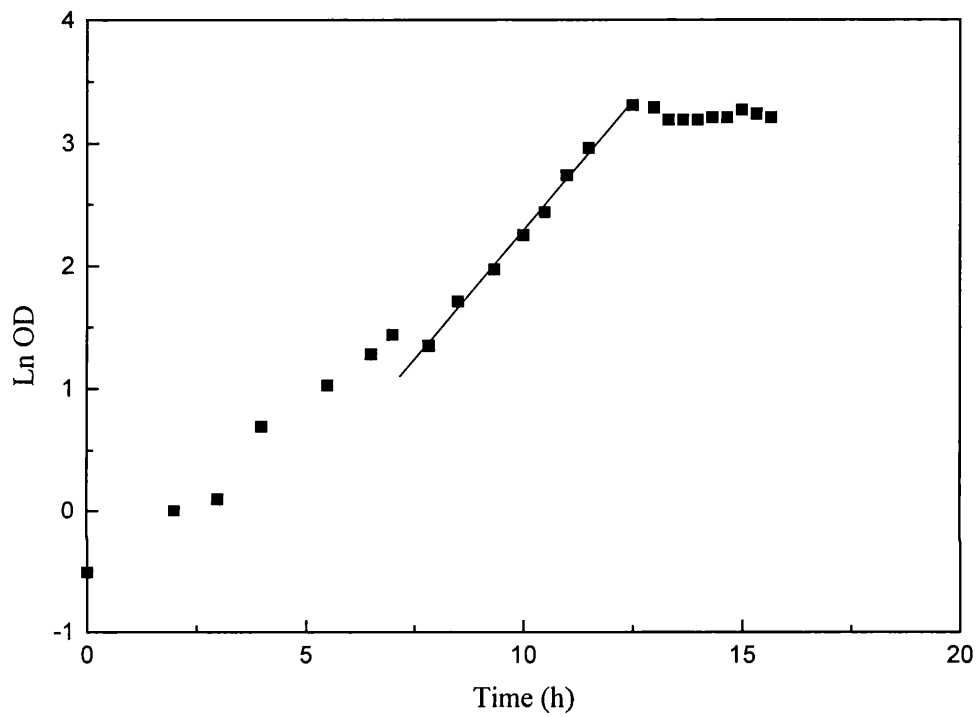


Figure 4.13: Productivity of 7 L batch fermentation of *A. calcoaceticus*. This figure illustrates the growth of *A. calcoaceticus* under conditions as detailed in section 3.6.3 and shows the growth rate during exponential phase (Δ gradient = 0.42 h^{-1}), calculated from ln OD (■).

4.3 Growth of *Escherichia coli* JM107/pQR210

4.3.1 Carbon source investigation

A recombinant *E. coli* strain containing a plasmid pQR210 with the CHMO gene from *A. calcoaceticus* was constructed (section 3.3). The gene was under the control of a tac promoter and was thus induced by the addition of IPTG to the culture. Shake flask experiments to assess the levels of CHMO expression in the recombinant *E. coli* strain JM107/pQR210 were performed. The construct was found to express active CHMO when grown on a proprietary nutrient complex medium (50 U gdc^{-1}). This medium contains some glucose which is known to repress the tac promoter so a complex medium (medium 1, table 3.3) with glycerol as the sole carbon source was used. The specific CHMO activity (330 U gdc^{-1}) was found to be increased six fold (Figure 4.14).

4.3.2 IPTG concentration investigation

Isopropyl thiogalactopyranoside (IPTG) is used to induce the expression of genes under the control of lac/tac promoters. It is however expensive to use and so the minimum required concentration for maximum expression should be used. Flasks with medium 1 were inoculated with an aliquot from a growing culture and incubated and monitored under the usual conditions.

After 6 hours varying amounts of IPTG were added and samples taken for analysis at intervals. Figure 4.15 shows that there is no significant difference between the induction of CHMO when the concentration of IPTG is 0.25 mM and above. It is interesting to note the apparent interruption to growth as the IPTG was added presumably as metabolism changed to produce CHMO. There was a lag of 80 minutes before CHMO activity could be detected and production of CHMO increased as the growth rate picked up once again. The specific activity reached a maximum of between 180 and 230 U g^{-1} dry cells 4 hours after addition of IPTG.

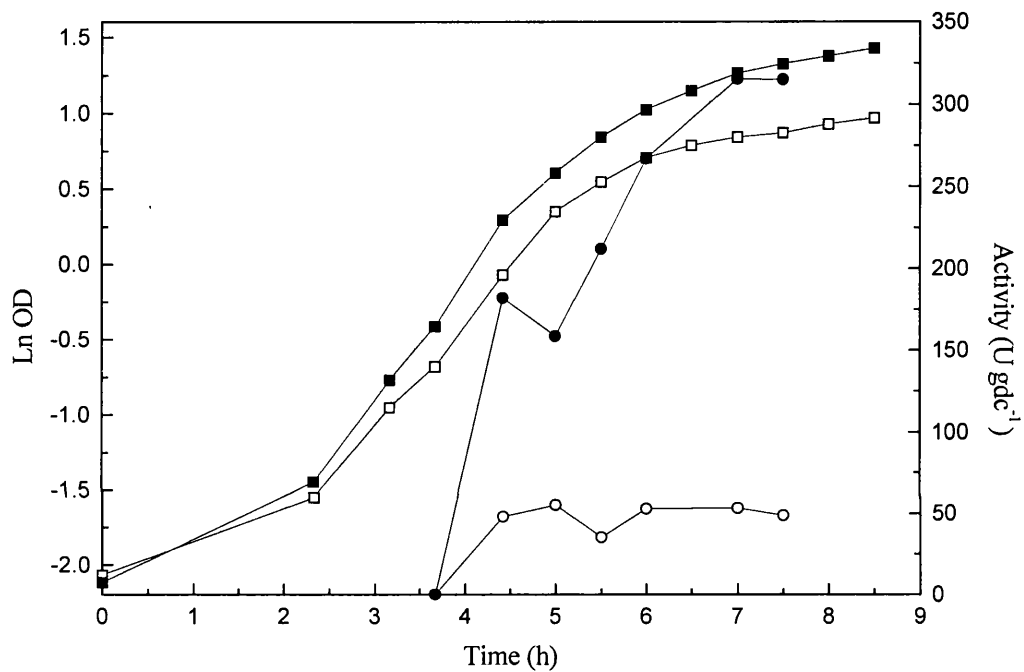


Figure 4.14: Expression of CHMO in recombinant *E. coli* in shake flasks. This figure shows the growth of *E. coli*, $\ln OD$ (■), and the specific CHMO activity (●) of crude homogenates, when grown on proprietary complex medium (open symbols) and medium 1 (closed symbols).

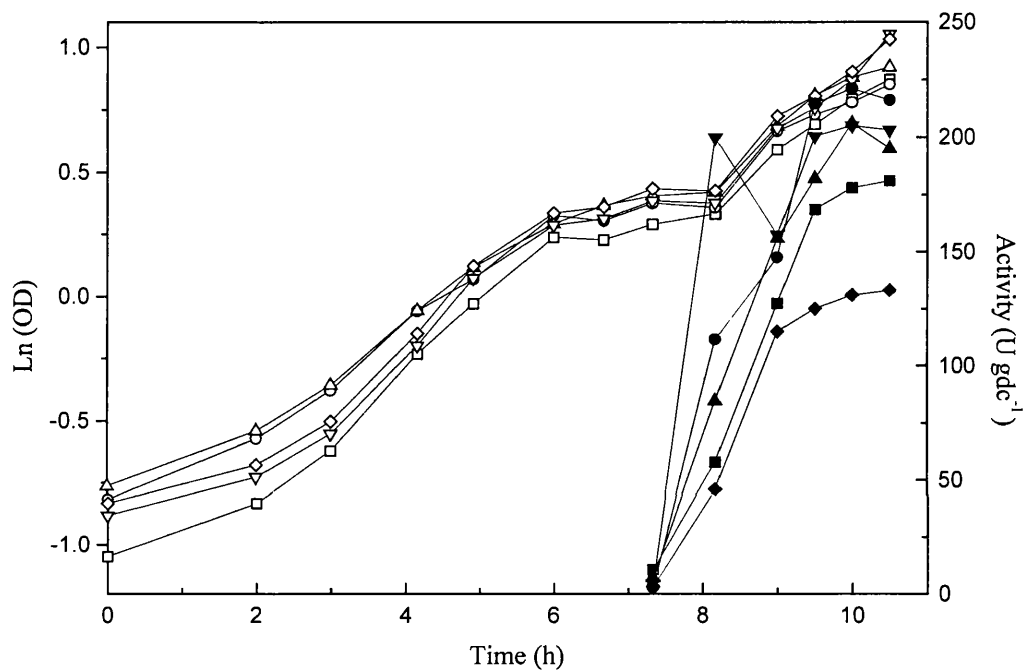


Figure 4.15: Effect of IPTG concentration on CHMO induction in shake flasks. This figure illustrates \ln OD (open symbols) and specific CHMO activity (closed symbols) for IPTG concentrations of 2 mM (■), 1 mM (●), 0.5 mM (▲), 0.25 mM (▼), and 0.1 mM (◆) added after 6 hours. No activity could be detected in fermentations where no IPTG was added. Error bars are omitted for clarity but were typically 5 to 8 %.

4.3.3 Plasmid retention during shake flasks fermentations

There are two main factors that could have affected the productivity when grown on defined medium. Protein expression could have been lower due to a lack of some nutrient or the loss of the plasmid from some of the cells. Cells that have lost the plasmid containing the CHMO gene will not produce the desired protein.

Plasmid stability is therefore vital to a highly productive fermentation. Table 4.3 illustrates the plasmid retention which was determined as described in section 3.7.5. The results show that the plasmid displayed good stability in shake flasks and are therefore likely to be of sufficient stability for fermenter growth.

Flask	Complex Medium 1			Defined Medium 3		
	6 h (%)	10 h (%)	22 h (%)	6 h (%)	12 h (%)	22 h (%)
1	99	99	95	100	98	94
2	100	100	97	99	97	88
3	98	97	94	96	98	91

Table 4.3: Plasmid stability of *E. coli* JM107/pQR210 in shake flasks.

4.3.4 Growth on complex medium

From these experiments the fermentation was scaled up to 7 L (5 L working volume) with 15 g L⁻¹ glycerol (medium 2, section 3.7.1) to find the growth and CHMO induction profile characteristics (Figure 4.16). The induction of CHMO was achieved by the addition of sufficient IPTG to give a final concentration of 0.5 mM.

A dry cell weight concentration of 7 g L⁻¹ (Figure 4.17) was achieved with a growth rate of 0.7 h⁻¹ giving a yield of ~ 0.5 g dry cells g⁻¹ glycerol. The values for OUR and CER are higher than previously achieved due to increased pressure within the vessel

caused by a partial blockage of the outlet filter by condensation of water in the off-gas. This allowed a greater cell concentration to be achieved before the fermentation conditions became oxygen limiting than would otherwise have been possible. Growth on this complex medium produced a large amount of foam that required large additions of antifoam.

CHMO production was induced after 3.5 hours when growth was exponential with a maximum specific enzyme activity of 800 U g^{-1} dry cells, two hours after induction. This is over twice the activity that was found in shake flasks most likely due to the increased mass transfer in the fermenter allowing more optimal metabolism.

This was investigated by repeating the fermentation with 30 g L^{-1} glycerol and with induction after 6 hours; the culture becoming oxygen limited during the production of CHMO (Figures 4.19 and 4.20).

The fermentation profile shows good agreement with the previous fermentation although there is less of a lag before exponential growth phase. The growth rate and the expression of CHMO is reduced (280 U gdc^{-1}) as the culture becomes oxygen limited. The dissolved oxygen tension during this period fell to 3 % with the gas flow rate at 1 v v^{-1} and the stirrer speed at 1100 rpm, the maximum for the vessel.

It was therefore important that subsequent fermentations be induced before any oxygen limitation.

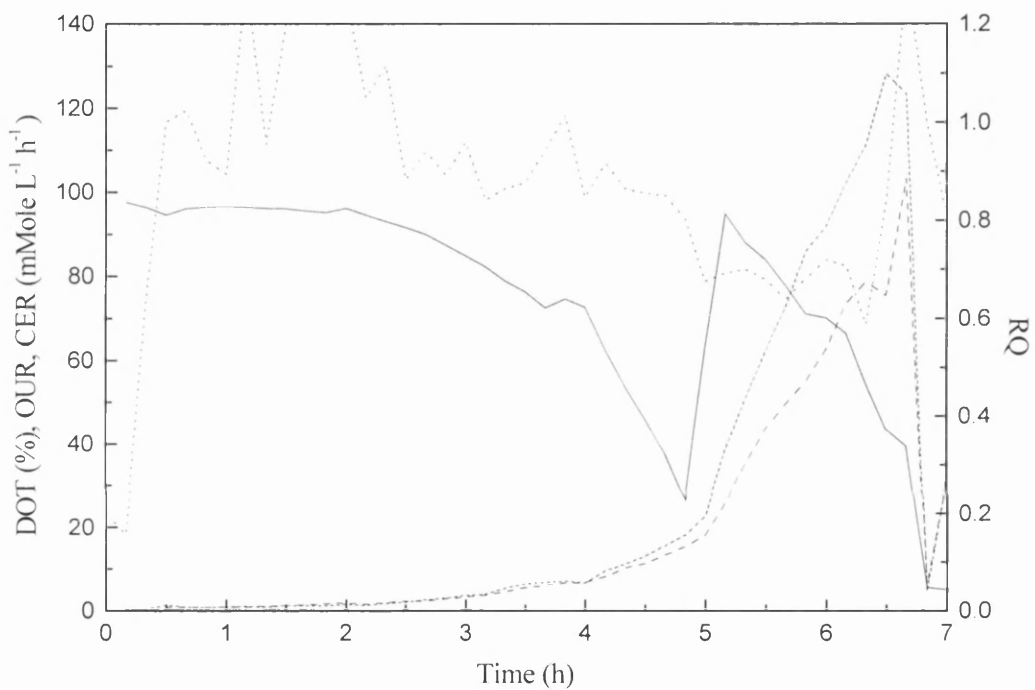


Figure 4.16: Fermentation profile for 7 L batch fermentation of *E. coli* JM107/pQR210 on complex medium. This figure shows the growth of *E. coli* as detailed in section 3.7.3 and illustrates the change in OUR (----), CER (---), DOT (—), and RQ (— · —) as the fermentation proceeds.

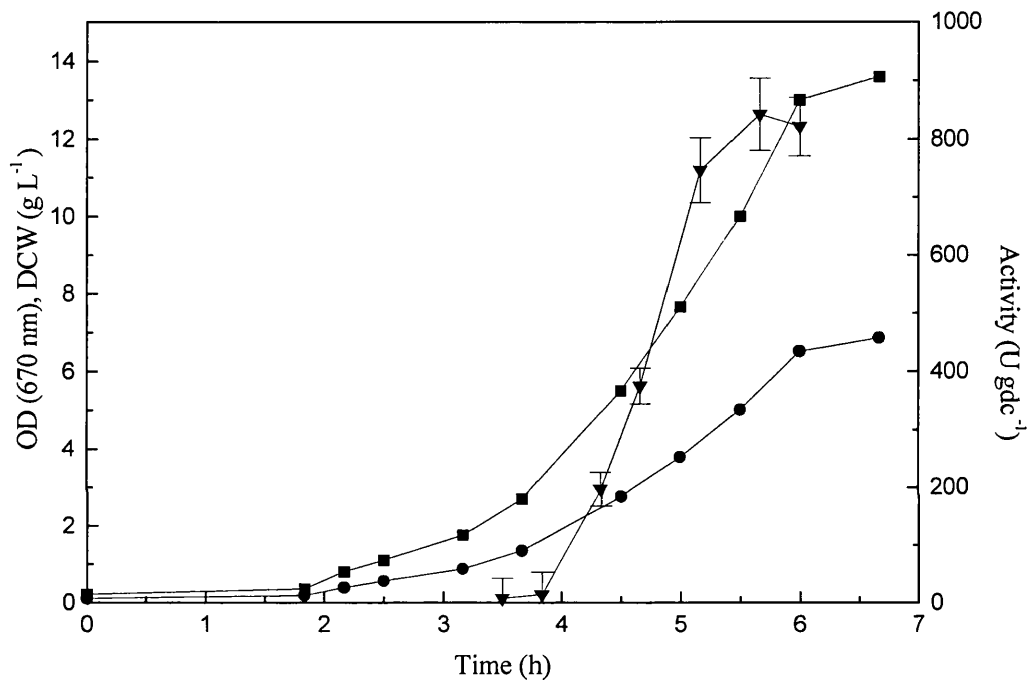


Figure 4.17: Productivity of 7 L batch fermentation of *E. coli* JM107/pQR210. This figure illustrates the production of active CHMO for the fermentation described by figure 4.17 as illustrated by OD (■), dry cell weight (●) and specific CHMO activity (▼).

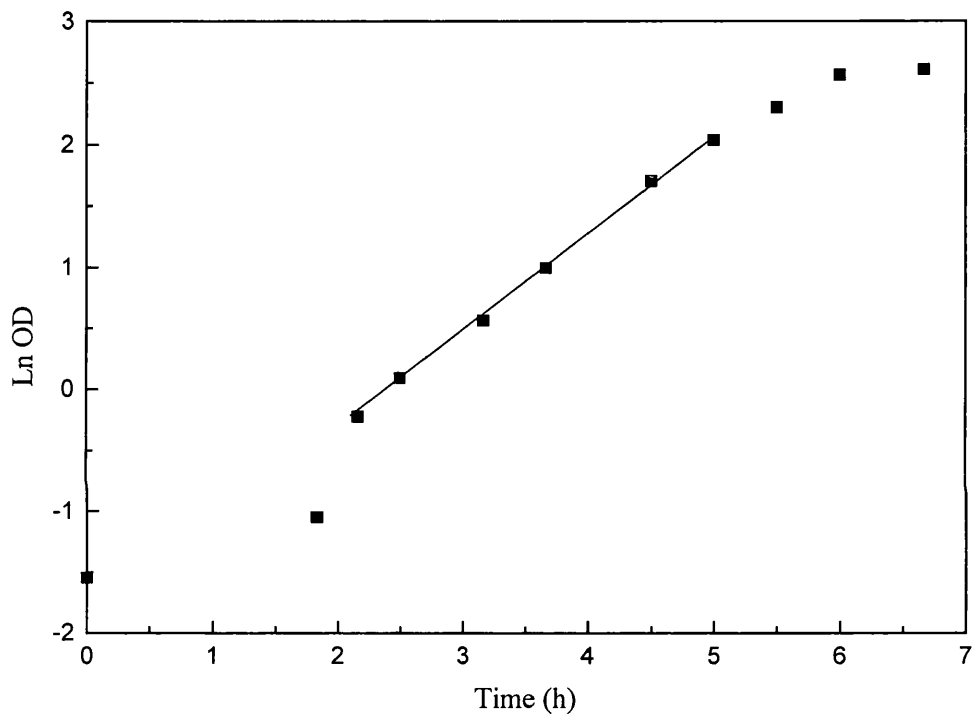


Figure 4.18: Productivity of 7 L batch fermentation of JM107/pQR210. This figure shows the growth of *E. coli* as described by figures 4.16 and 4.17 and shows the growth rate during exponential phase (\blacktriangle gradient = 0.70 h^{-1}) calculated from ln OD (\blacksquare).

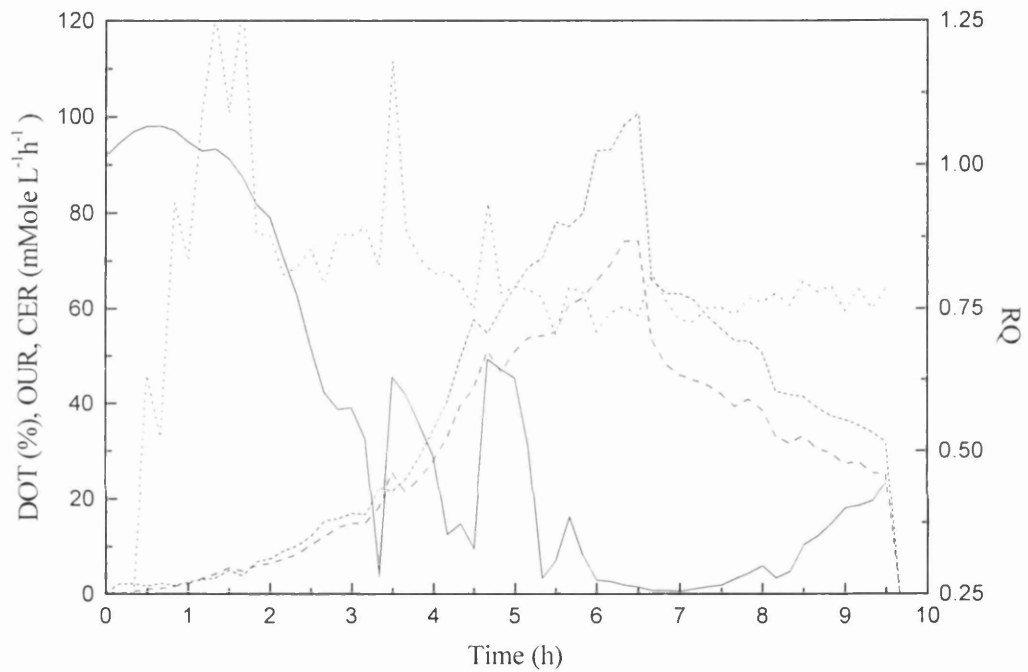


Figure 4.19: Fermentation profile for 7 L batch fermentation of JM107/pQR210 with oxygen limitation. This figure shows the growth of *E. coli* as detailed in section 3.7.3 and illustrates the change in OUR (----), CER (---), DOT (—), and RQ (— · —) as the fermentation proceeds.

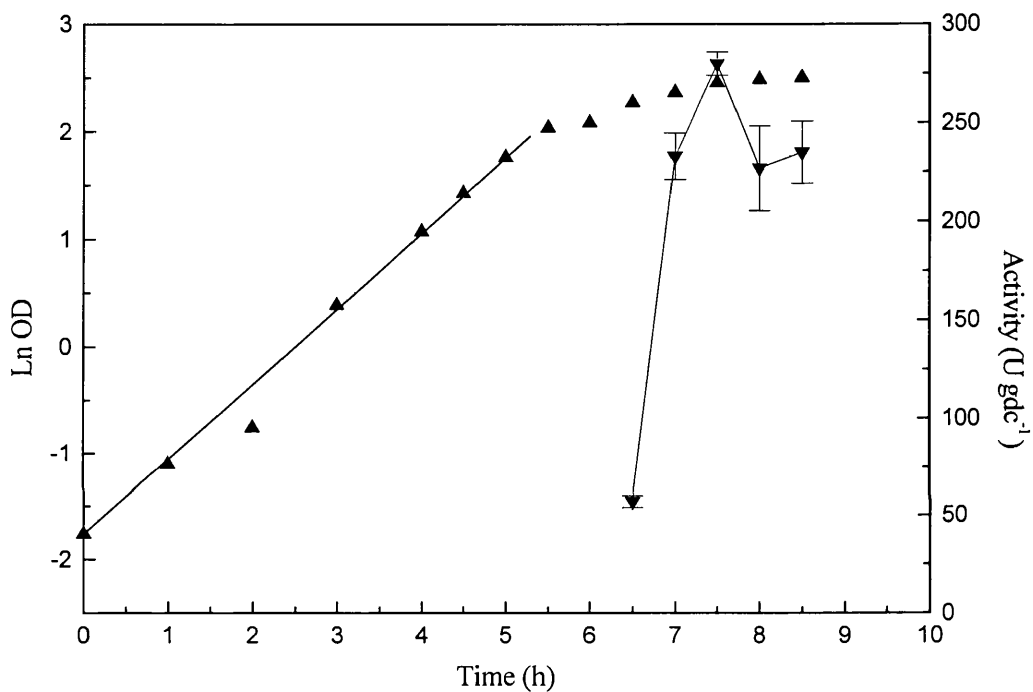


Figure 4.20: Productivity of 7 L batch fermentation of JM107/pQR210 with oxygen limitation. This figure illustrates the production of active CHMO for the fermentation described by figure 4.19 as illustrated by the specific CHMO activity (▼) and constant growth rate calculated from dry cell weight calculations (▲ gradient = 0.71 h⁻¹).

4.3.5 Growth on defined medium

Defined minimal media are preferred for industrial fermentations so it was considered necessary to examine any changes that such a medium may have on productivity. A defined medium would also allow the implementation of a fed batch regime to increase maximum cell density and hence productivity, without the foaming problems encountered with a complex proteinaceous medium.

A defined medium was chosen (media 3-6, section 3.7.1) that was known to be a good medium for this strain of *E. coli* (Hobbs *et al.* 1996).

To maximise productivity from the fermentation it would be necessary to grow the cells to the highest cell concentration possible. This would require a fed batch regime since dissolved oxygen concentration has been shown to be an important factor in the expression of CHMO. The growth rate can be controlled so as not to exceed the oxygen transfer capabilities of the fermenter.

Initial experiments used medium 6 (section 3.7.1) with 15 g L⁻¹ glycerol so as to gain data that would be required for future fed batch fermentations.

Figure 4.21 shows a typical fermentation profile. The growth rate was significantly lower ($\mu = 0.43 \text{ h}^{-1}$) than with a complex medium. The growth rate estimated from the natural logarithm of OUR and CER was 0.47 h^{-1} which showed good agreement with that taken from OD measurements.

The culture grew to a dry cell weight of 7 g L⁻¹, (Figures 4.22 and 4.23) with a yield on glycerol of 0.47 g g⁻¹. These data were used to control fed batch fermentations using the algorithms outlined in section 3.7.4.

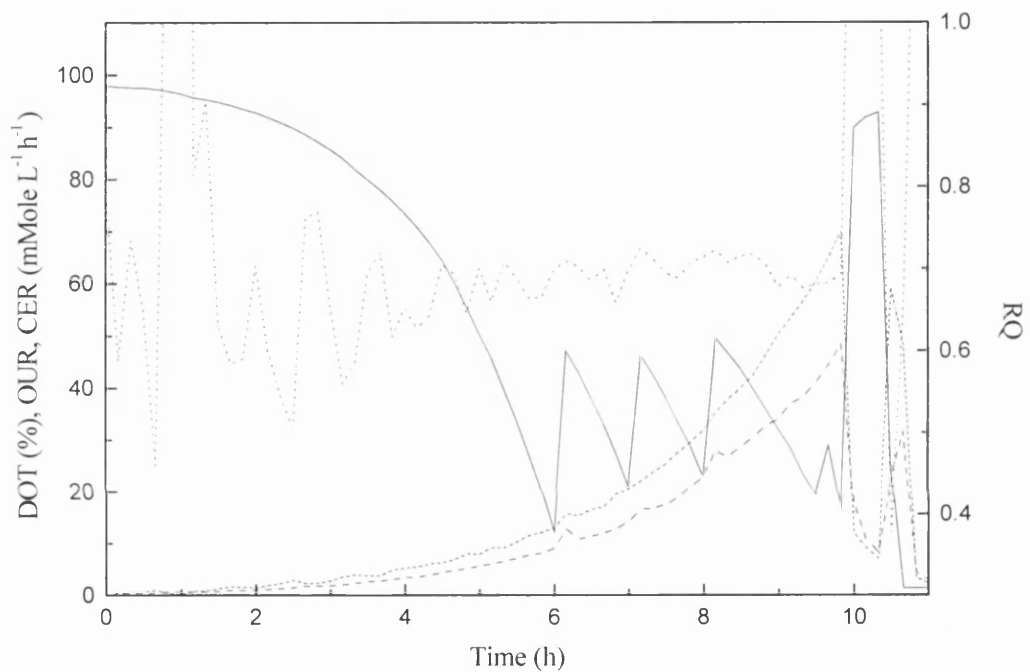


Figure 4.21: Fermentation profile for 7 L batch fermentation of *E. coli* JM107/pQR210 on defined medium. This figure shows the growth of *E. coli* as detailed in section 3.7.3 and illustrates the change in OUR (----), CER (---), DOT (—), and RQ (— · —) as the fermentation proceeds.

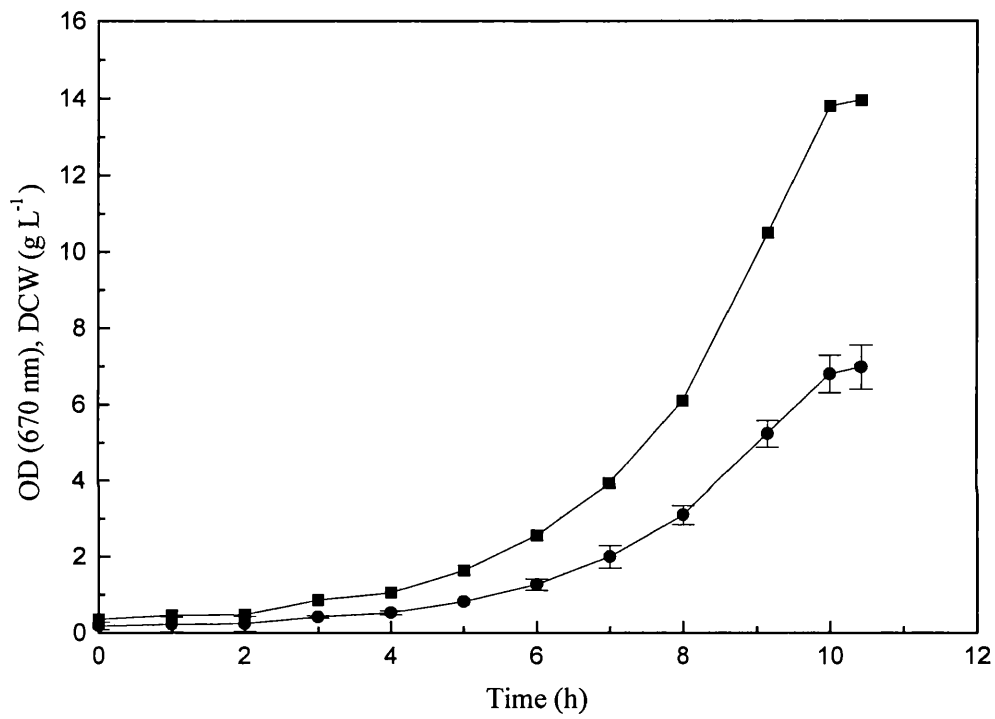


Figure 4.22: Biomass production in 2L batch fermentation of JM107/pQR210 on defined medium. This figure illustrates the growth of *E. coli* as described in figure 4.21 and illustrates optical density (■) and dry cell weight (●) measured as detailed in section 3.1.1

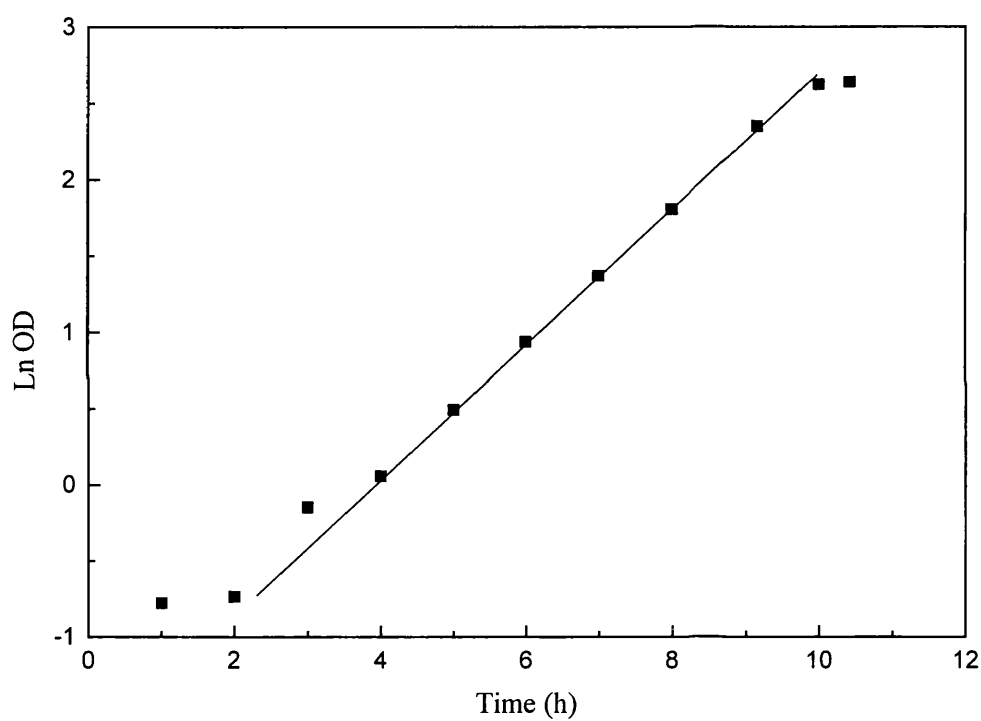


Figure 4.23: Biomass production in 7 L batch fermentation of JM107/pQR210 on defined medium. This figure illustrates the growth of *E. coli* under conditions as described by figures 4.21 and 4.22 and shows the growth rate during exponential phase (■ gradient = 0.43 h^{-1}).

4.4 Induction of cyclohexanone monooxygenase

4.4.1 Batch fermentation

As previously mentioned any effects of the defined medium on the productivity of the fermentation must be investigated. Figures 4.24 to 4.29 show 7 L batch fermentations with medium 4 (15 g L⁻¹ glycerol) with induction of CHMO after 8 and 10 hours respectively. The fermentation profile matches the previous experiment although there is a longer lag (2 h) before the exponential growth phase. The growth rates were 0.44 h⁻¹ and 0.43 h⁻¹ calculated from OD measurements and the final cell concentration were 7.1 g L⁻¹ and 5.12 g L⁻¹.

After induction with sufficient IPTG to give a final concentration of 0.5 mM (147 g), the maximum amount of CHMO activity was found 2 hours after induction. At this time there was still sufficient dissolved oxygen to ensure that there were no effects of oxygen limitation. The specific activity reached a maximum of 48 and 56 U gdc⁻¹ which is approximately 16 times lower than when complex medium was used.

There was a slight drop in the percentage of cells containing plasmids, but this is too small a change to account for the lower activity and the second fermentation had a lower plasmid percentage (85 %) but greater activity.

4.4.2 Batch fermentation with supplementation

The loss of CHMO activity when grown on defined minimal medium would have resulted in a significant decrease in productivity over the complex medium fermentation and therefore a large process volume would be required for the same amount of catalyst.

The effect of supplementation of the medium was investigated. Yeast extract and tryptone were chosen as these were the major constituents of the complex medium.. The batch fermentation was repeated with 20 g L⁻¹ glycerol and the addition of 10 g of both yeast extract and tryptone when CHMO expression was induced.

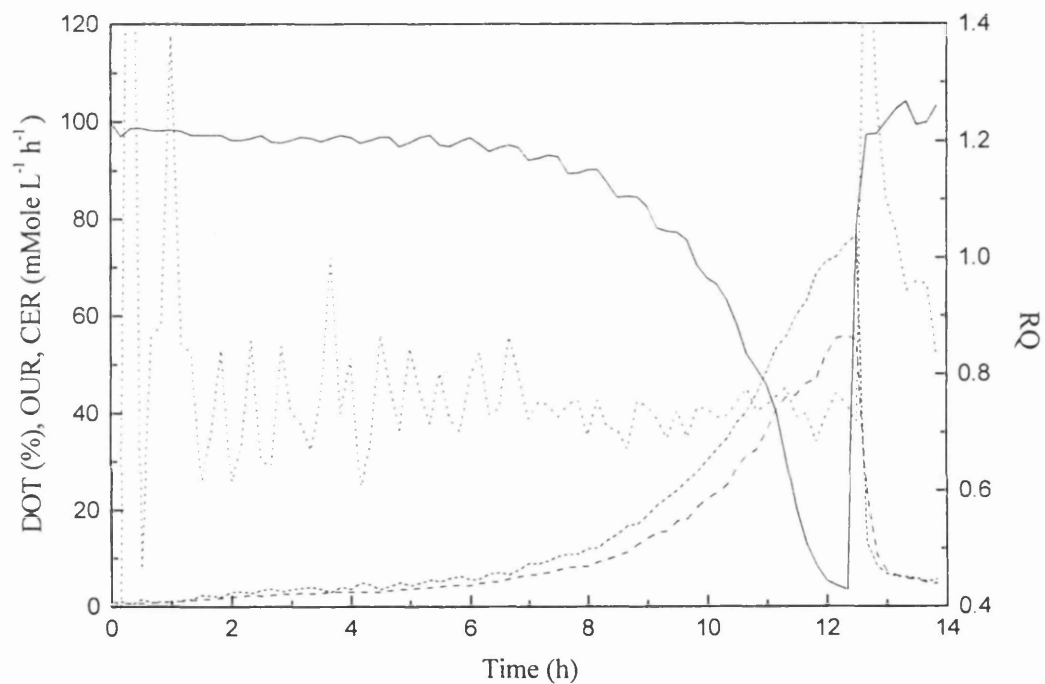


Figure 4.24: Fermentation profile for 7 L batch fermentation of JM107/pQR210 on defined medium with induction of CHMO at 8 hours. This figure shows the growth of *E. coli* as detailed in section 3.7.3 and illustrates the change in OUR (----), CER (---), DOT (—), and RQ (· · · · ·) as the fermentation proceeds.

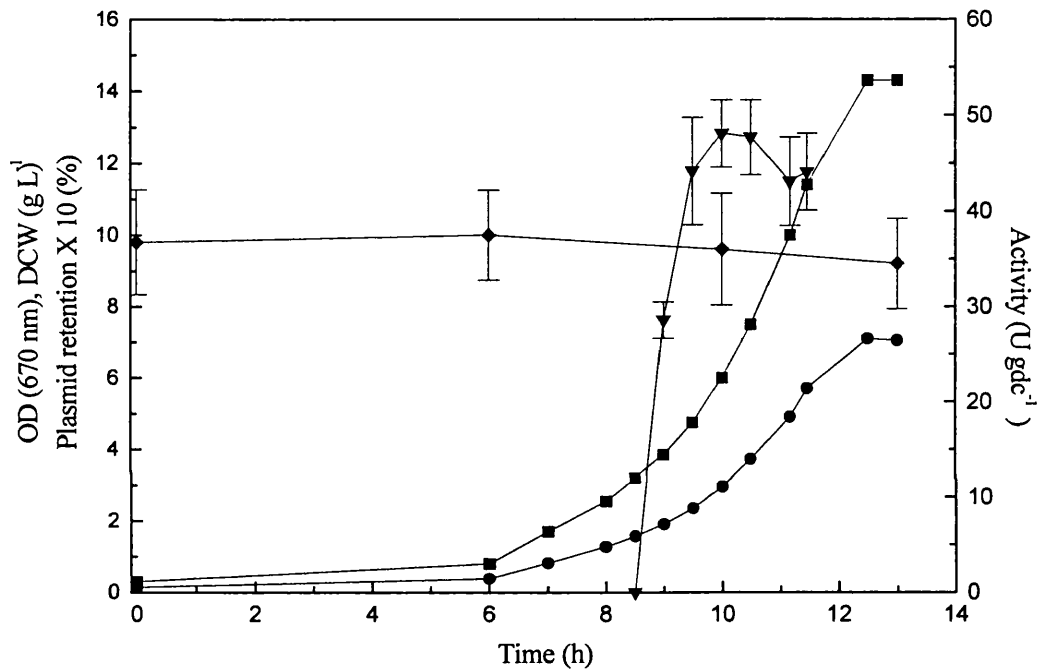


Figure 4.25: Productivity of a batch fermentation of *E. coli* JM107/pQR210 on defined medium with induction of CHMO at 8 h. This figure illustrates the production of active CHMO for the fermentation described by figure 4.24 as illustrated by OD (■), dry cell weight (●) and specific CHMO activity (▼). The figure also illustrates the percentage cells containing plasmid throughout the fermentation (◆).

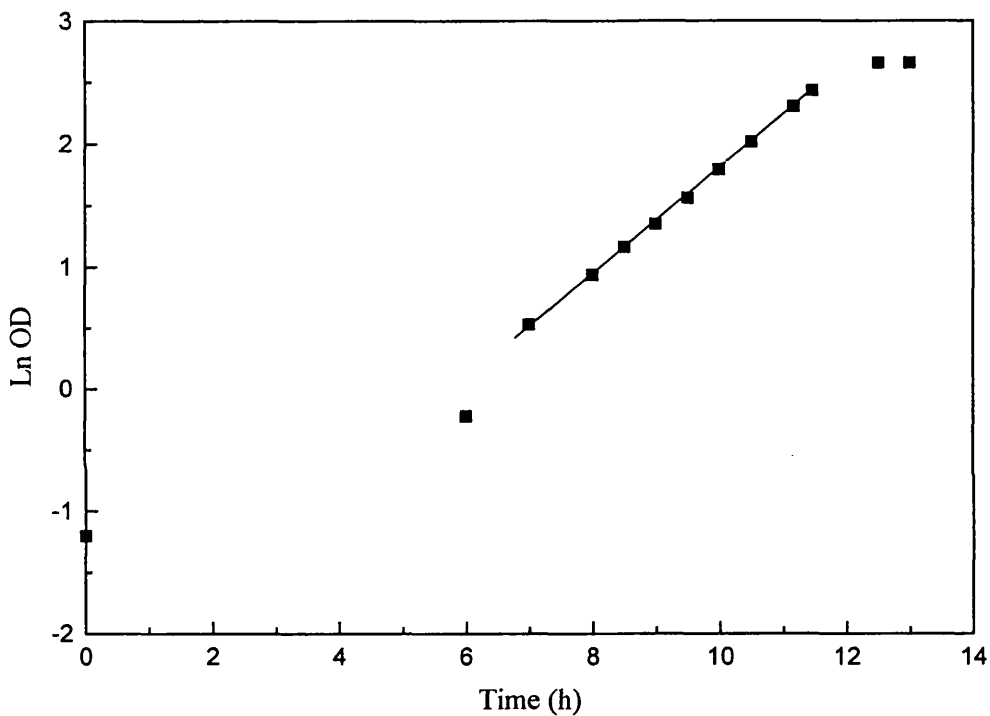


Figure 4.26: Productivity of batch fermentation of *E. coli* JM107/pQR210 on defined medium with induction of CHMO at 8 h. This figure illustrates the growth of *E. coli* under conditions as described by figures 4.24 and 4.25 and shows the growth rate during exponential phase (■ gradient = 0.44 h^{-1}).

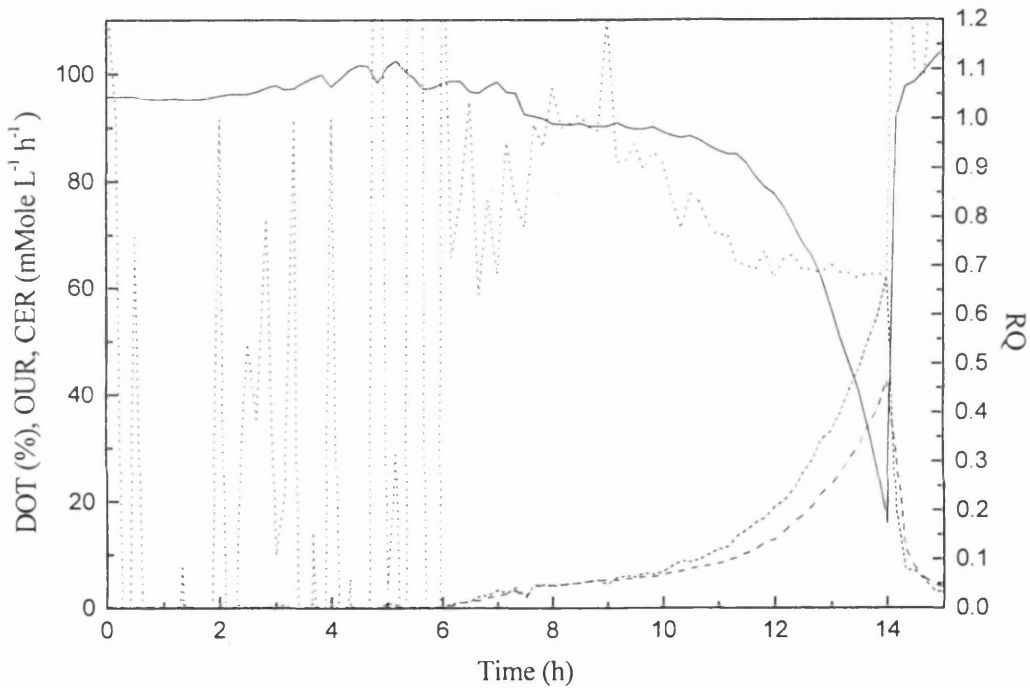


Figure 4.27: Fermentation profile for 7 L batch fermentation of *E. coli* JM107/pQR210 on defined medium with induction of CHMO at 10 h. This figure shows the growth of *E. coli* as detailed in section 3.7.3 and illustrates the change in OUR (----), CER (---), DOT (—), and RQ (— · —) as the fermentation proceeds.

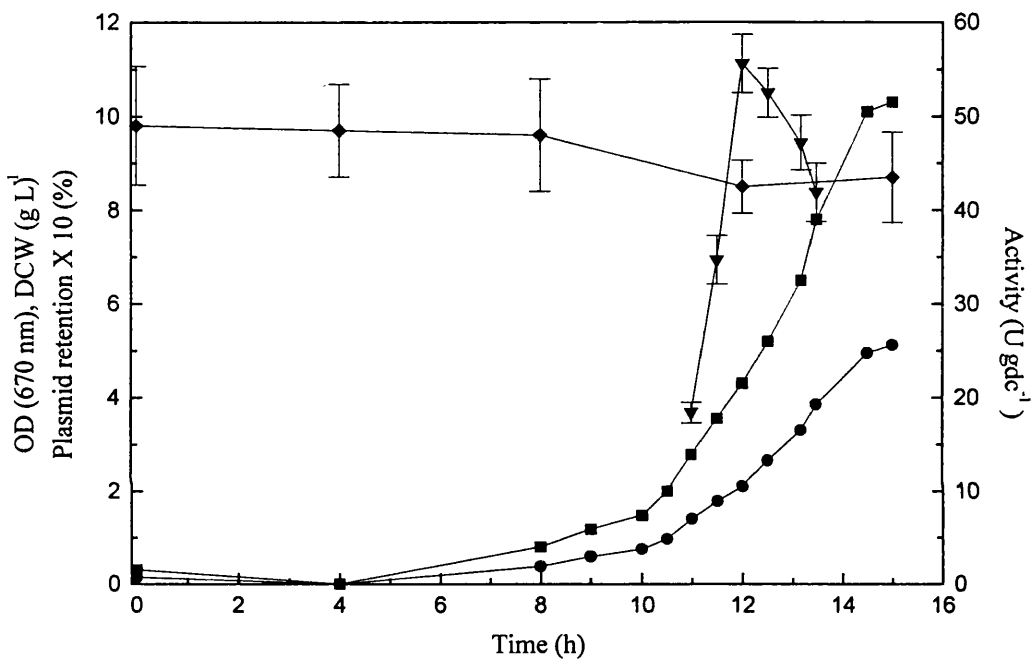


Figure 4.28: Productivity of a batch fermentation of *E. coli* JM107/pQR210 on defined medium with induction of CHMO at 10 h. This figure illustrates the production of active CHMO for the fermentation described by figure 4.27 as illustrated by OD (■), dry cell weight (●) and specific CHMO activity (▼). The figure also illustrates the percentage cells containing plasmid throughout the fermentation (◆).

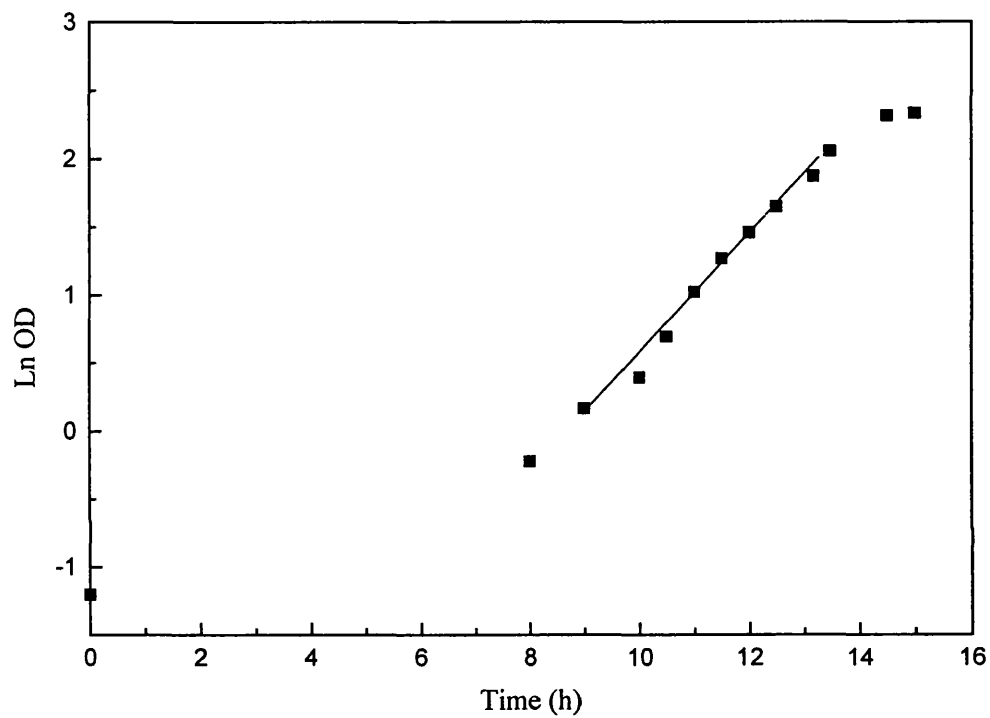


Figure 4.29: Productivity of batch fermentation of *E. coli* JM107/pQR210 on defined medium with induction of CHMO at 10 h. This figure illustrates the growth of *E. coli* under conditions as described by figures 4.27 and 4.28 and shows the growth rate during exponential phase (■ gradient = 0.43 h^{-1}).

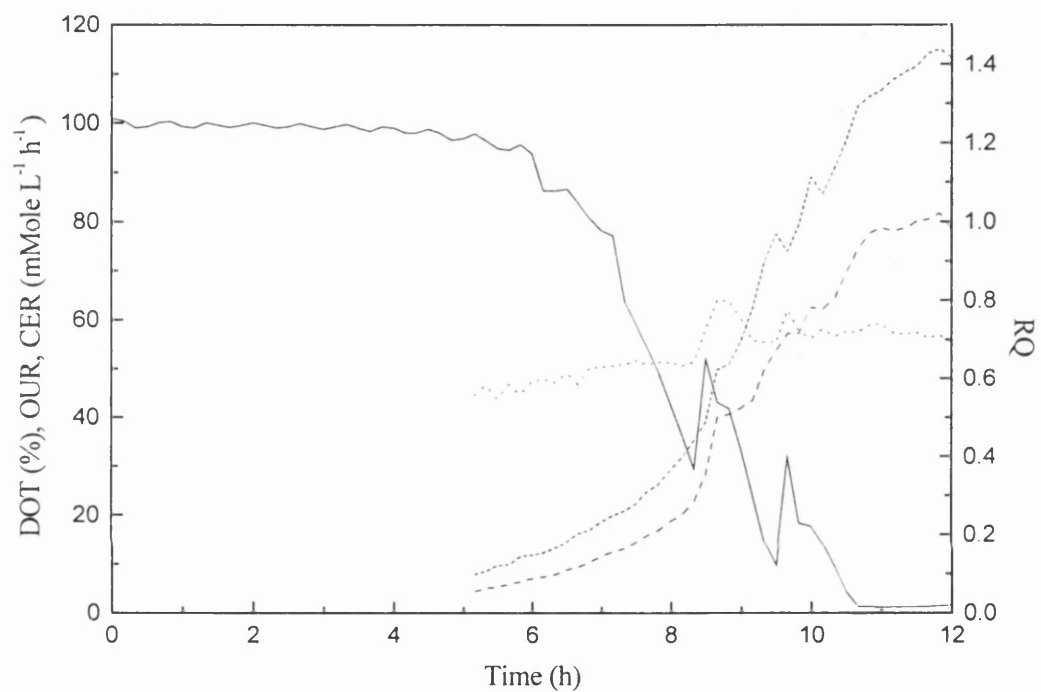


Figure 4.30 Fermentation profile for a 7 L batch fermentation of *E. coli* JM107/pQR210 on defined medium with media supplementation and induction of CHMO at 7.7 h. This figure shows the growth of *E. coli* as detailed in section 3.7.3 and illustrates the change in OUR (----), CER (---), DOT (—), and RQ (— · —) as the fermentation proceeds.

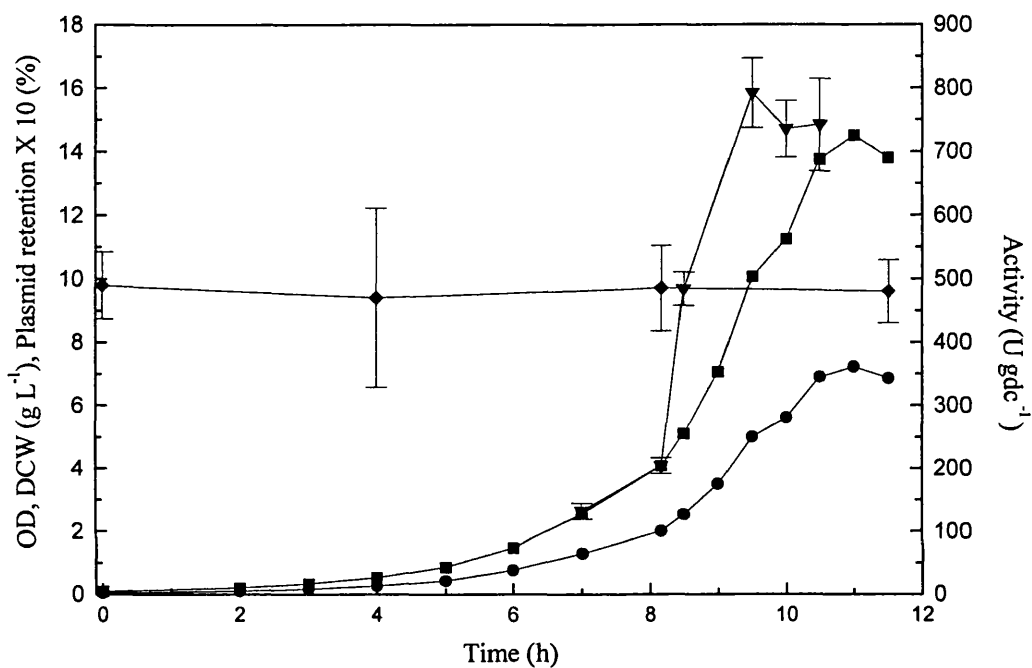


Figure 4.31: Productivity of 7 L batch fermentation of *E. coli* JM107/pQR210 on defined medium with supplementation and CHMO induction at 7.7 h. This figure illustrates the production of active CHMO for the fermentation described by figure 4.30 as illustrated by OD (■), dry cell weight (●) and specific CHMO activity (▼). The figure also illustrates the percentage cells containing plasmid throughout the fermentation (◆).

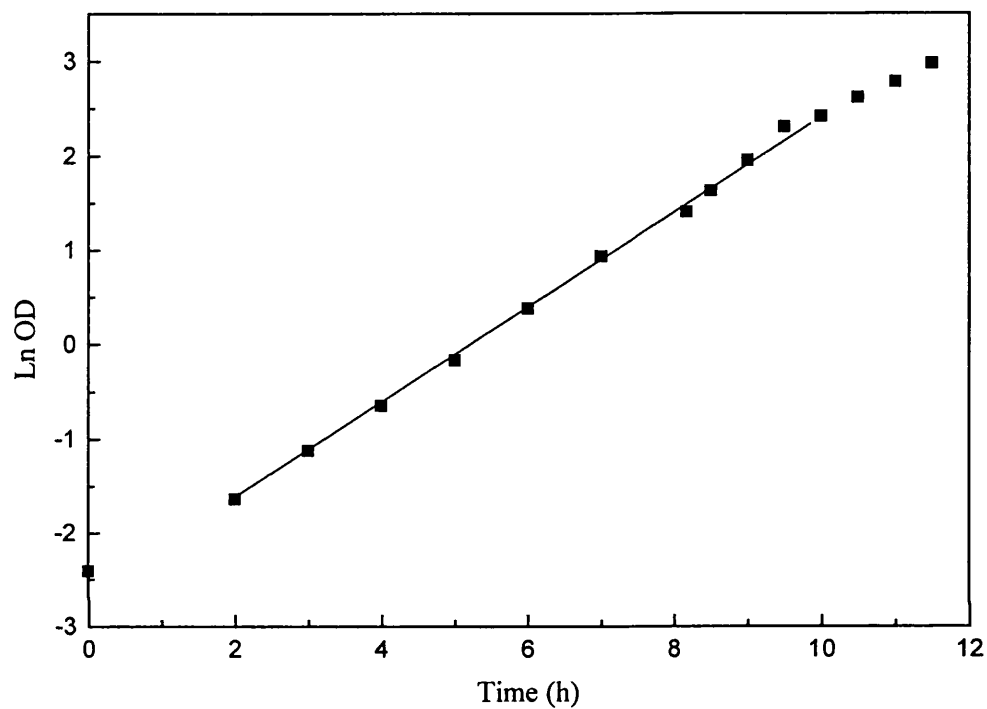


Figure 4.32: Biomass production in a 7 L batch fermentation of *E. coli* JM107/pQR210 on defined medium with supplementation and CHMO induction at 7.7 h. This figure illustrates the growth of *E. coli* under conditions as described by figures 4.30 and 4.31 and shows the growth rate during exponential phase (■ gradient = 0.49 h^{-1}).

Figures 4.30 to 4.32 show the fermentation followed the expected profile with a growth rate of 0.49 h^{-1} . CHMO production was induced at 7.66 hours and the maximum activity of 792 U gdc^{-1} found after approximately 2 hours. At maximum CHMO activity the cell concentration was 5 g L^{-1} and the dissolved oxygen tension was above 20 % saturation. The addition of the complex nutrients gave the same level of activity as the complex medium fermentation.

4.4.3 Fed batch exponential feeding

A fed batch strategy allows greater biomass to be produced, without the problems associated with oxygen limitation by restricting the growth rate, (Paalme *et al.* 1990, Riesenberg *et al.*, 1991). In addition the maintenance of a low constant growth rate has often been reported to increase the stability of recombinant organisms (Yoon and Kang, 1994, Hellmuth *et al.* 1994) and increase productivity.

Yeast extract and tryptone were added to fed batch fermentations at the time of induction as this had been proven to be necessary for maximum expression during batch fermentations on minimal medium.

Figures 4.33 to 4.38 show the data from a typical fermentation with defined medium 4 and 3. The LabView software was set up as described in section 3.7.4 with feed solution 4 ($\mu = 0.15 \text{ h}^{-1}$). CHMO production was induced after 20.5 and 20 h respectively and reached a maxima of 436 and 388 U gdc^{-1} approximately 2.5 hours later. Induction was effected by the addition of IPTG at a point during the controlled growth rate that would ensure that the culture did not become oxygen limited during CHMO synthesis.

The growth rates during feeding as determined by optical density measurements were both 0.14 h^{-1} . When calculated from regressed OUR data the growth rates were both 0.14 h^{-1} , which shows good agreement and shows that the control was adequate. When regressed CER data were used the growth rates were estimated as 0.13 h^{-1} and 0.12 h^{-1} .

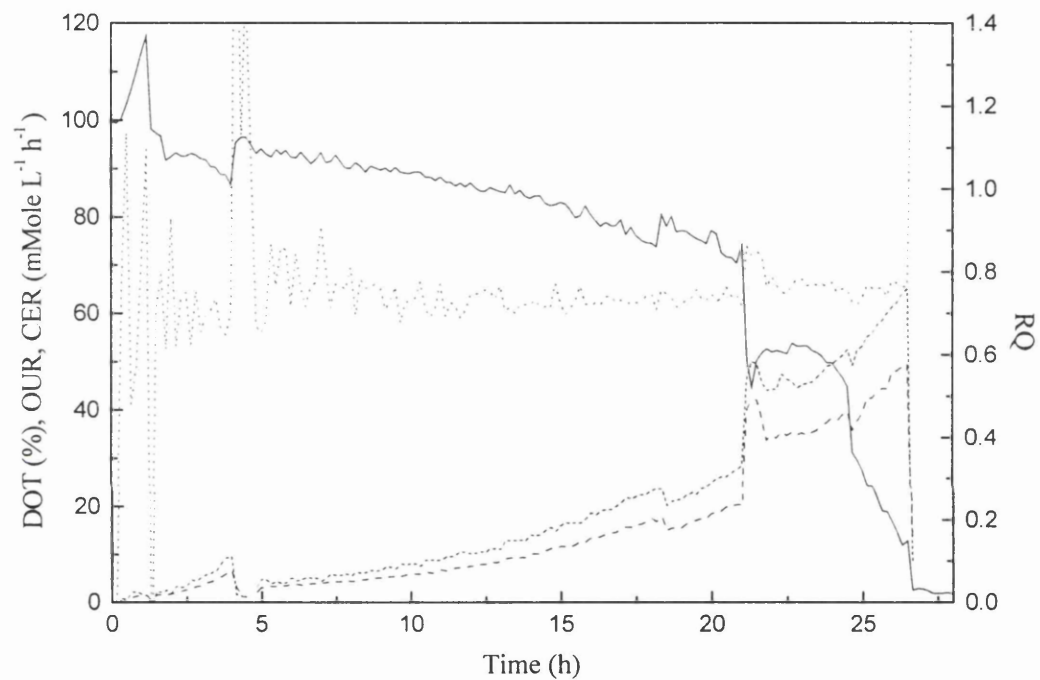


Figure 4.33: Fermentation profile for a 7 L fed batch fermentation of *E. coli* JM107/pQR210 with induction of CHMO at 20.5 h. This figure shows the growth of *E. coli* as detailed in section 3.7.4 and illustrates the change in OUR (----), CER (---), DOT (—), and RQ (· · · · ·) as the fermentation proceeds.

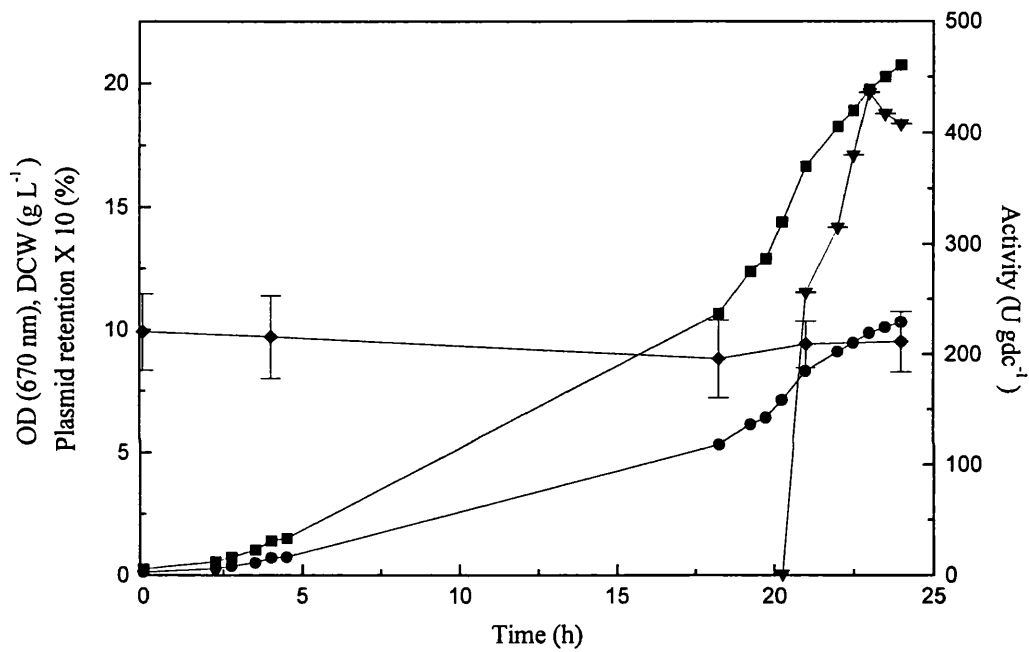


Figure 4.34: Productivity of a 7 L fed batch fermentation of *E. coli* JM107/pQR210 with induction of CHMO at 20.5 h. This figure illustrates the production of active CHMO for the fermentation described by figure 4.33 as illustrated by OD (■), dry cell weight (●) and specific CHMO activity (▼). The figure also illustrates the percentage cells containing plasmid throughout the fermentation (◆).

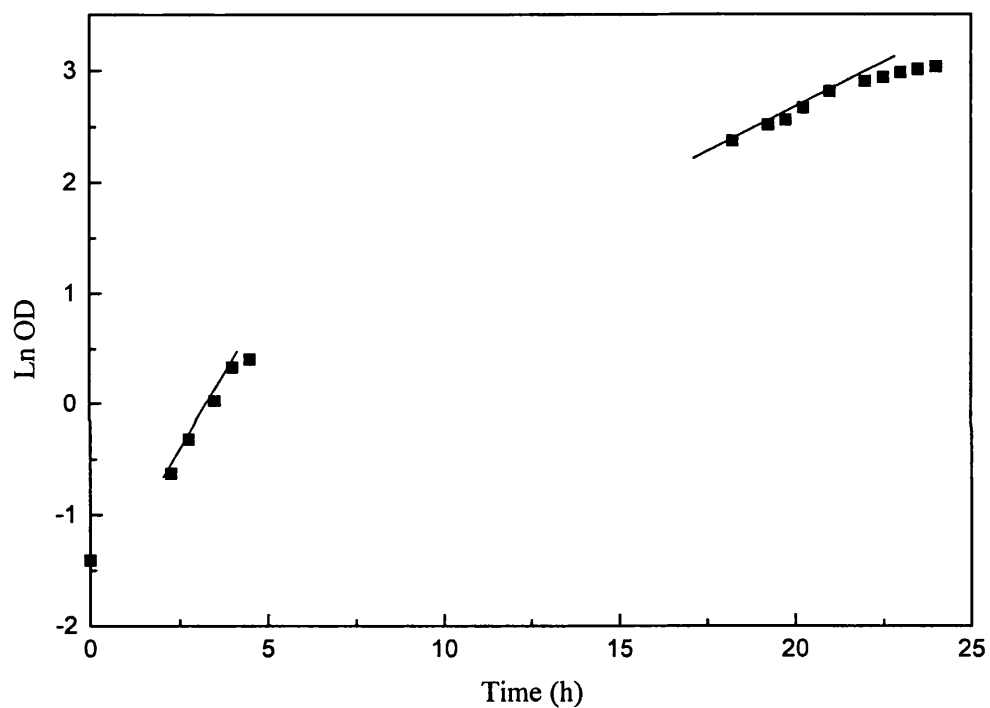


Figure4.35: Productivity of a 7 L fed batch fermentation of *E. coli* JM107/pQR210 with CHMO induction at 20.5 h. This figure illustrates the growth of *E. coli* under conditions as described by figures 4.33 and 4.34 and shows the growth rate during the initial exponential phase (■ gradient = 0.49 h^{-1}) and during the fed stage (0.144 h^{-1}).

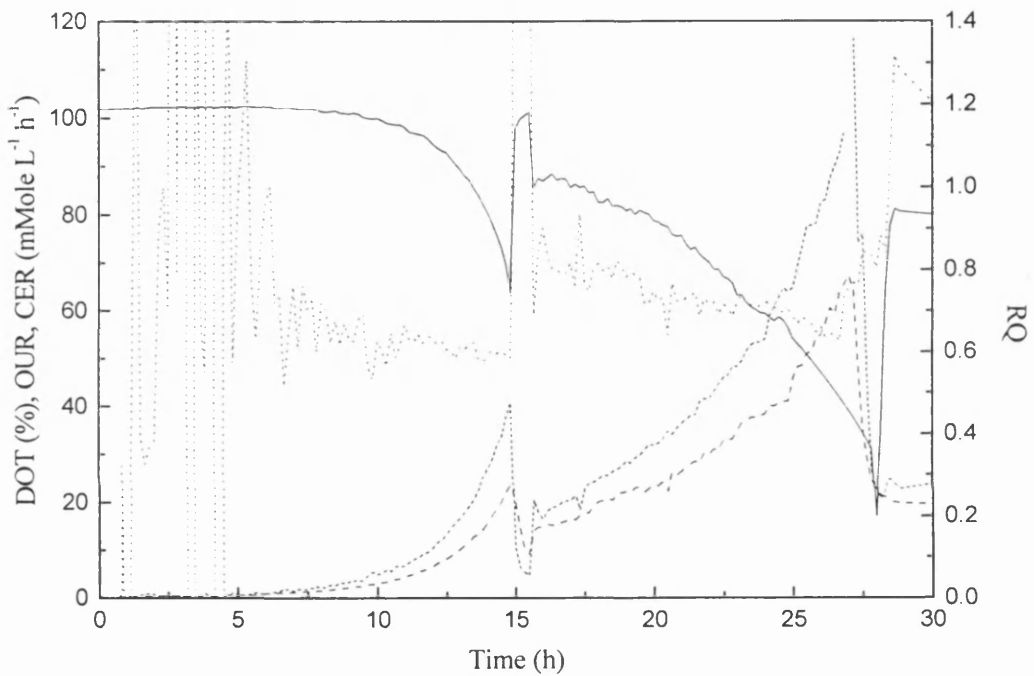


Figure 4.36: Fermentation profile for a 7 L fed batch fermentation of *E. coli* JM107/pQR210 with increased initial glycerol concentration and CHMO induction at 20 h. This figure shows the growth of *E. coli* as detailed in section 3.7.4 and illustrates the change in OUR (----), CER (---), DOT (—), and RQ (.....) as the fermentation proceeds.

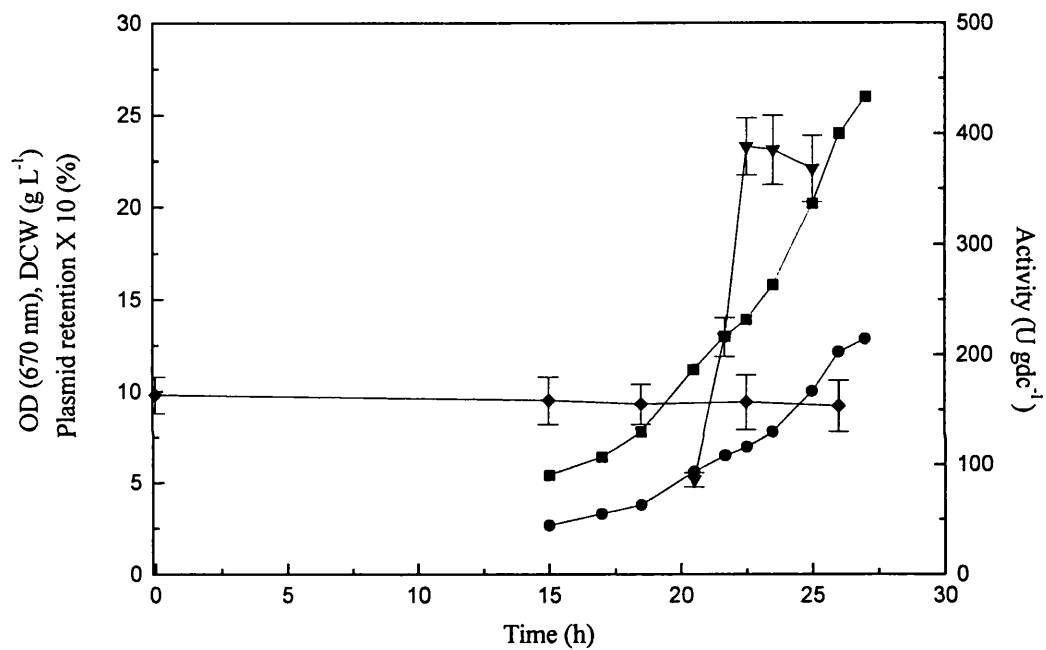


Figure 4.37: Productivity of a 7 L fed batch fermentation of *E. coli* JM107/pQR210 with increased initial glycerol concentration and CHMO induction at 20 h. This figure illustrates the production of active CHMO for the fermentation described by figure 4.36 as illustrated by OD (■), dry cell weight (●) and specific CHMO activity (▼). The figure also illustrates the percentage cells containing plasmid throughout the fermentation (◆).

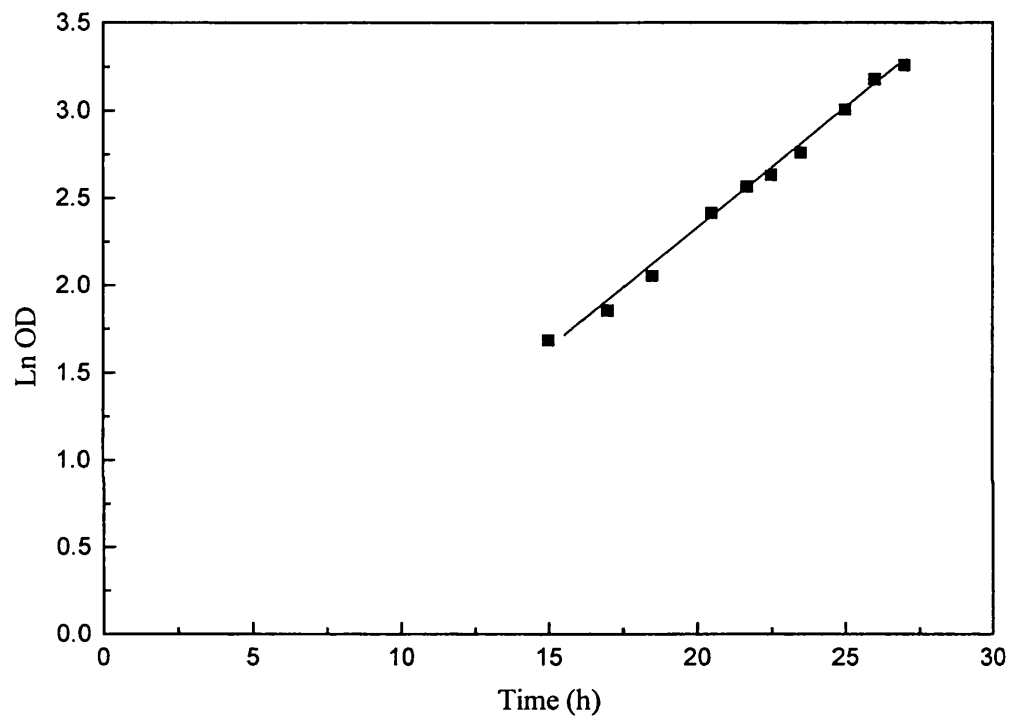


Figure 4.38: Productivity of a 7 L fed batch fermentation of *E. coli* JM107/pQR210 with increased initial glycerol concentration and CHMO induction at 20 h. This figure illustrates the growth of *E. coli* under conditions as described by figures 4.36 and 4.37 and shows the growth rate during the fed stage (■ gradient = 0.14 h^{-1}).

4.4.4 Fed batch linear feeding

Controlled exponential feeding allowed the production of greater biomass without oxygen limitation. Exponential feeding still does not allow the cells to reach the maximum biomass that the medium would support without reaching oxygen limitation. To further increase biomass the pumps that control the feed addition can be set to a fixed output when the exponential feeding has reached a point where oxygen limitation may become a problem.

Figures 4.39 to 4.44 show typical fermentations where the feed pumps have been set to a constant value either after a period of controlled growth rate feeding (Figures 4.39 to 4.41) or directly after the batch phase (Figures 4.42 to 4.44).

Figures 4.39 to 4.41 show a controlled fed batch fermentation (medium 3) where the feed was set at a constant rate when the OUR reached $50 \text{ mMole L}^{-1} \text{ h}^{-1}$ after exponential feeding to give a growth rate of 0.15 h^{-1} . The growth rate gradually decreased from this point and CHMO production was induced after 31.5 hours. A dry cell weight of 19 g L^{-1} was achieved from glycerol additions equivalent to a total of 50 g L^{-1} . Activity reached a maximum of 100 U gdc^{-1} after 35 hours.

Figures 4.42 to 4.44 show a constant rate fed batch fermentation (medium 3) where the glycerol feed (355 g L^{-1}) rate was set at 11.09 g h^{-1} . A dry cell weight of 24 g L^{-1} was achieved from glycerol additions equivalent to a total of 75 g L^{-1} . CHMO production was induced after 26.25 hours and reached a maximum of 122 U gdc^{-1} after 29.25 hours.

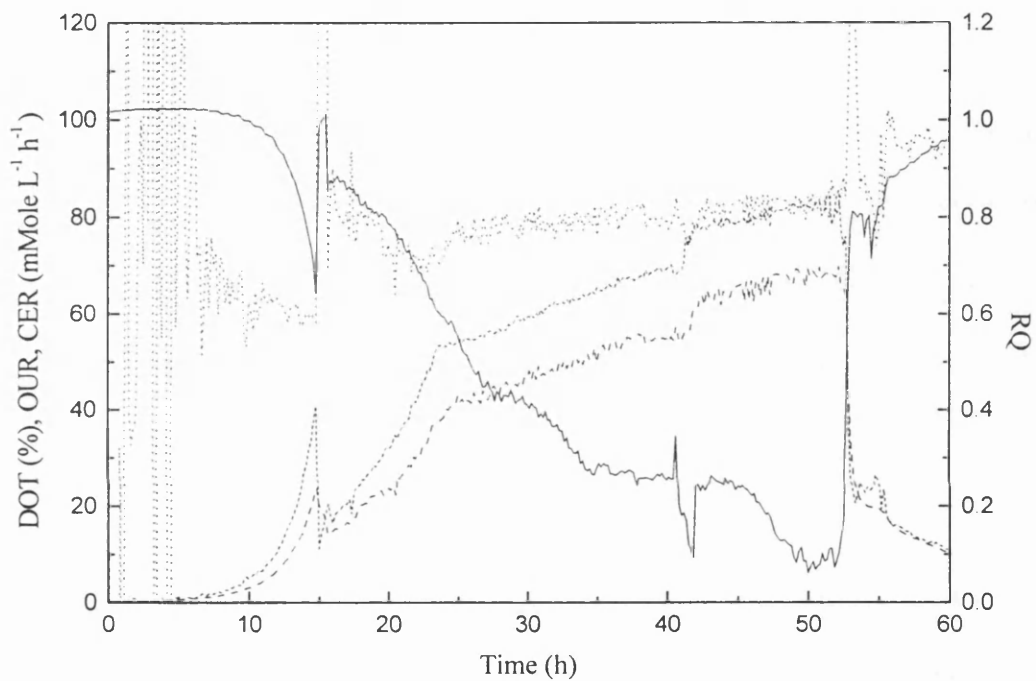


Figure 4.39: Fermentation profile for a 7 L exponential then linear fed batch fermentation of *E. coli* JM107/pQR210. This figure shows the growth of *E. coli* as detailed in section 3.7.4 and illustrates the change in OUR (----), CER (---), DOT (—), and RQ (.....) as the fermentation proceeds. The exponential feeding was started at 15 h, set to linear after 24 h and CHMO induced at 30.5 h

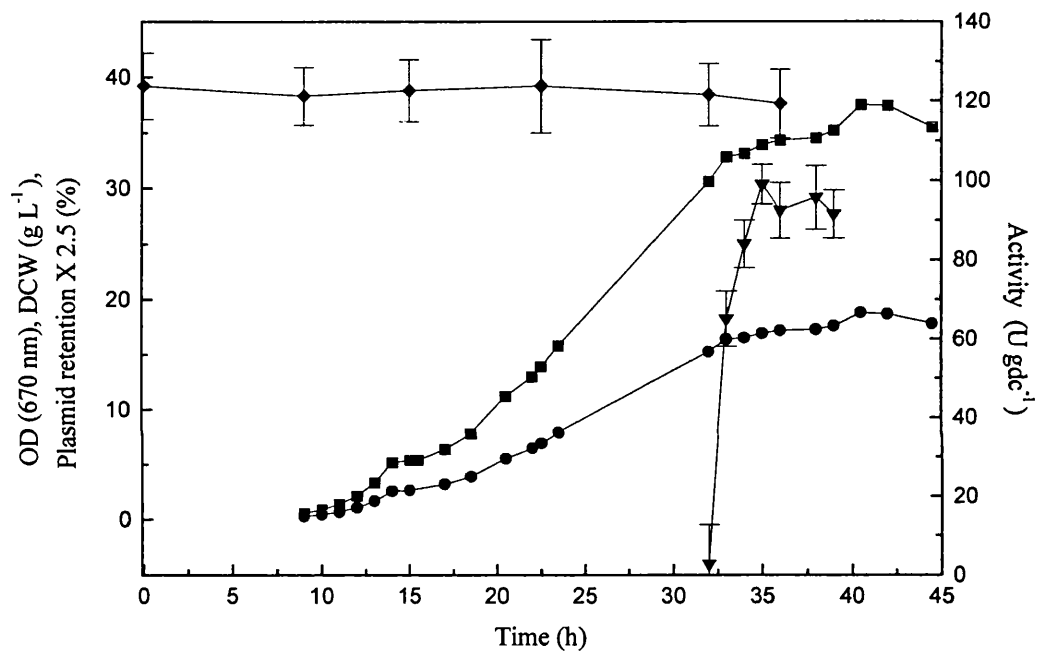


Figure 4.40: Productivity of a 7 L exponential then linear fed batch fermentation of *E. coli* JM107/pQR2107. Illustrating optical density (■), dry cell weight (●), CHMO activity (▼), and plasmid percentage (◆). This figure illustrates the production of active CHMO for the fermentation described by figure 4.39 as illustrated by OD (■), dry cell weight (●) and specific CHMO activity (▼). The figure also illustrates the percentage cells containing plasmid throughout the fermentation (◆).

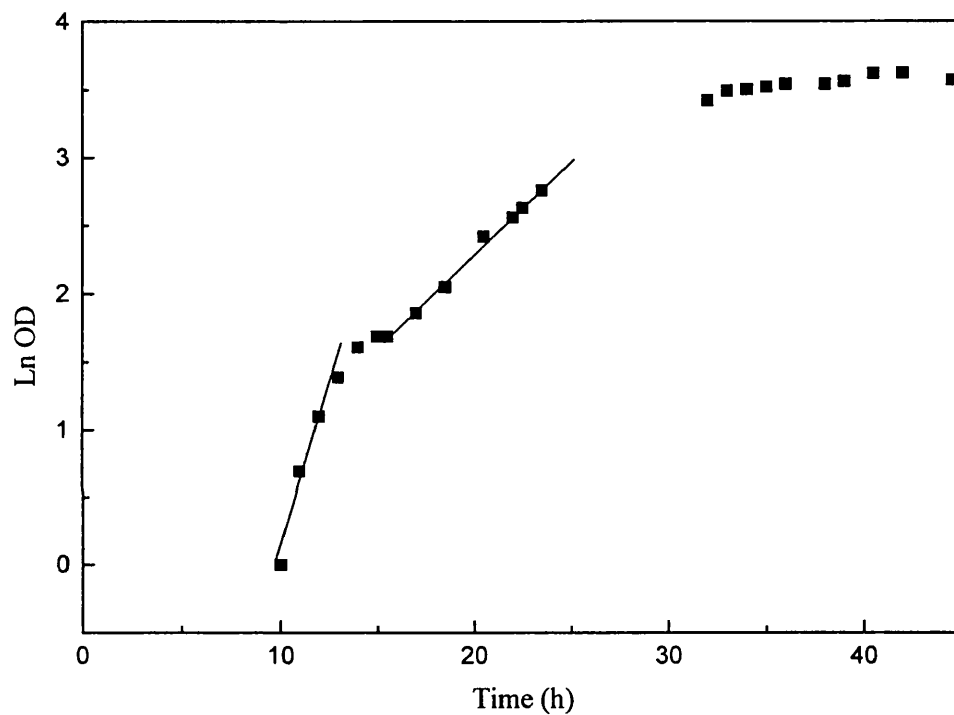


Figure 4.41: Productivity of a 7 L exponential then linear fed batch fermentation of *E. coli* JM107/pQR2107. This figure illustrates the growth of *E. coli* under conditions as described by figures 4.39 and 4.340 and shows the growth rate during the initial exponential phase fed stage (■ gradient = 0.44 h^{-1}) and the exponential fed stage (0.143 h^{-1}).

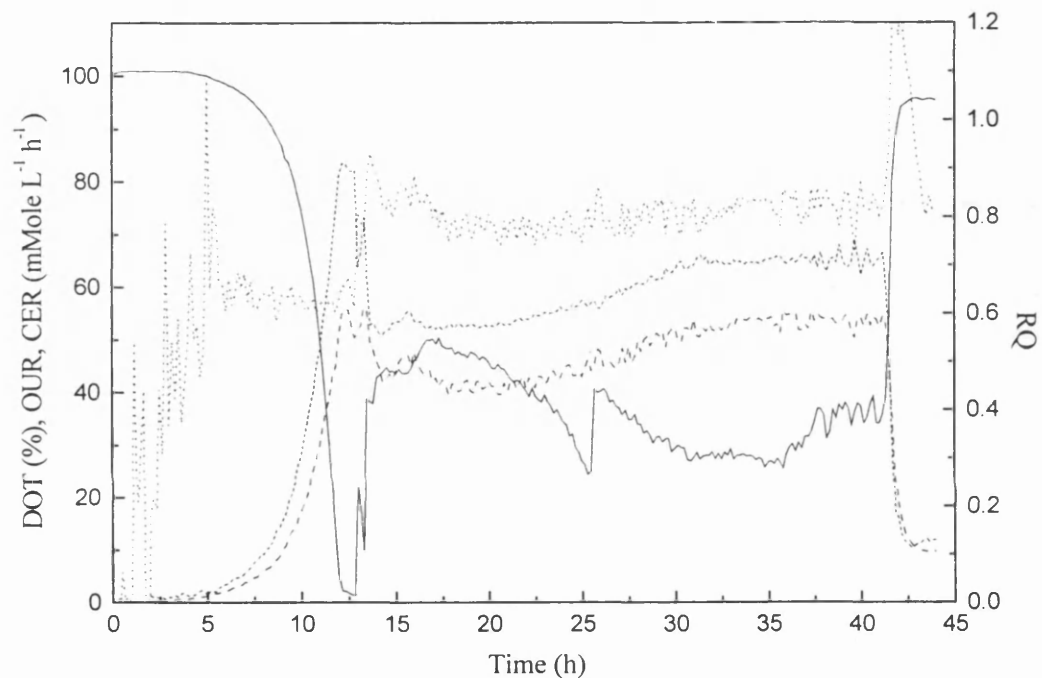


Figure 4.42: Fermentation profile for a 7 L linear fed batch fermentation of *E. coli* JM107/pQR210. This figure shows the growth of *E. coli* as detailed in section 3.7.4 and illustrates the change in OUR (----), CER (---), DOT (—), and RQ (.....) as the fermentation proceeds. The linear feeding was started at 14 h and CHMO induced at 26.25 h

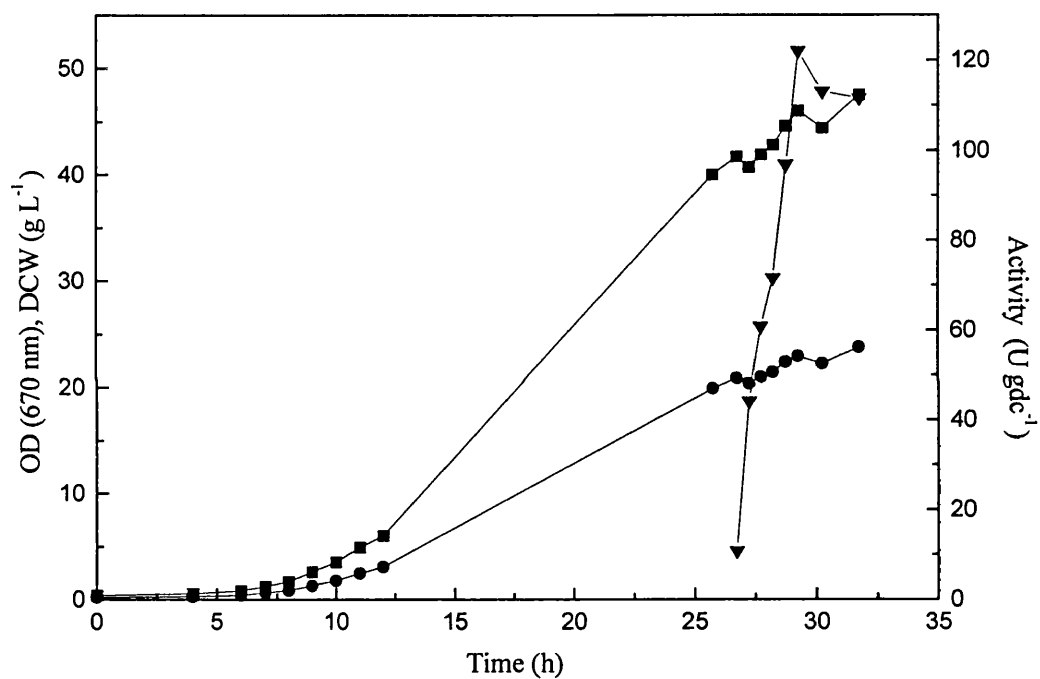


Figure 4.43: Productivity of a 7 L fed batch fermentation of *E. coli* JM107/pQR210. This figure illustrates the production of active CHMO for the fermentation described by figure 4.42 as illustrated by OD (■), dry cell weight (●) and specific CHMO activity (▼). The figure also illustrates the percentage cells containing plasmid throughout the fermentation (◆).

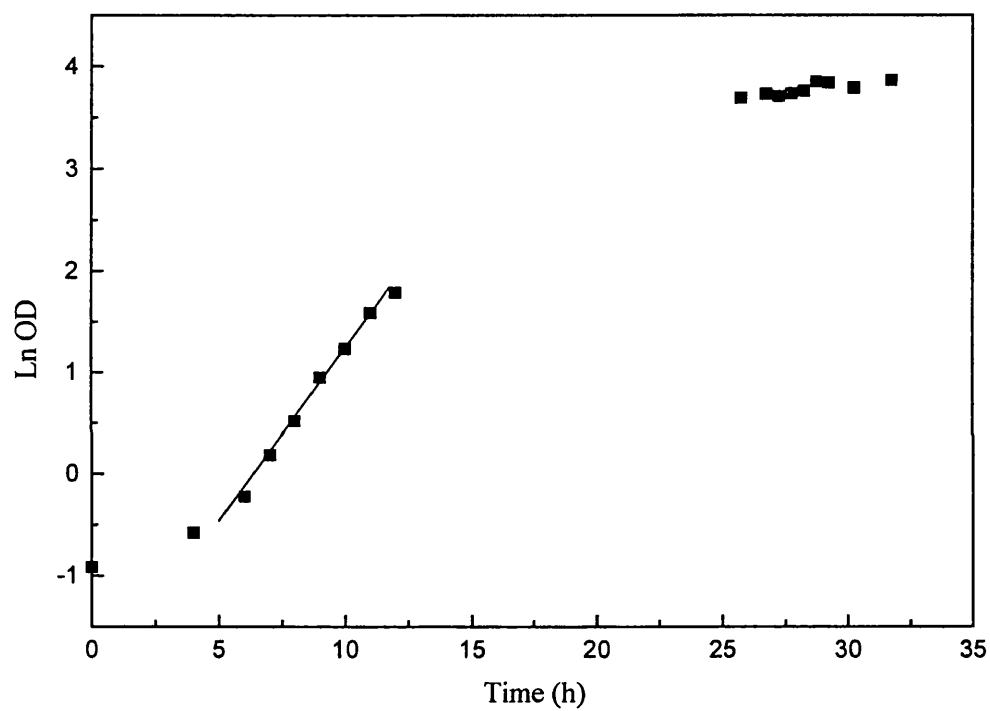


Figure 4.44: Productivity of a 7 L fed batch fermentation of *E. coli* JM107/pQR210. This figure illustrates the growth of *E. coli* under conditions as described by figures 4.42 and 4.43 and shows the growth rate during the initial exponential phase fed stage (■ gradient = 0.38 h^{-1}).

4.5 Stability of stored catalysts

4.5.1 Whole cells

An important factor in the usefulness of any biocatalyst is the length of time that the catalyst can be stored without losing significant amounts of activity. This period of time determines the size of fermentation and the frequency with which they will be required. The relative stability of stored CHMO in whole cells and crude homogenate would determine their relative usefulness as catalysts.

Whole cells of both *A. calcoaceticus* and *E. coli* were prepared and stored as described in section 3.8.3. The stability profiles of CHMO activity in *A. calcoaceticus* cells stored at -18 °C are shown in Figure 4.45. The figure illustrates that stability did not change significantly when the cells were stored in glycerol and that the cells had lost only 40 % of their activity after 5 months. The error bars in figures 4.45 to 4.47 represent the standard deviation calculated from five repeat samples.

In *E. coli* cells, as illustrated by Figure 4.46, CHMO activity is stable when stored in a buffered 50 % glycerol solution for over 6 months without a significant loss of activity. The cells have retained half of the original activity after nearly two years of storage.

4.5.2 Homogenate

Clarified homogenate of *E. coli* was prepared and stored as described in section 3.8.4. Figure 4.47 shows the stability profile for CHMO activity under a variety of conditions. Activity is lost very rapidly at 4 °C with no measurable activity after 3 weeks of storage with the addition of sodium azide or ampicillin to inhibit bacterial growth. When stored at -18 °C there is a gradual loss of activity with a loss of 50% activity after approximately 5 months. When the homogenate is stored with an equal volume of glycerol at -18 °C there is no significant change in activity after 5 months.

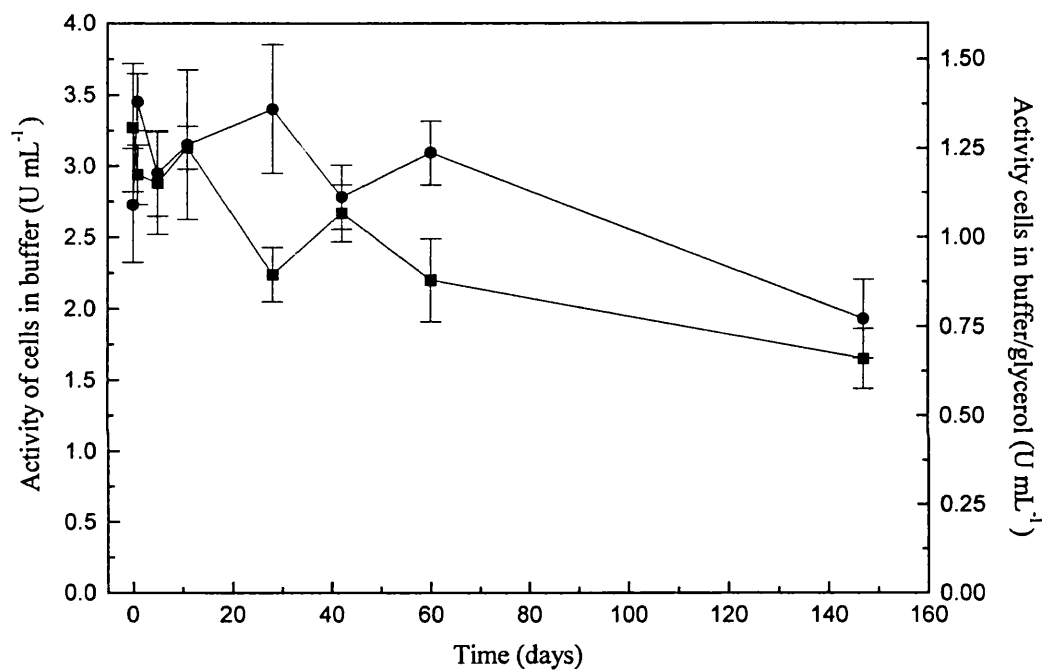


Figure 4.45: Stability of CHMO activity in *A. calcoaceticus* cells stored at -18 °C. This figure illustrates the change in CHMO activity with time of cells stored in phosphate buffer (■), and cells stored in phosphate buffer/glycerol (●).

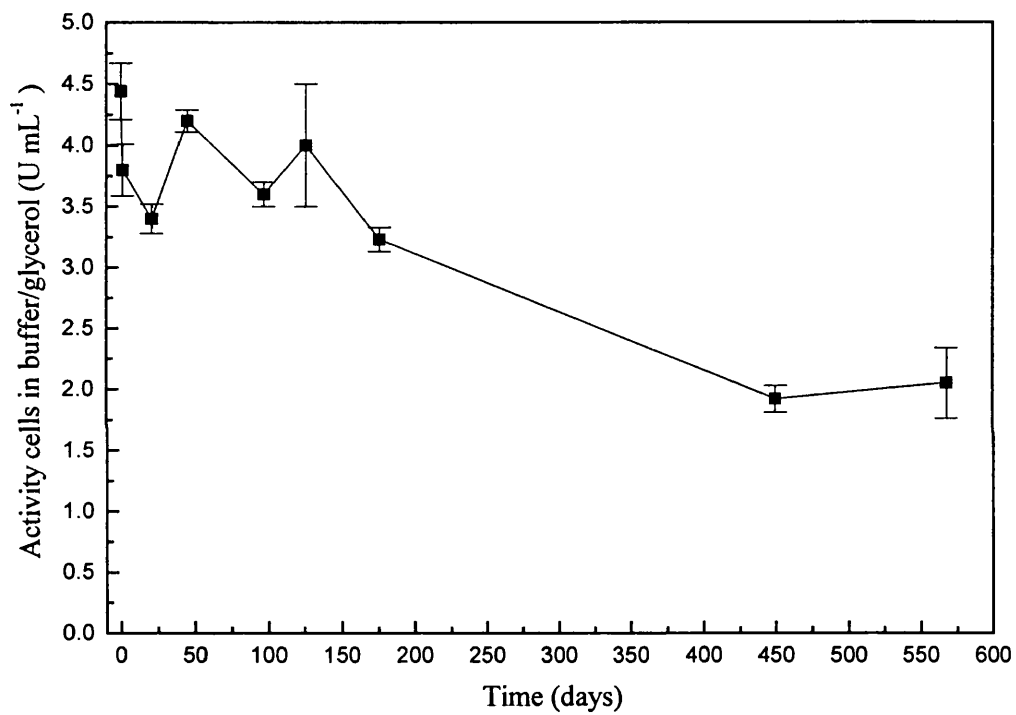


Figure 4.46: Stability of CHMO activity in *E. coli* cells stored at -18 °C. This figure illustrates the change in CHMO activity in cells stored in phosphate buffer/glycerol (■).

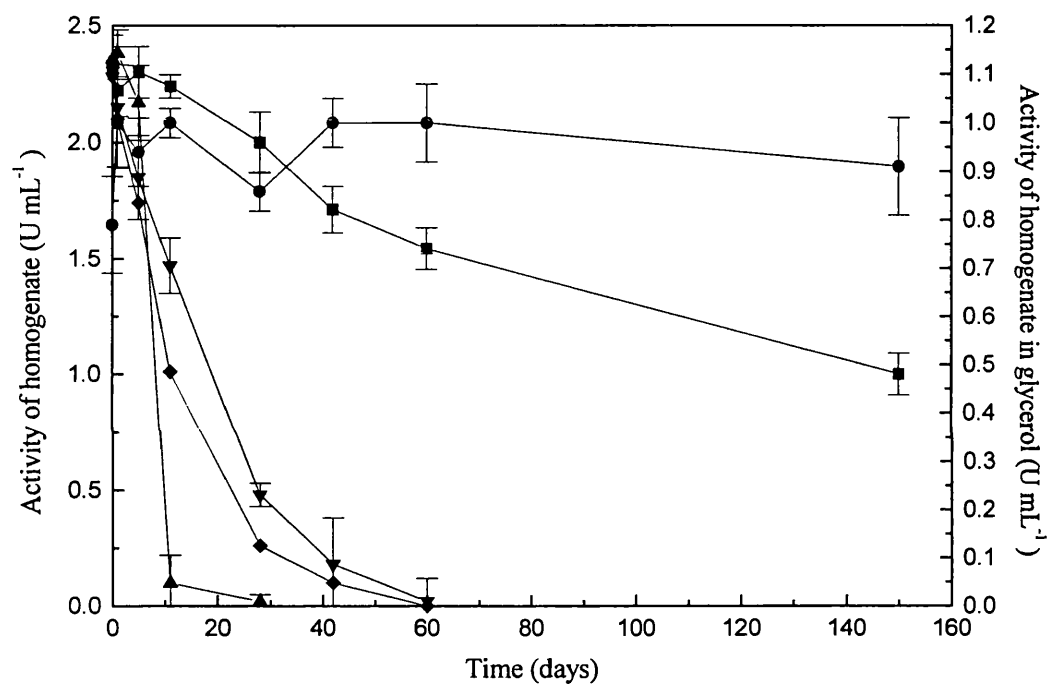


Figure 4.47: Stability of CHMO activity in clarified homogenate of *E. coli*. This figure illustrates the change in CHMO activity of *E. coli* homogenate stored at 4 °C (▲), 4 °C with 0.02 % addition of sodium azide (▼), 4 °C with 50 µg mL⁻¹ ampicillin (◆), -18 °C (■), and mixed with an equal volume of glycerol and stored at -18 °C (●).

4.6 Biotransformations - whole cell *Acinetobacter calcoaceticus*

4.6.1 Biotransformation of cyclohexanone

Whole cells of *A. calcoaceticus* were grown and prepared, and biotransformations carried out in an orbital shaker as detailed in section 3.9.1. The reactions were buffered to pH 7 as at this pH any potential instability of the lactone products would be reduced. pH 9 is the optimum for maximum enzyme activity (Trudgill, 1990) but under these conditions the possibility of lactone ring opening is increased.

Figure 4.48 illustrates a typical biotransformation of cyclohexanone, the natural substrate of the enzyme. The whole cells contain cyclohexanol dehydrogenase enzymes which are clearly driven in the reverse direction to produce cyclohexanol. Due to the action of the lactone dehydrogenase enzyme no lactone products could be detected. The presence of a substrate for the cyclohexanol degradation pathway confers stability to the CHMO activity as can be seen (Figure 4.49) by the fall in activity after 2 hours and the loss of activity by 5 hours.

4.6.2 Biotransformation of 2-ethyl cyclopentanone

The biotransformation of 2-ethyl cyclopentanone (figure 4.50) followed a similar pattern to that of cyclohexanone. This racemic substrate allows the examination of a chiral resolution. Based on relative retention time to other cyclic alcohols the unknown species was most likely 2-ethyl cyclopentanol. Lactone products could not be detected implying that the lactone product was a substrate for the lactone dehydrogenase enzyme. The concentration of alcohol produced was significantly lower than that produced in the biotransformation of the more simple cyclohexanone substrate, only reaching a concentration of 1 mM.

2-ethyl cyclopentanone did not confer the same stability to the CHMO activity as cyclohexanone. Figure 4.51 shows that activity fell at the same rate as the control cell suspension.

4.6.3 Biotransformation of 4-methyl cyclohexanone

4-methyl cyclohexanone was found not to confer stability to CHMO and cyclohexanol was added as a co-substrate to insure that sufficient activity remained throughout the biotransformation. Figure 4.52 shows a typical reaction profile. The concentrations of reactants and products were measured in both the supernatant and in sonicated cell extracts (figures 4.52 and 4.53). The unknown was most likely 4-methyl cyclohexanol, based on retention time, again produced by the cyclohexanol dehydrogenase enzyme catalysing the reverse reaction. The levels produced were similar to that of cyclohexanol when cyclohexanone was the substrate reaching a concentration of approximately 10 mM. No lactone products were found so 4-methyl cyclohexanone is as expected, a substrate for the lactonase enzyme.

The intracellular concentrations of all components were found to be similar and low, reaching a maximum concentration of 1 mM shortly after addition.

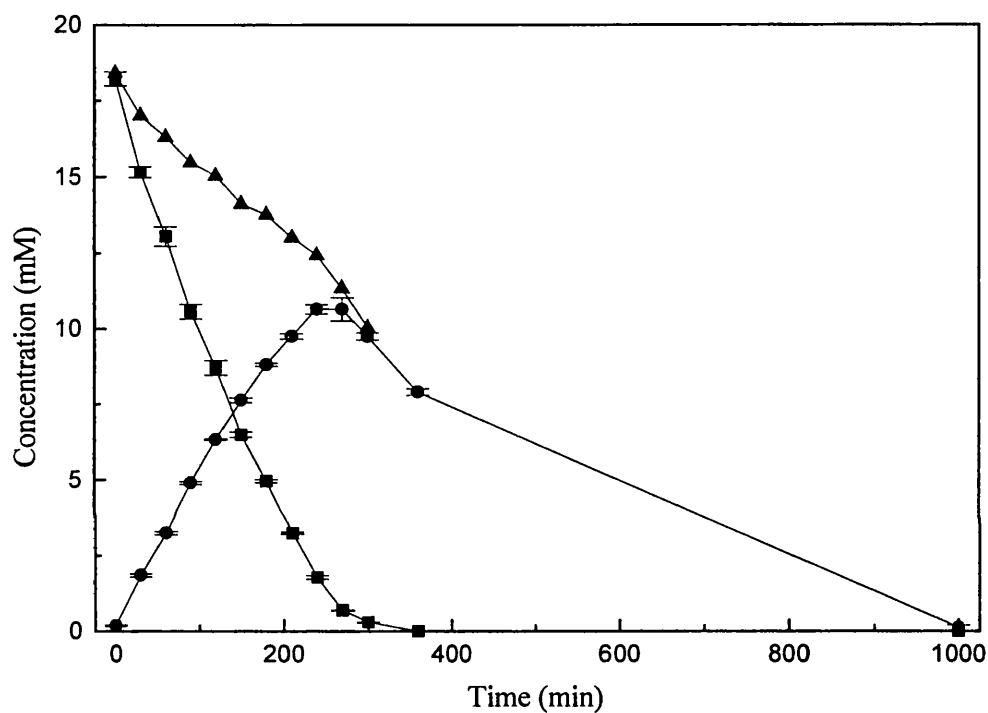


Figure 4.48 Biotransformation of cyclohexanone by whole cell *A. calcoaceticus*. This figure shows the biotransformation of cyclohexanone (■) by whole cell *A. calcoaceticus* under the conditions detailed in section 3.9.1. The production of cyclohexanol (●) and the cumulative concentration of the two (▲) are illustrated. No lactone products were detected.

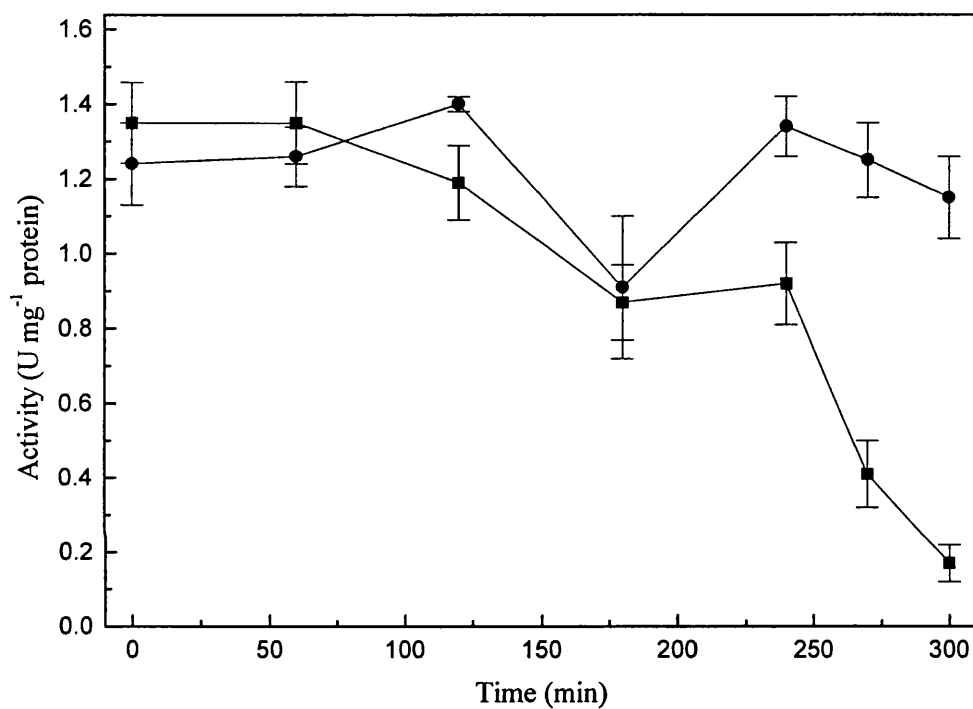


Figure 4.49 Specific activity of cyclohexanone monooxygenase during the cyclohexanone biotransformation described by figure 4.48. This figure illustrates the increased stability of CHMO within the *A. calcoaceticus* cells when 20 mM cyclohexanone is added (●), compared to the control of cells in buffer alone (■).

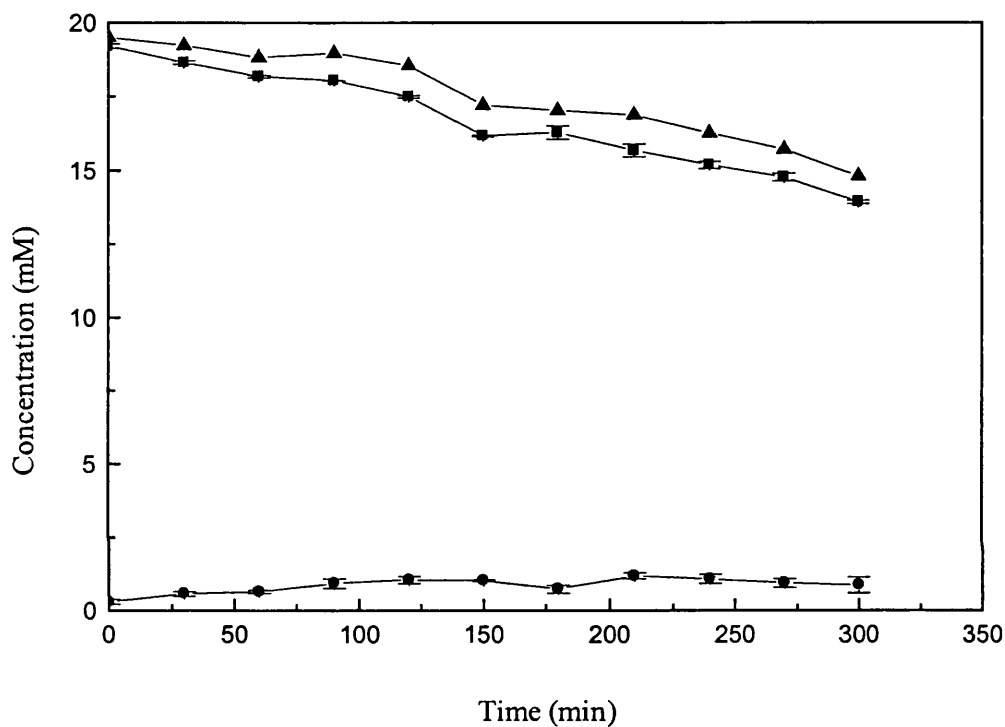


Figure 4.50 Biotransformation of 20 mM 2-ethyl cyclopentanone by whole cell *A. calcoaceticus*. This figure shows the biotransformation of 2-ethyl cyclopentanone (■) by whole cell *A. calcoaceticus* under the conditions detailed in section 3.9.1. The production of an unknown (●) (believed to be 2-ethyl cyclopentanol by GC retention time) and the cumulative concentration of the two (▲) are illustrated. No lactone products were detected

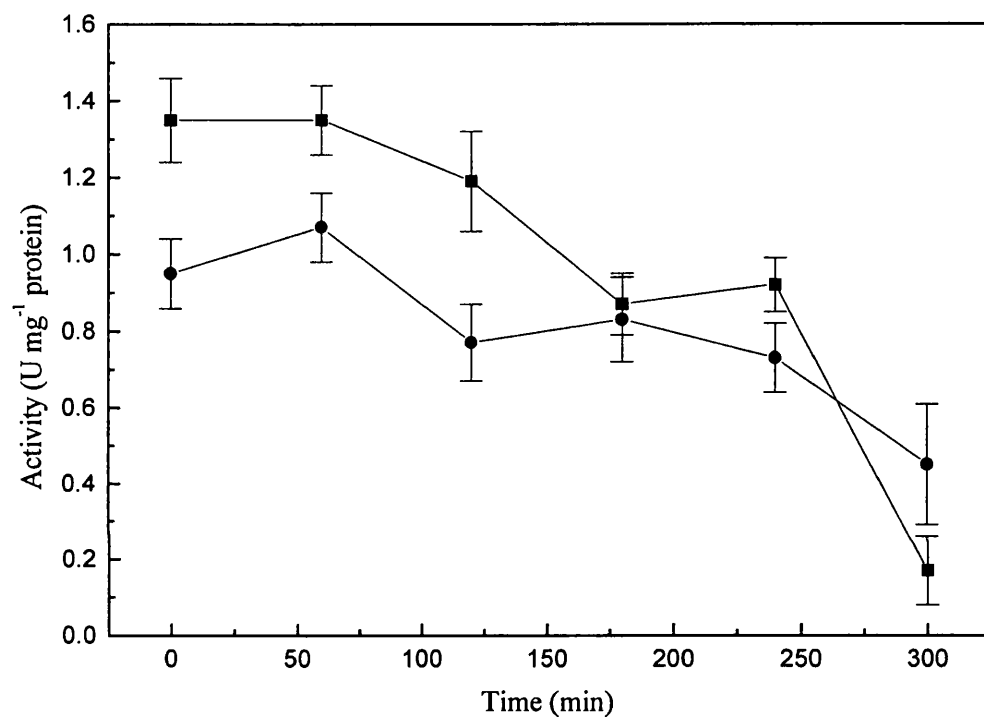


Figure 4.51 Specific activity of cyclohexanone monooxygenase during a 20 mM 2-ethyl cyclopentanone biotransformation described by figure 4.50. This figure illustrates the stability of CHMO within the *A. calcoaceticus* cells when 20 mM 2-ethyl cyclopentanone is added (●), compared to the control of cells in buffer alone (■).

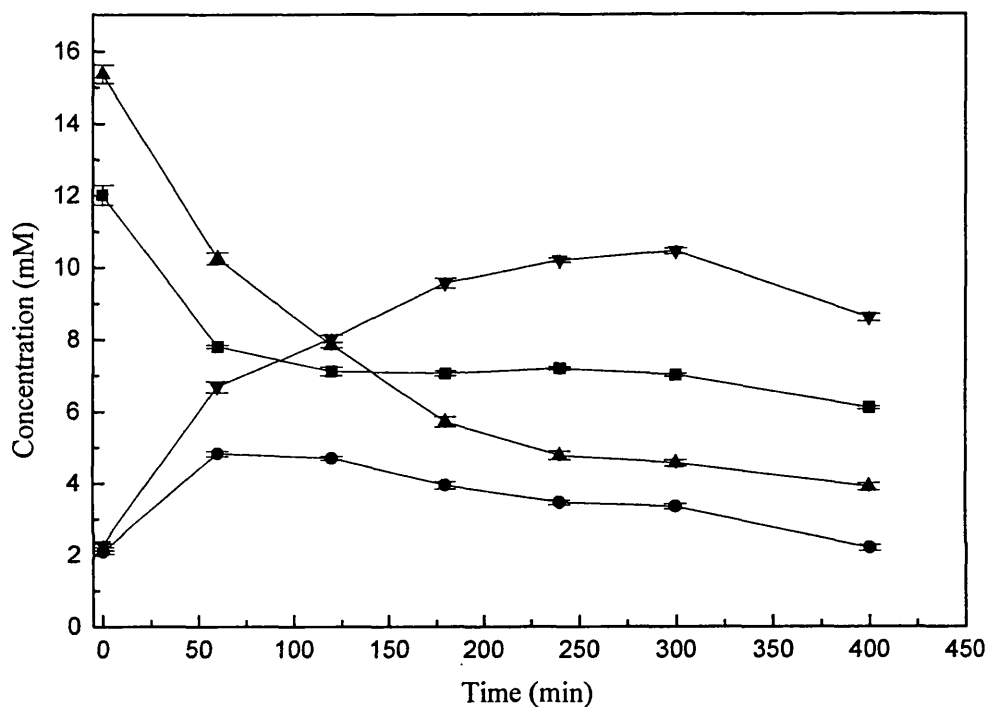


Figure 4.52 Biotransformation of 20 mM 4-methyl cyclohexanone, with cyclohexanol co-substrate, by whole cells of *A. calcoaceticus*. This figure shows the biotransformation of 4-methyl cyclohexanone (▲) and cyclohexanol (■) by whole cells of *A. calcoaceticus* under the conditions detailed in section 3.9.1. The production of cyclohexanone (●) and an unknown intermediate (believed to be 4-methyl cyclohexanol from GC retention time) are illustrated. All species were identified in the supernatant. No lactone products were detected.

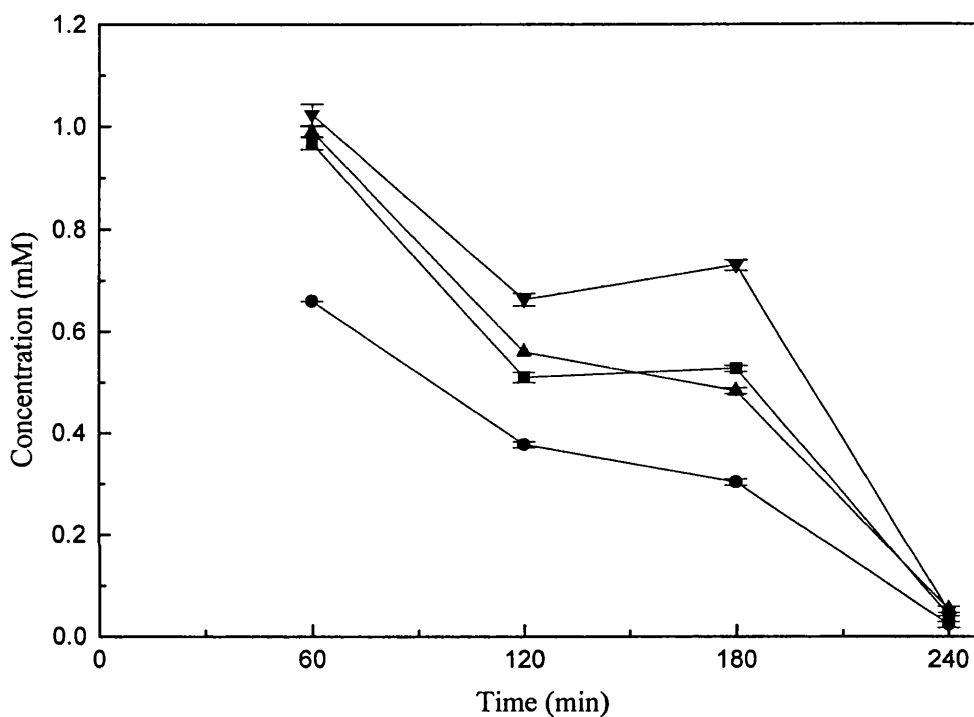


Figure 4.53 Biotransformation of 20 mM 4-methyl cyclohexanone, with cyclohexanol co-substrate, by whole cells of *A. calcoaceticus*. This figure shows the biotransformation of 4-methyl cyclohexanone (▲) and cyclohexanol (■) by whole cells of *A. calcoaceticus* under the conditions detailed in section 3.9.1. The production of cyclohexanone (●) and an unknown intermediate (believed to be 4-methyl cyclohexanol from GC retention time) are illustrated. All species were identified in intracellular fluid. No lactone products were detected.

4.7 Biotransformation - *Acinetobacter calcoaceticus* homogenate

4.7.1 Biotransformations of 4-methyl cyclohexanone

A. calcoaceticus homogenate was prepared as described in section 3.8.2 and biotransformations were performed as section 3.9.2.

The results of the whole cell biotransformations showed that the lactone products of the chosen substrates were substrates for the lactonase enzyme and thus no lactone products could be found. Therefore for homogenate biotransformations the addition of an inhibitor of lactonase activity would be required. Literature suggested that tetraethylpyrophosphate (TEPP) is an effective inhibitor of the lactonase enzyme (Donoghue *et al.*, 1975). After careful consideration this chemical, belonging to the organophosphate group, was considered to be too toxic for routine use even on a small scale.

Isatoic anhydride has been used in to inhibit dehydrogenase activity with purified enzyme but it is not as effective as TEPP and has not been found to be an inhibitor when whole cell catalysts are used.

Crude homogenate was found to require the addition of NADPH to allow the reaction to proceed. Figure 4.54 shows the disappearance of 4-methyl cyclohexanone with and without the addition of a stoichiometric quantity of NADPH.

Figure 4.55 shows a typical reaction profile for 20 mM biotransformation of 4-methyl cyclohexanone. Once again no lactone products could be identified. The isatoic anhydride interfered with the reaction and slowed down the rate. The unknown intermediate, most likely the alcohol, has been produced much more slowly and has not been totally transformed. Unlike in whole cells the CHMO activity was not protected by the presence of added cyclohexanol (Figure 4.56).

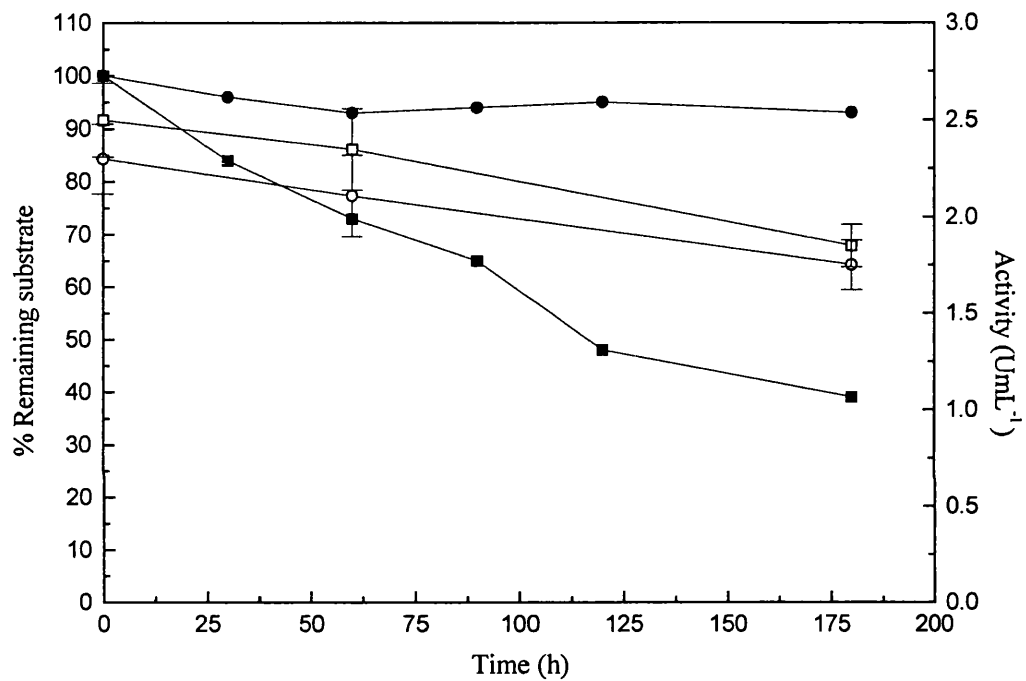


Figure 4.54 Biotransformation of 20 mM 4-methyl cyclohexanone by *A. calcoaceticus* homogenate under the conditions described in section 3.9.2. This figure shows the loss of substrate (closed symbols) and the CHMO activity (open symbols) with (■), and without (●) the addition of 40 mM NADPH. No lactone products could be identified.

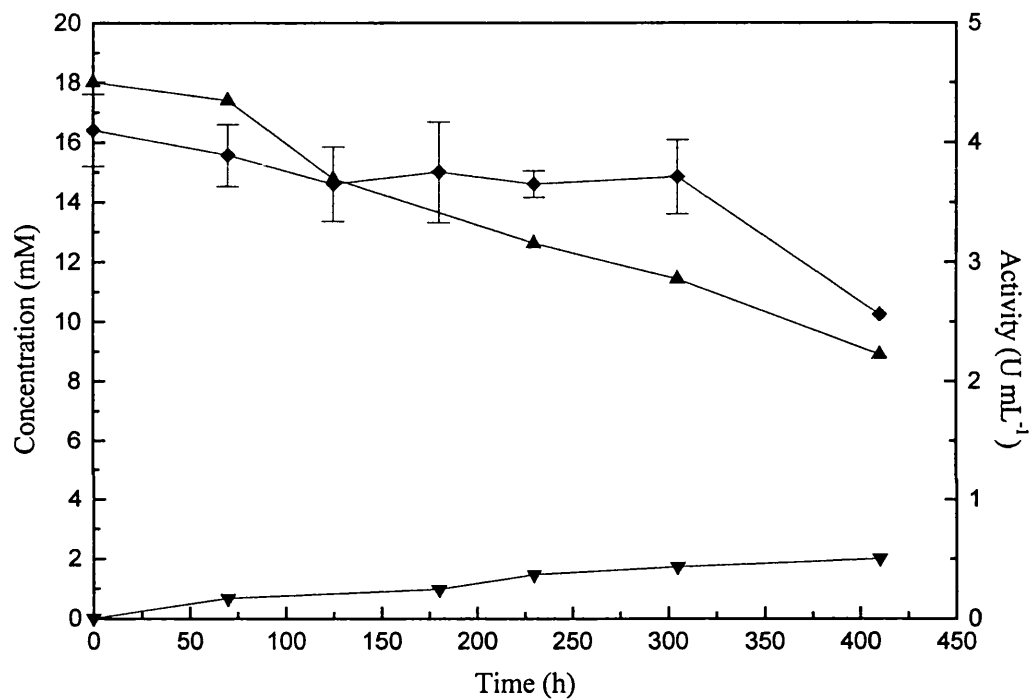


Figure 4.55 Biotransformation of 20 mM 4-methyl cyclohexanone by *A. calcoaceticus* homogenate with the addition of isatoic anhydride. This figure shows the effect of isatoic anhydride on the biotransformation of 4-methyl cyclohexanone (▲), production of the unknown (▼) (believed to be 4-methyl cyclohexanol from GC retention time), and CHMO activity (◆).

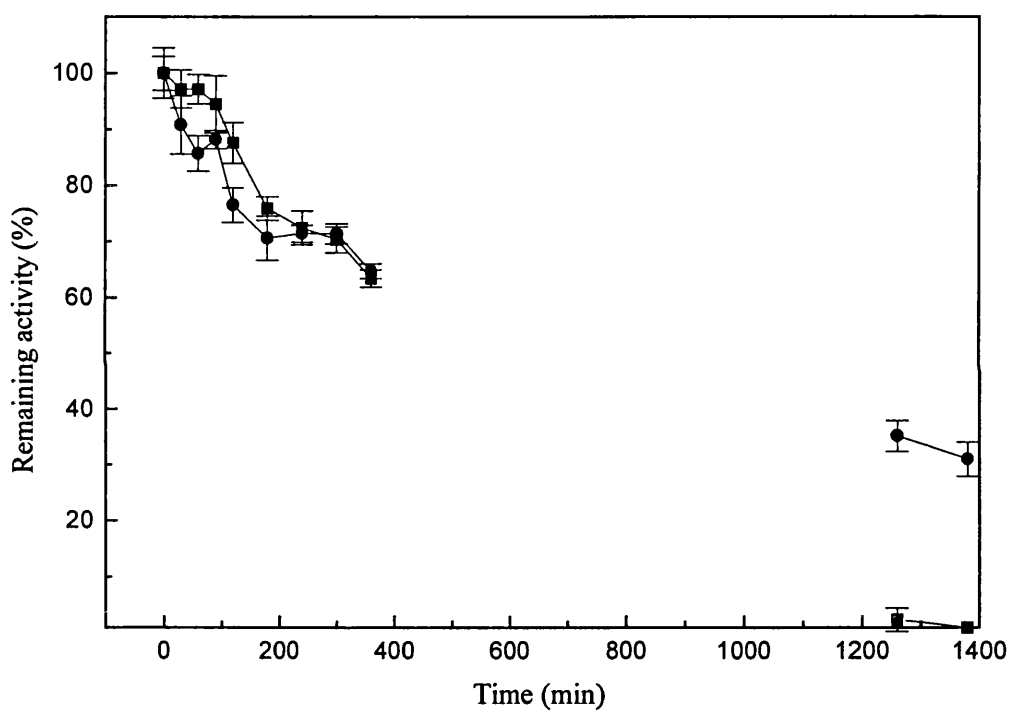


Figure 4.56 Stability of CHMO in *A. calcoaceticus* homogenate. This figure shows the effect on CHMO stability in buffered homogenate with the addition of 20 mM cyclohexanol (●), and without (■). Cyclohexanol does not confer the same stability to homogenate as was evident with whole cells.

4.7.2 Biotransformation of 2-methyl cyclohexanone

2-methyl cyclohexanone was chosen because the column was unable to resolve the enantiomers of substituted cyclopentanone as mentioned in section 2.2.2. Figure 4.57 shows a typical profile for a 20 mM biotransformation. No lactone products could be found indicating that the lactone dehydrogenase enzyme was not inhibited by the presence of isatoic anhydride. The enzyme showed a distinct preference for one enantiomer with the enantiomeric excess being approximately 30 %. No cyclic alcohol products of the back reaction of cyclohexanol dehydrogenase could be found.

4.8 Biotransformations - whole cell *Escherichia coli*

Whole cells of *E. coli* were grown and prepared, and biotransformations carried out in an orbital shaker as detailed in section 3.9.1. The reactions were buffered to pH 7 for reasons outlined previously (section 4.6.1).

Figure 4.58 shows a typical reaction with whole cells and 20 mM 2-ethyl cyclopentanone. Lactone product was identified but as discussed earlier the column was unable to resolve the enantiomers of the ketone substrates lactone product. It can be seen that the maximum concentration of lactone product is approximately 2 mM while the concentration of ketone has fallen by 5 mM. The control shows that the additional losses of ketone could not be attributed to evaporation.

4.9 Biotransformations - *E. coli* homogenate

The data for *E. coli* homogenate biotransformation was kindly supplied by Rachel Stones, Dept. Biochemical Engineering, University College London.

Figure 4.59 shows the stereoselective biotransformation of 20 mM 2-methyl cyclohexanone. Lactone products could be identified from their relative retention times and the two isomers are clearly resolved. The absolute conformations of these isomers

were not determined. Figure 4.60 illustrates the change in enantiomeric excess of one enantiomer over the other as the reaction proceeded. The e.e. of the lactone fell to 45 % and the e.e. of the remaining ketone 60% after 6 hours. At this point the yield of lactone was 30 % and 35 % of the ketone was recovered.

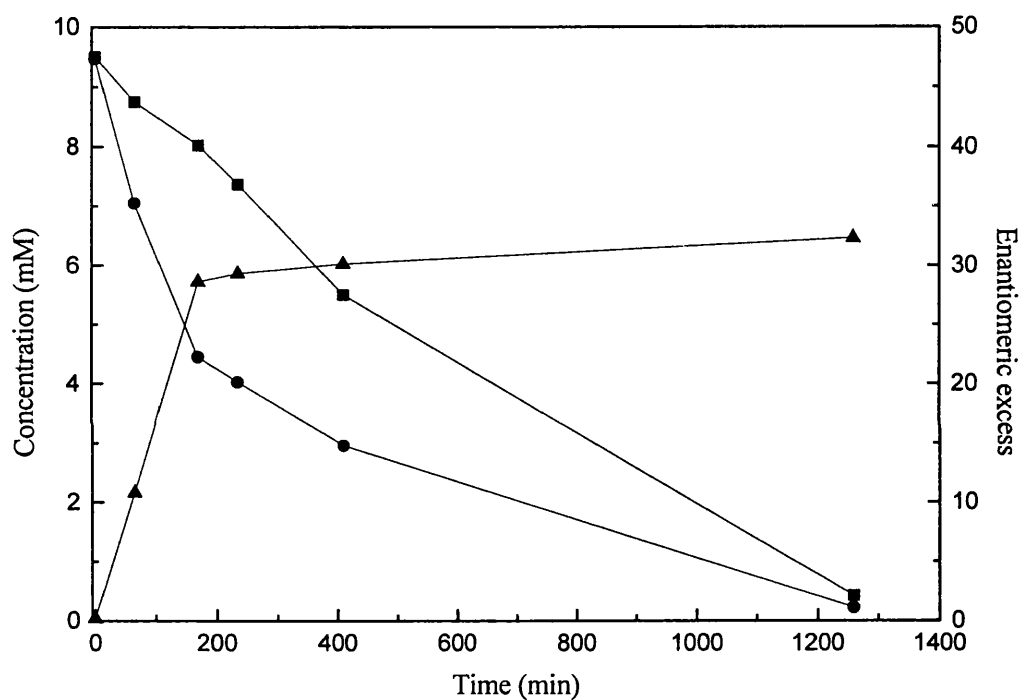


Figure 4.57 Biotransformation of 20 mM 2-methyl cyclohexanone by *A. calcoaceticus* homogenate with isatoic anhydride. This figure shows the selectivity of the enzyme as illustrated by the relative concentration of one enantiomer of 2-methyl cyclohexanone (■) over the other (●), and the enantiomeric excess of one over the other (▲). No lactone products could be identified.

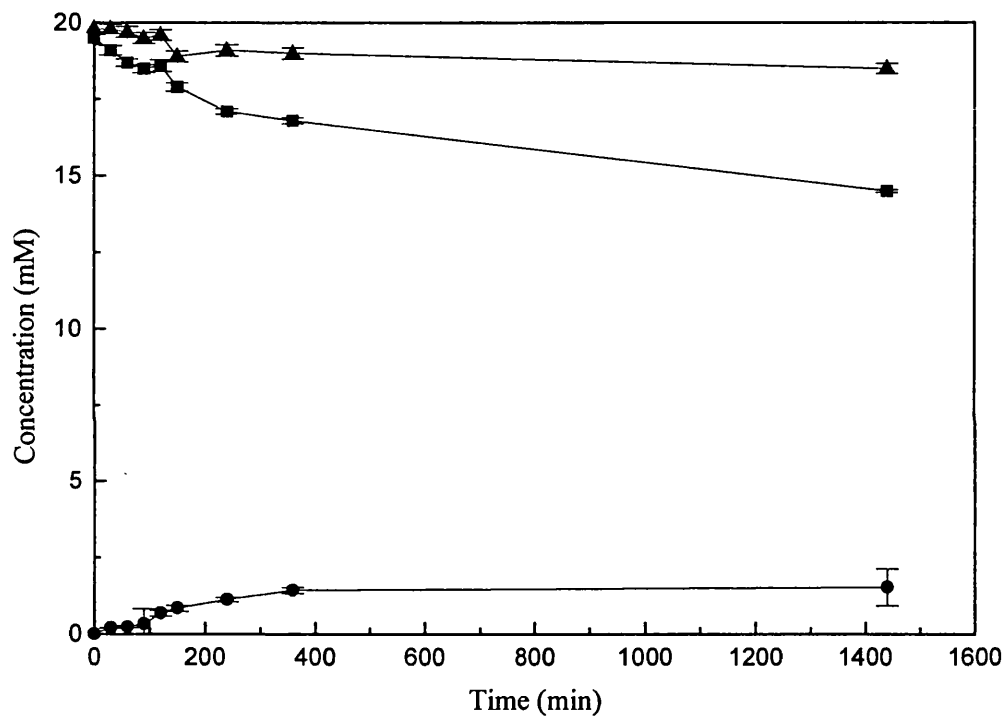


Figure 4.58 Biotransformation of 20 mM 2-ethyl cyclopentanone by whole cells of *E. coli*. This figure gives the results of a typical biotransformation and illustrates the poor conversion of 2-ethyl cyclopentanone (■), to the corresponding lactone (●), and the losses of ketone due to evaporation (▲).

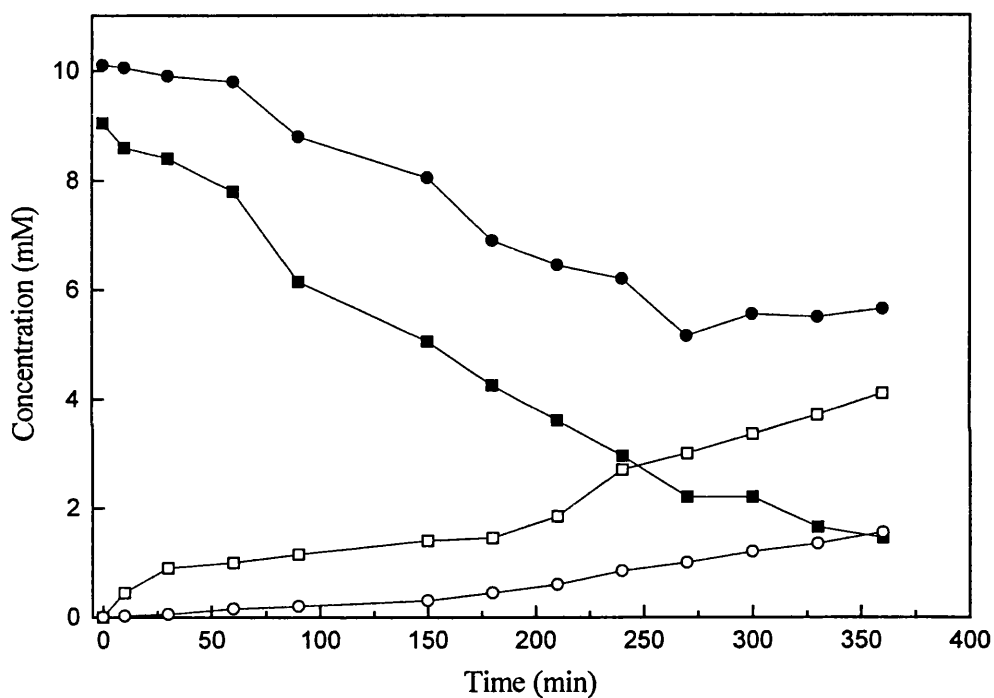


Figure 4.59: Biotransformation of 20 mM 2-methyl cyclohexanone by *E. coli* homogenate. This figure shows the selectivity of the enzyme as illustrated by the relative concentration of one enantiomer of the substrate, 2-methyl cyclohexanone (■) over the other (●), and the concentration of one isomer of the product, 2-methyl caprolactone (□) over the other (○).

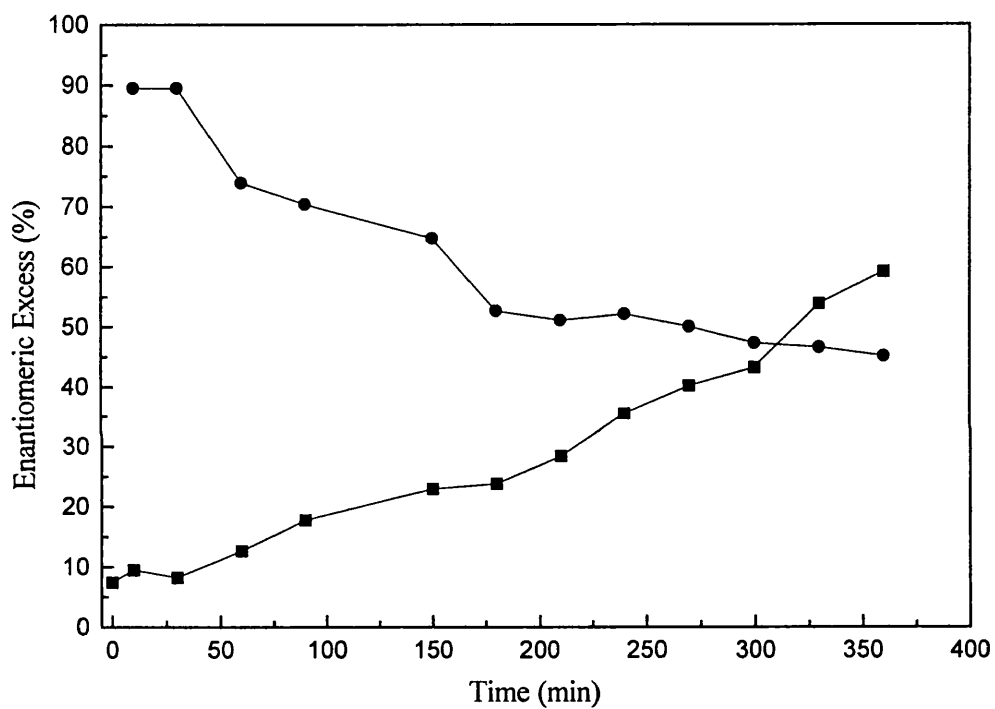


Figure 4.60: Biotransformation of 20 mM 2-methyl cyclohexanone by *E. coli* homogenate. This figure illustrates the enantiomeric excess of ketone substrate (■), and lactone product (●), for the biotransformation as described by figure 4.59.

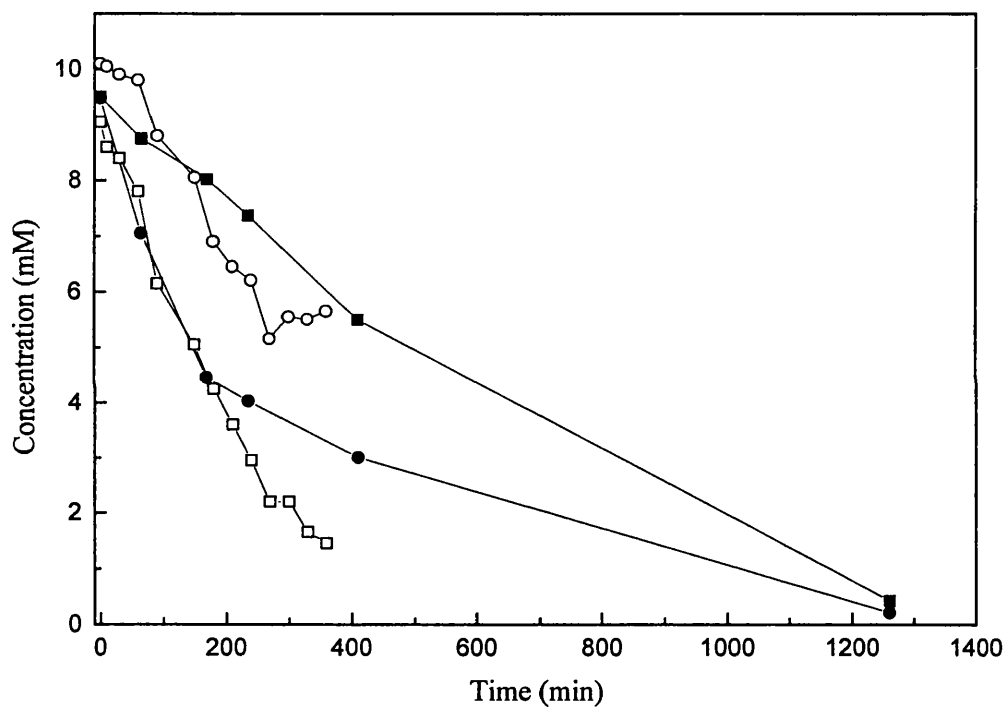


Figure 4.61 Comparison between *A. calcoaceticus* and *E. coli* homogenate biotransformation of 2-methyl cyclohexanone. This figure shows the increased utilisation of 2-methyl cyclohexanone by *E. coli* homogenate illustrated by the concentrations of the two isomers of the ketone in the *A. calcoaceticus* (■ and ●) and *E. coli* (□ and ○) reactions.

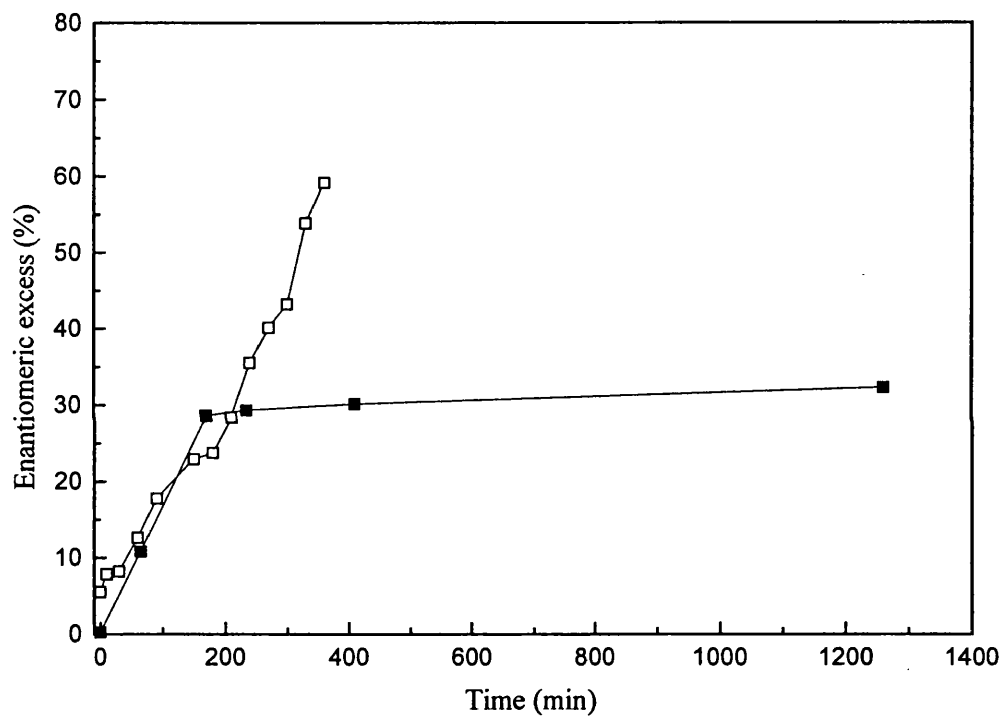


Figure 4.62 Comparison between *A. calcoaceticus* and *E. coli* homogenate biotransformation of 2-methyl cyclohexanone. This figure illustrates the enantiomeric excess of one isomer of the ketone substrate over the other in the *A. calcoaceticus* (■) and *E. coli* (□) reactions described by figure 4.61.

5 DISCUSSION

5.1 Biocatalyst production in *Acinetobacter calcoaceticus*

5.1.1 Carbon source investigation

Growth of *A. calcoaceticus* using cyclohexanol as the sole carbon source was found to be impractical for a number of reasons. There is a large lag phase, typically 9 hours, which was due in part to variability in the inoculum. There was large variability in the growth in shake flasks and predicting the optimum time for transfer to the fermenter was difficult. Inoculum transfer to the fermenter typically occurred between 16 and 25 hours after inoculation of the shake flask. There was still variation in the lag phase in the fermenter, however, when the inocula were at almost identical optical densities after the same length of time.

Due to the toxicity of cyclohexanol to the cells above approximately 1 g L^{-1} cyclohexanol had to be added to the vessel at intervals. The flammability of cyclohexanol prohibited its use in large quantities in the process area so a continuous feed was not possible.

The medium (table 3.2) provided sufficient nutrients to produce 15 g L^{-1} dry cells as shown when glutamate was used as the carbon source (figure 4.10). With cyclohexanol as the sole carbon source only 3 g L^{-1} was produced regardless of further additions. This was most likely due to an accumulation of toxic metabolites or the stress on the cell membranes of maintained exposure to cyclohexanol.

Biocatalyst production was therefore separated into biomass production and induction of cyclohexanone monooxygenase.

The use of succinate as a carbon source was found to be problematic due to foaming. The quantity of base required to neutralise the acid prior to inoculation, and the subsequent need for acid as the substrate was consumed during the fermentation caused a large increase in the salt concentration. Large volumes of antifoam were required to suppress foaming which caused a significant drop in the gas transfer and did not allow the biomass to be increased beyond 4 g L^{-1} . The long fermentation time required the need for automatic antifoam addition which proved to be unreliable. The foam produced was found to be slow to break down after addition of PPG solution. The automatic control could not be tuned to deal with this problem and allowed the foam to either block the off-gas filter or continued to dose large amounts of antifoam which suppressed oxygen transfer.

Succinate offered some advantage over cyclohexanol as carbon source with a much shorter fermentation time, 20 h compared to 50 h, and reduced need for operator supervision. The requirement for large volumes of flammable solvent and spark proof facilities are also removed. The advantages of succinate over cyclohexanol are significant for ease of process operation but negligible in terms of productivity. Further carbon sources were therefore investigated.

Glutamate was found to be a good carbon source and did not produce excessive amounts of foam as had other organic acid substrates. The need for pH readjustment during media make up was reduced compared to succinate with a corresponding reduction in the amount of pH control required. The growth rate was double that which had been achieved with succinate which offered significant process advantages. The growth profile was similar to that of succinate with a similar lag phase of 5 hours. Fermentations with glutamate as a substrate were found to be more reproducible than with either cyclohexanol or succinate. This was due to more reproducible growth in the inoculum shake flasks allowing transfer when the cells were in the optimum condition. The fermentation proceeded without the need for excessive volumes of antifoam allowing good oxygen transfer to be maintained throughout. As mentioned previously the medium allowed the production of up to 14 g L^{-1} from 30 g L^{-1} glutamate. This was the maximum biomass achievable without the fermentation becoming oxygen

limited. The dissolved oxygen tension (data not shown) was maintained above 15 % throughout the fermentation illustrated by figure 4.7.

Throughout the fermentation no CHMO activity could be detected. As expected cyclohexanone monooxygenase is therefore not constitutively produced by *A. calcoaceticus* but is instead only produced when the cells are exposed to a cyclic alcohol or ketone. Both substrates have been found to induce activity (Sandey 1991) but the actual induction method is not clear since the alcohol is oxidised to the ketone and *vice versa*.

When cyclohexanol was added at the end of the fermentation (section 4.2.4) induction of CHMO had not been achieved after 5 hours. The most likely explanation is that, as had been seen previously with cells grown exclusively on cyclohexanol, there is a significant lag of up to 9 hours before growth occurs. This is attributable to the switching of metabolism to include the cyclic alcohol degradation pathway. The cells cannot be maintained routinely on a solid medium containing cyclohexanol so this lag is inevitable if cultures are stored on plates and shake flask inocula are grown on media not containing cyclohexanol.

For this reason all further fermentations were inoculated with cells that had been grown on glutamate and cyclohexanol as co-substrates.

5.1.2 CHMO production

The larger scale 7 L *A. calcoaceticus* fermentations illustrated in figures 4.9 and 4.11 show distinct evidence of diauxic growth with a very clear switch between substrates. The change in RQ demonstrates the difference in the oxidation states of the two substrates with cyclohexanol requiring more oxygen to be fully metabolised.

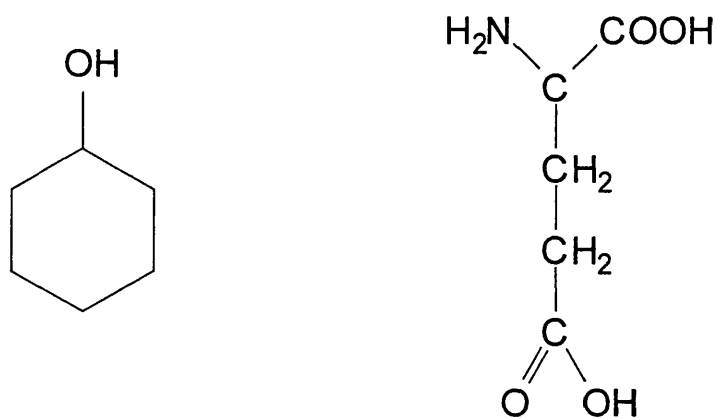


Figure 5.1: Carbon sources for *A. calcoaceticus*

Table 5.1 summarises the results of the carbon source investigation to maximise biomass produced. The advantage of glutamate as a carbon source is very clearly illustrated producing significantly more biomass in a much more reasonable time. After addition of cyclohexanol at the end of the fermentation the cells produced CHMO to the same level that had been found when cyclohexanol had been the sole carbon source.

Carbon source	Biomass (g L ⁻¹)	Growth rate (h ⁻¹)	CHMO (U gdc ⁻¹)
Cyclohexanol	3	0.16	25
Succinate	4	0.22	-
Glutamate	14	0.44	25

Table 5.1: Summary of carbon source investigation.

The fermentation profiles illustrated in Figures 4.9 and 4.11 show good agreement. In the first fermentation the inducing cyclohexanol (1 g L⁻¹) was added 1.5 hours after the fermentation had become oxygen limited and glutamate had become exhausted as evident from the rapid decline in cellular respiration. CHMO was induced

to approximately 25 U gdc^{-1} (Figure 4.10) 90 minutes later and was seen to rapidly decline once the cyclohexanol was exhausted. The second fermentation (Figure 4.11) was induced immediately upon the exhaustion of glutamate as indicated by a sudden drop in the OUR and CER. Twice as much cyclohexanol as the previous fermentation was added and the CHMO reached a maximum of 20 U gdc^{-1} . The activity is not seen to fall as rapidly because the cells are metabolising cyclohexanol for longer. As previously seen in shake flasks the cells rapidly lose activity once the cyclohexanol is consumed. This effect can be minimised by the addition of cyclohexanol just prior to harvesting the cells to maximise productivity. Increasing the concentration of the alcohol has a negative effect on CHMO production most likely due to cellular membrane damage by the solvent (Sandey, 1991).

For large scale production of the biocatalyst the rapid decline of activity after induction could dramatically reduce the productivity of the fermentation if the conditions are not carefully monitored and controlled. The time taken to process large volumes of cells would make it difficult to maintain high levels of activity.

The use of glutamate and cyclohexanol as growth substrates followed by induction by cyclohexanol addition has increased the productivity of the fermentation from 75 to 350 U L^{-1} . The time for the fermentation has also been reduced from 50 to 15 hours. The productivity if defined as units of CHMO produced per litre per hour has therefore increased from $1.5 \text{ U L}^{-1} \text{ h}^{-1}$ to $23 \text{ U L}^{-1} \text{ h}^{-1}$. This represents a significant advantage in both processing time and cost.

5.2 Biocatalyst production in *Escherichia coli*

5.2.1 Over expression of CHMO in an *E. coli* construct

Dr. Sejal Patel (UCL) excised the fragment of DNA containing the CHMO gene from *A. calcoaceticus* and inserted it into a high copy number plasmid pQR210 in an *E. coli* host (lab strain JM107). The gene was placed under the control of a *tac* promoter, a hybrid of *lac* and *trp* promoters (de Boer *et al.*, 1983) that has much increased productivity over the parental promoters (Amann *et al.*, 1983). The construct was selected for by ampicillin resistance conferred by the presence of the gene encoding for β -lactamase in the plasmid. The addition of ampicillin to the growth medium could therefore be used to prevent the accumulation of plasmid free cells. Induction of the recombinant CHMO could be stimulated by the addition of IPTG to the growth medium. IPTG, which is an analogue of lactose, is not metabolised by the cells and so its concentration and inducing effect is maintained.

The over-expression of CHMO from recombinant *E. coli* cells should allow for much greater productivity over *A. calcoaceticus* and due to the much greater understanding of *E. coli* fermentations an easier process for biocatalyst production.

The construct was found to produce active CHMO protein with glycerol as the carbon source (Figure 4.1). Glycerol was chosen as the carbon source because growth on sugars tends to inhibit the *tac* promoter. There is also evidence that at high cell concentrations the production of acetate from incomplete sugar metabolism may reduce the production of recombinant protein (Lee, 1996). This strain of *E. coli* has been successfully grown on glycerol at UCL to 20 g L⁻¹ by Dr. Gordon Hobbs to produce recombinant transketolase (Hobbs *et al.*, 1996).

5.2.2 Plasmid stability

The production of large scale enzyme biocatalyst requires a progression in the scale of culture to the final fermenter volume required. It is vital therefore that the cells are in the best condition possible at each stage to maintain high productivity. As mentioned previously in section 4.3.3 the loss of plasmid from the cells during any of these stages will dramatically reduce the production of recombinant CHMO. It was vital to assess the stability of the plasmid and how prone the cells were to segregational plasmid instability. Table 4.3 shows that after 22 hours growth in a shake flask there is some loss of plasmid especially when grown on defined medium. The most likely explanation for this phenomenon is the well documented process of secretion of the β -lactamase. β -lactamase, which confers ampicillin resistance, is secreted into the periplasm where it degrades the ampicillin, reducing the effective concentration with time (Georgiou *et al.*, 1988). As the concentration decreases so the likelihood of plasmid loss increases. The plasmid free cells are believed to have a faster growth rate than those still containing a plasmid since they have a lower metabolic burden. However, the loss of plasmid containing cells in this recombinant strain has been shown to be minimal during the likely fermentation time.

5.2.3 IPTG concentration

IPTG which is required to induce the *tac* promoter and hence production of CHMO is expensive and the required concentration must therefore be as low as possible. Figure 4.15 shows that the minimum concentration required for CHMO induction that was approaching the maximum achieved is 0.25 mM. Further increase to the concentration had little effect on productivity. This was not unexpected since the compound is known to be a very strong inducer and, since it is not metabolised, the concentration required is therefore low. Increasing the concentration has no effect once the production of recombinant enzyme is at its maximum rate. To insure that expression was at its maximum a concentration of 0.5 mM was used for subsequent fermentations to allow for any losses of IPTG due to chemical reactions or thermal instability.

5.2.4 Growth and production of CHMO on complex media

Initial fermentations used complex medium for growth with glycerol as a carbon source. The cells grew at a growth rate of 0.7 h^{-1} and reached a maximum cell concentration of 6 g L^{-1} before the oxygen demand became greater than the maximum the vessel could supply. The components of the complex medium caused significant amounts of foaming and thus required the addition of significant quantities of antifoam. A large concentration of antifoam is undesirable for a number of reasons. The surfactant nature of antifoams means that they act as a barrier to gas transfer and thus reduce the fermenter's ability to supply oxygen. The need to remove antifoam during downstream processing can also be a problem as it can reduce homogeniser efficiency and make protein purification difficult.

During the fermentation illustrated by figures 4.16 to 4.18 CHMO production was induced after 3 hours when the cells were in the exponential growth phase. Over 800 U gdc^{-1} of CHMO were produced. This is an improvement over the shake flask production where 300 U gdc^{-1} were produced. The maximum activity was reached much more quickly in the fermenter and the lag in production which had been seen in shake flasks was not present. This was most likely due to the increased oxygen transfer in the fermenter which has been reported to be of great importance when producing recombinant proteins (Bhattacharya and Dubey, 1997).

A repeat fermentation with increased concentration of glycerol that allowed the fermentation to become oxygen limited was performed. Figures 4.19 and 4.20 show the profile of such a fermentation. The cells grew at an exponential rate (0.7 h^{-1}) until 6 hrs when oxygen became limiting and growth continued, albeit at a continually decreasing growth rate, until the nutrients were exhausted after 9.5 hours. CHMO induction was attempted after 6 hours when the fermentation was growth limited on oxygen as indicated by the decline in OUR and CER. Only 250 U gdc^{-1} of CHMO activity were induced indicating that cells require a well oxygenated environment for maximum protein production. The oxygen limitation did not effect the rate of CHMO production with the maximum activity found after approximately 2 to 2.5 hours after induction in both cases.

The problem of foaming when grown on complex medium and the inherent variation in product specification make clearly defined media the preferred choice for industrial fermentations.

5.2.5 Initial study of growth and production of CHMO on defined media

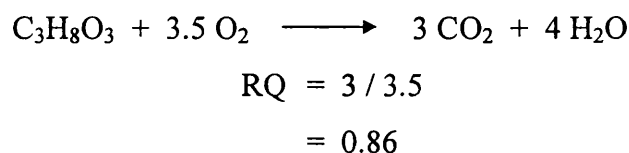
As stated earlier the defined medium used was chosen because it was known to support the growth of strain JM107 to at least 20 gdc L⁻¹ (Hobbs *et al.*, 1996). Initially batch fermentations were carried out to gain data that would be required for any subsequent fed batch fermentations.

The complex medium fermentations showed that induction of CHMO must be achieved while dissolved oxygen is at a sufficient concentration to prevent any limitation to growth. This information meant that the glycerol concentrations would have to be kept at a level that would allow OUR to remain below approximately 80 mMole L⁻¹ h⁻¹ since this is the maximum transfer rate achievable by the vessel with the DOT maintained above 20 %. To achieve this transfer rate the stirrer was operating at maximum output of 1100 rpm and the air flow rate was 1 v v⁻¹ min⁻¹. Further increases in the gas flow rate caused excessive foaming and some cavitation around the impeller which has serious implications for the mixing conditions in the vessel.

Figures 4.21 to 4.23 show a typical profile for a batch fermentation on defined medium. After a lag period of approximately two hours an exponential growth phase began. The exponential growth phase continued at 0.43 h⁻¹ until 9.5 hours when the glycerol became exhausted. This growth rate is significantly slower than when the complex medium is used (0.7 h⁻¹). This is expected since the cells have to synthesise many more components from basic chemicals that would be supplied by the complex medium. The stirrer was increased throughout the fermentation to maintain the DOT above 10 % at all time and preferably above 20%. From 15 g L⁻¹ glycerol a dry cell concentration of 7 g L⁻¹ was achieved. Figure 4.21 illustrates clearly that an OUR of 60 is the maximum achievable with a DOT above 20%. At this point the gradient of the curve shows that after another 30 minutes the DOT would be zero.

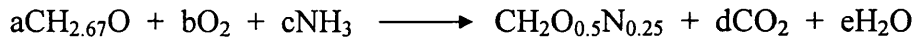
The effect, if any, on the production of CHMO when using defined medium had to be investigated. Figures 4.18 and 4.20 show the profiles for identical fermentations where induction of CHMO was initiated by the addition of IPTG during the exponential growth phase. Due to scheduling difficulties the inocula for these fermentations were not in the ideal condition. Figures 4.21, 4.24 and 4.27 should show identical growth profiles. The shake flasks used for inoculation were incubated for too long in the second two fermentations. This has resulted in a much increased lag phase from 4 hours in the first fermentation, where the inoculum was in mid exponential growth phase, to 6 and 8 hours respectively, where the inocula had been allowed to grow to stationary phase. Once the exponential growth phase had been reached the profiles are very similar. All reached a maximum growth rate of approximately 0.44 h^{-1} with a maximum OUR of $65 \text{ mmole L}^{-1} \text{ h}^{-1}$ and a cell density of 7 g L^{-1} , with the exception of the fermentation illustrated by figures 4.20 and 4.21 which reached only 5 g L^{-1} . This loss of yield can be explained by the increased lag phase where the cells were recovering from the stationary conditions in the inoculum. When the inocula cultures have reached the stationary phase the potential for plasmid loss from some cells is increased. This can lead to a greater proportion of non plasmid bearing cells in the inoculum. The figures show however that there was little if any loss of plasmid containing cells throughout the fermentations. The increased lag phase can thus be explained by the reduced number of viable cells entering the vessel from the seed flask and that the cells would have been in the stationary phase and nutrient depleted.

The respiratory quotient settled at 0.74 after initial noise. If the glycerol had been completely oxidised an RQ of 0.86 would be expected since 1 mole of glycerol produces 3 moles of carbon dioxide from the consumption of 3.5 mole of oxygen.



This shows that some or all of the glycerol is not being fully oxidised. The discrepancy is due in the main part to the incorporation of carbon in the construction of cell mass and to a lesser extent the production of organic acids. Organic acids tend to be produced

when the cells are not supplied with sufficient oxygen and the fermentation becomes anaerobic. Under the fermentation conditions present there should not have been anaerobic conditions. Assuming that to be the case the above equation can be replaced with one taking into account the carbon utilised by cell mass by estimating the elemental composition of the cells (Atkinson and Mavituna, 1983).



$$\text{C: } a = 1 + d$$

$$\text{H: } 2.67a + 3c = 2 + 2e$$

$$\text{O: } a + 2b = 0.5 + 2d + e$$

$$\text{N: } c = 0.25$$

To solve the simultaneous equations requires a further relationship which can be taken from the growth yield on glycerol; 0.47 gdc g^{-1} . The yield on glycerol is therefore equal to formula weight of dry cells divided by the formula weight of cells multiplied by the exponent a .

Solving the equations gives: $a = 1.76$, $b = 0.99$, $c = 0.25$, $d = 0.76$ and $e = 1.72$. The RQ can be simply calculated from d/b to give 0.77 . This value is very close to the observed value when considering that the formula is based on average cell composition.

When induced by the addition of IPTG the maximum activity was much lower than had been achieved with complex growth medium. As discussed in section 4.4.1 the small loss of plasmid does not account for this loss in active protein. The loss of activity would make a defined medium fermentation very costly since no increase in productivity would be gained even if the cell density could be increased dramatically by a fed batch regime.

The loss of activity could be due to this cell strain requiring additional nutrients to produce CHMO at the desired level. To make an assessment of exactly what this nutrient or nutrients may be would be very time consuming. The complex medium fermentations had shown that the CHMO could be produced to 900 U gdc^{-1} so yeast extract and tryptone were subsequently added at the time of induction.

Figures 4.30 to 4.32 show the results of this fermentation. Glycerol at a concentration of 20 g L^{-1} was inadvertently added. This combined with the increased oxygen requirement for the metabolism of the components of the yeast extract and tryptone increased the demand to greater than that which could be supplied. Consequently the DOT fell to zero and the OUR reached $100 \text{ mMole L}^{-1} \text{ h}^{-1}$. The early portion of the data was lost due to a problem with the mass spectrometer gas analyser. The inoculum was in the ideal condition for this fermentation which has minimised the lag phase. CHMO was produced after induction and reached a maximum of 800 U gdc^{-1} after approximately 2 hours. The maximum CHMO activity was recorded before the DOT fell to a level that had previously been shown to reduce the enzyme titre. This is comparable to cells grown and induced on complex growth medium. Many of the advantages of a defined medium are still maintained since the majority of the growth phase is on a defined medium. The problems of foaming and lack of reproducibility that can occur with complex medium are removed but the productivity of the complex medium can be maintained.

This information gave the required operating conditions for the fed batch fermentation development.

5.2.6 Development of fed-batch fermentation

A fed batch fermentation would allow the cell concentration to be increased and hence increase the productivity of the fermentation. To further increase the biomass in a batch fermentation would require increased oxygen supply by supplementation of sparging air with oxygen. A fed batch system allows the growth rate to be controlled and hence the oxygen demand can be controlled to below that which the fermenter is capable of supplying. As discussed in section 4.4.3 it has been widely reported that reducing the growth rate of a recombinant *E. coli* fermentation reduces the loss of plasmids from the cells and can enhance the production of recombinant protein.

5.2.7 Constant growth rate

During batch fermentation the cells grow at the maximum growth rate (μ_{\max}) for that particular medium. Reducing this growth rate by controlled addition of the carbon source may increase the production of CHMO. A fed batch fermentation was attempted with the LabView controlled pumps set to deliver glycerol at a rate that would produce a growth rate of 0.15 h^{-1} . Figures 4.33 and 4.36 show the gas profiles for two fed batch fermentations where the initial glycerol concentration in the medium was 1 g L^{-1} and 5 g L^{-1} respectively.

The depletion of the limited supply of glycerol in the batch phase was shown by a rapid decline in the OUR and CER and a corresponding rise in the DOT. The biomass concentration was estimated from optical density at this point and the pumps controlling the glycerol feed turned on to initiate the fed-batch phase of the fermentation.

The gas profile (figure 4.3) is as would be expected until the point of IPTG addition. There is a sudden rapid increase in the OUR and CER profile and a small increase in the RQ that then settles to the original level. This could be due to an explosion of growth due to the addition of the complex medium components at this time or the change in metabolic pathways to produce the recombinant protein. The values of OUR and CER are lower than would be expected however when compared to those obtained from the second fermentation. This indicates that growth was interrupted by the addition of IPTG and the complex nutrients. There is no evidence of this phenomenon in subsequent fermentations however. The pressure in the vessel had increased again due to a partially blocked air filter. It was discovered that the cooling water for the condensers had inadvertently been connected to the incorrect supply and was not sufficiently cool to efficiently condense the moisture in the off-gas. The increased pressure may have damaged some of the cells which may explain the uncharacteristic gas profile during induction.

The profile for the second fermentation shows that growth was not interrupted by the addition at 20.5 hours. The cells were induced to produce CHMO before the maximum biomass achievable with this medium was reached because earlier experiments had shown that dissolved oxygen was important for good expression of

active protein. Figures 4.36 to 4.38 illustrate that CHMO activity had reached a maximum when DOT had fallen to only 50 %.

The RQ appeared very unstable in all fermentations due to small errors in the readings of relative oxygen and carbon dioxide. This was due to the sparge gas composition not being measured directly but taken instead from an average value. The gas analyser reference air pump had been malfunctioning intermittently and had produced uneven gas flow. For this reason average values from the room were taken as reference and so did not take into account any changes in the actual composition of the feed air source throughout the fermentation.

In the second fermentation (Figures 4.36 to 4.38) there was an increase in the RQ value once the fermentation had been switched to the constant growth rate phase which then fell slowly to the original value. This increase in RQ due to a relative increase in CO₂ evolution would tend to indicate that the cells were incorporating less carbon into cell mass and respiring more indicating a higher requirement for maintenance energy.

The production of CHMO in each case follows a similar profile (figures 4.34 and 4.37) reaching a maximum approximately 2.5 hours after induction. The second fermentation produced 10 % less maximum activity, 388 U gdc⁻¹ compared to 436 U gdc⁻¹. This is difficult to explain since the fermentations were essentially identical. In the first fermentation the OUR and CER data are very different to the second after induction and would tend to indicate a lower growth rate, this was not evident in dry cell weight determinations over the same period however. In the second fermentation the RQ is seen to decline steadily during the controlled growth rate phase indicating that less CO₂ was being produced. The production of organic acids or greater incorporation of carbon into the cells could account for this discrepancy. The production of organic acids by *E. coli* is well documented (Luli and Strohl, 1990; Pan *et al.*, 1987) but is usually associated with a oxygen limitation and therefore incomplete oxidation of the carbon source. This change in metabolism could account for the slight loss in CHMO activity.

5.2.8 Constant feed rate

When considering the implications for scaling up such a fermentation, maximum gassed power must be taken into consideration. The maximum oxygen supply rate of larger fermenters is lower and can be assumed to be in the region of $50 \text{ mmole L}^{-1} \text{ h}^{-1}$ for a 1500 L vessel. An exponentially fed fermentation will still allow the fermentation to become oxygen limited. To reach the maximum achievable biomass without oxygen limitation for a given medium would therefore require a constant feed rate of glycerol to maintain an OUR close to but not exceeding the maximum achievable by the vessel.

Figure 4.39 shows a fed batch fermentation where after the initial batch phase the pumps were set to deliver sufficient glycerol to allow a growth rate of 0.15 h^{-1} . During the batch phase the cells grew as expected from previous fermentations with a growth rate of 0.44 h^{-1} . When the limited carbon source (5 g L^{-1}) was depleted the cell concentration was 2.4 gdc L^{-1} which was a yield of 0.48 gdc g^{-1} . During the exponential feeding phase a total of 84 mL of feed (700 g L^{-1}) was added corresponding to 58.8 g glycerol. The DCW had increased by 5.5 g L^{-1} (22.4 g) indicating a yield of 0.38 g g^{-1} . The RQ fell steadily throughout the period of controlled growth from ≈ 0.8 to 0.74 the expected value for batch fermentation. A possible explanation is the production of organic acid during the batch phase of growth. If at this lower growth rate the production of acid was reduced and the acid produced during the batch phase were utilised by the cells, the amount of carbon dioxide produced would be greater. This would have the combined effect of raising the RQ. As the acid was used by the cells the amount of carbon dioxide produced would gradually decrease to the level expected.

When the OUR had reached a value of $50 \text{ mmole L}^{-1} \text{ h}^{-1}$ the pumps were set to deliver a constant feed at that rate of addition reached at that point. As the rate of glycerol added is constant the oxygen requirement to metabolise it should also be constant and it would be expected that for a constant volume the OUR and CER would also remain constant. As feed is added there is an increase in volume but this was taken into consideration when calculating the values by taking data from LabView and inputting it into the spreadsheet for OUR and CER calculations. There was a gradual and linear increase however with a much smaller but steady increase in the RQ. During linear feeding the cells are growing at a constantly decreasing growth rate which is clearly

indicated in figures 4.40 and 4.41. The increase in OUR and CER is accompanied by a corresponding decrease in the DOT indicating that the demand for oxygen was increasing throughout feeding.

The previously mentioned organic acid production and subsequent metabolism could explain this increase in RQ but the amount of acid produced is unlikely to have been sufficient to cause an elevated RQ for the length of the period of the linear feeding. The most likely explanation is an increase in the maintenance energy requirements of the cell. As the growth rate decreases the proportion of energy that is utilised by the cells for maintenance becomes more significant until a point is reached where the feed rate of glycerol is no longer sufficient to support an increase in biomass.

When induced with CHMO after 31.5 hours the production of CHMO was rapid reaching a maximum of 100 U gdc^{-1} after 3.5 hours. The time taken to reach maximum activity was slightly longer than when induction occurred during the period of controlled growth rate. This is due to the metabolism of the cells being at a generally lower rate due to the very low growth rate. The addition of complex nutrients at this stage as had been indicated as a requirement during earlier fermentations produced no noticeable change in metabolism. Neither OUR, CER or RQ showed any significant change after induction although towards the end of the induction period (defined as when maximum CHMO activity had been reached) there was a period when the DOT stopped decreasing. There is no associated change in the gas analysed however. After 40 hours there was no measurable increase in dry cell weight although the cells continued to respire at approximately the same rate.

In the second fermentation illustrated by figures 4.42 to 4.44 constant feed rate was started immediately after batch phase with no period of constant growth rate. The OUR and CER were much greater in the batch phase due to the pumps being switched on after 8 hours of growth thus effectively increasing the amount of glycerol available for exponential growth. The RQ slowly increased during feeding as in the previous fermentation around ≈ 0.8 . The cells reached a greater concentration than in the previous fermentation with an average yield of 0.34 gdc g^{-1} glycerol. After induction the maximum activity of 120 U gdc^{-1} was reached after 3 hours

5.3 Stability of stored catalysts

5.3.1 Whole cells

An important factor when considering which form of biocatalyst to use is the stability of that catalyst during storage. Both *A. calcoaceticus* and *E. coli* showed that under the storage conditions tested active CHMO can be maintained for many months (Figures 4.45 and 4.46). The addition of a cryo-protectant such as glycerol while offering no advantage to the stability of CHMO does allow the cells to be stored in a viable condition for use in whole cell biotransformations. In the case of *E. coli* the cells have retained half of their original activity after some 24 months when stores at $-18\text{ }^{\circ}\text{C}$. The variability in the data is due to the method of sampling. When material was prepared for freezing it was dispensed in aliquots so that the bulk was not disrupted by thawing after each time point and there was likely to have been some variability in the cell concentration dispensed.

This means that active CHMO can be produced on a large scale and stored for use in future biotransformations. Samples from the cells removed from storage after 150 days were diluted and plated onto agar and incubated. When examined after 32 hours there was an average of 300 discreet colonies from the cells stored in glycerol and only ten or twenty from those stored without. A freshly grown culture, of a similar cell concentration, plated under the same conditions produced confluent growth. Although this showed that the storage conditions are adequate for maintaining CHMO activity, it does not necessarily infer that the cells would be useful for whole cell biotransformation.

When used as a biocatalyst the cell must be metabolising to recycle NADPH and facilitate the biotransformation. Cells that have been frozen, while viable, are unlikely to be in an optimum condition and may require a period for recovery before efficient function.

As discussed earlier the CHMO activity was found to decrease rapidly at the end of the fermentation once the cyclohexanol was exhausted. When the cells had been harvested, i.e. removed from the culture medium by centrifugation, the reduction in CHMO activity with time was greatly reduced. When the cells were resuspended in

buffered solution the cells maintained CHMO activity for a number of hours at room temperature typically losing activity after 5 or 6 hours (Figure 4.49). This shows that the rapid decline in CHMO activity experienced at the end of fermentation was due to metabolic activity within the cells. Presumably the removal of nutrients from the cells slows down metabolism and hence the destruction of the enzyme.

5.3.2 Homogenate

A. calcoaceticus homogenate was not tested for stability. If the biocatalyst was required in a homogenate or purified form, there would be no advantage in producing enzyme by *A. calcoaceticus* fermentation. As previously discussed, *E. coli* is a far more productive vehicle for producing the catalyst in this form.

Figure 4.47 shows the stability of clarified homogenate under a variety of conditions. All samples originated from the same batch of cells and were stored under the same physical conditions. It is very clear that the activity is lost very rapidly when the homogenate is stored at 4 °C even when sodium azide or ampicillin was added to prevent contaminating microbial growth. There was a slight improvement in stability when anti-microbial agents were added indicating that a small proportion of the loss in activity could have been due to bacteria utilising the enzymes in the homogenate as an energy source. The remainder of the loss therefore, is likely to be due to the action of protease enzymes naturally present in *E. coli*. The action of these enzymes can be inhibited by the addition of chemicals but when planning biotransformations the system should be kept as simple as possible with the minimum amount of potential interfering chemistry.

It is interesting that when stored with glycerol present the activity appears to be maintained more effectively than with buffer solution alone (Figure 4.47). The gradual decline of activity in the homogenate stored in buffer alone would indicate that the effect is not due to assay interference since the effect should have been observed in the early samples as well. As the same batch of homogenate was used for all storage conditions, the protein concentration and hence activity in the samples stored with glycerol was approximately half that of the buffer only homogenate. It is possible that

this dilution infers stability to the homogenate or that the reduced water activity due to the presence of glycerol inhibits the action of degrading enzymes.

5.4 Biotransformation - *A. calcoaceticus* whole cells

5.4.1 Stability of CHMO activity during biotransformations

The stability of CHMO activity during a reaction was vital to the success of the reaction and a significant factor to the usefulness of whole cells as a biocatalyst. Figure 4.49 shows the stability of CHMO activity in *A. calcoaceticus*, during a cyclohexanone biotransformation. After 300 minutes there was no loss of activity compared to the control cells without addition of the substrate. Figure 4.48 shows that at this point there was still a significant concentration of cyclohexanol present in the medium and it must therefore be this or the presence of its metabolites that infer this stability. The presence of cyclohexanol, which induces the production of CHMO, must either be continuing to stimulate the production of new CHMO and balancing the proteolysis or repressing the proteolysis.

Figure 4.51 shows that the presence of 2-ethylcyclopentanone does not have the same CHMO activity protecting activity that was present in the cyclohexanone biotransformation. This cyclic ketone was likely to have been a substrate for CHMO and the lactonase enzyme since no lactone production was observed.

2-ethylcyclopentanone can however be seen to be a poor substrate for the alcohol dehydrogenase as there was very little 2-ethylcyclopentanol produced. It is possible therefore that it is the presence of the alcohol that maintains the CHMO activity. Studies by earlier workers have shown that cells grown on cyclohexanol or cyclohexanone exhibit the same pattern of enzyme production and that either substrate promotes the production of all the enzymes in the pathway (Sandey and Willetts, 1992). For future whole cell biotransformations, cyclohexanol was added as a co-substrate to maintain the activity of CHMO.

5.4.2 Cyclohexanone

For *A. calcoaceticus* cells to produce biotransformation products the cells must have a mechanism that allows the diffusion, facilitated or otherwise, of both simple and complex cyclic alcohols, ketones and lactones through the cell wall and membrane. Figure 4.58 shows the results of a typical biotransformation of cyclohexanone. All species were identified and quantified by their relative retention times when compared to standards analysed by GC (section 3.1.2). No products of CHMO could be identified as expected by the over-metabolism of the lactone product by the later enzymes in the pathway (figure 1.8).

It can be seen that cyclohexanol dehydrogenase is catalysing the reverse reaction to produce cyclohexanol. This reaction is running at approximately the same speed as the monooxygenase catalysed lactonisation indicated by the fact that after 300 minutes the ketone has disappeared and the alcohol has reached a concentration of 10 mM. From this point on CHMO produces lactone at the same rate that the alcohol dehydrogenase produces ketone since no further cyclohexanone could be measured.

5.4.3 2-ethyl cyclopentanone

The use of 2-ethyl cyclopentanone as a substrate for CHMO was chosen to illustrate the chiral resolution potential of the enzyme. It was hoped that the lactone product might not be a suitable substrate for the lactonase enzyme and hence lactone products would be identified. Figure 4.50 illustrates a typical profile for a 20 mM biotransformation. No lactone products could be identified. It was not possible to purchase a standard substituted alcohol or lactone but the retention times of peaks could be estimated based on the retention time of cyclohexanol and caprolactone relative to cyclohexanone. Therefore, the unknown peak present in small concentration is most likely the corresponding substituted alcohol. The reaction proceeds at a much slower rate than with cyclohexanone and there is very little alcohol produced. The concentration of 2-ethyl cyclopentanol reaches a maximum of 1.2 mM indicating that this is not such a good substrate for the dehydrogenase enzyme as cyclohexanone. The

lactone produced is however a good substrate for the lactonase since no evidence of further lactones could be found. The reaction appeared to have stopped after approximately 400 minutes and when the CHMO activity was measured it was found to be very low.

5.4.4 4-methyl cyclohexanone

4-methyl cyclohexanone was chosen as a substrate because it is a pro-chiral compound. The structure of the molecule is such that when an oxygen is inserted into the ring a chiral molecule is formed. Figure 4.52 shows a typical biotransformation where cyclohexanol has been added as a co-substrate to maintain the CHMO activity. The data illustrates that the biotransformation of 4-methyl cyclopentanone is very rapid and the production of the unknown intermediate, which for reasons discussed earlier was considered to be 4-methyl cyclopentanol, follows a similar pattern to that of the cyclohexanone biotransformation (Figure 4.58). The alcohol reaches a maximum concentration of approximately 10 mM after 300 minutes.

The cyclohexanone is initially transformed very rapidly but then reaches a level of 7 mM and is slowly metabolised. Very little cyclohexanone was measured reaching a maximum concentration of 5 mM. This is not surprising since the rate of lactonisation by CHMO is known to be rapid. The production of 4-methylcyclohexanol from the back reaction of the dehydrogenase has occurred at approximately the same rate as when cyclohexanone had been added. When comparing the results from 2-ethyl cyclopentanone it can be seen that the substitution at the two position, or the use of a cyclopentanone derivative, slows down the reaction rates of both the dehydrogenase and monooxygenase enzymes.

Previous workers have shown that there is little difference between cyclohexanone and cyclopentanone (Donoghue *et al.*, 1976) as a substrate. The loss of activity with the 2 substituted ketone is most likely due to steric hindrance in the active site.

The cell contents were checked to ensure that none of the substrates were stored in the cells. When the reactions were sampled, the supernatant was analysed by GC for

cyclic components. The cells were washed with buffer twice, resuspended, and sonicated to release intracellular components. After treatment to remove protein the supernatant was analysed for cyclic components. The wash solutions were also analysed by GC and found to contain only unquantifiable traces of alcohol and ketone.

Figure 4.53 shows that initially the concentrations reached as much as 1 mM when the cell contents were resuspended in 1 mL of buffer. The wet cell weight was approximately 25 mg, or approximately 25 μL , indicating that the maximum concentration within the cell was in the region of 40 mM one hour after addition. As a proportion of the total however, very little of the reactants and products were contained within the cells. The intracellular concentrations are in a similar ratio to the bulk in the supernatant with the exception of the sample taken at 240 minutes. The intracellular concentrations were very close to zero at this point which is difficult to explain. As previously mentioned, there were no measurable reaction components in the wash buffer, just an unquantifiable trace in the first wash. The cell disruption buffer was equivalent in volume to the wash buffer so any significant leakage would have been observed. A possible explanation is that the rate of reaction has slowed to a point where it is equal to the rate of diffusion across the cell wall and membrane.

5.5 Biotransformation - *E. coli* whole cells

The greater productivity of *E. coli* fermentation makes the use of the recombinant catalyst an attractive option. The lack of a native lactonase enzyme in the *E. coli* host strain should allow the production of lactone without further metabolism. Figure 4.58 shows a typical whole cell biotransformation of 2-ethyl cyclopentanone. The biotransformation of 4-methyl cyclohexanone produced very similar results (data not shown). The results show that *E. coli* whole cells are a poor catalyst for the biotransformation of this type of compound.

Lactone product was identified by relative retention time but at less than half of the concentration of ketone lost. A control to assess losses through evaporation showed that while this may account for some of the additional loss there was most likely another cause of ketone or lactone loss. The lactone could have been chemically degraded, i.e.

the ring opened during the reaction. The disparity appears at the beginning of the reaction however, in a time scale in which the lactone is known to be stable under these conditions (Hogan, unpublished data). The other possibility is that *E. coli* possesses some other enzyme mechanism for the slow degradation of either the ketone or the lactone.

The enantiomers of either the lactone or ketone could not be resolved by the analytical technique available. The low conversion could be due to a number of factors. It is possible that the cell structure of *E. coli* does not have the correct properties to enable these cyclic compounds to diffuse into the cells thus reducing reaction rates. *A. calcoaceticus* has evolved to grow on cyclic hydrocarbons as a sole carbon source and as such must have machinery in place to allow the diffusion of such compounds or their active transport in and out of the cells. *E. coli* may not be able to recycle the NADPH required for the reaction. In this case the reaction would be initially as rapid as diffusion would allow until the pool of NADPH had been oxidised. In *A. calcoaceticus* whole cells the pathway includes reactions that recycle the NADPH without the need for any other substrate for a second pathway. Should whole cell *E. coli* require NADPH to be added this negates any advantage to using the more active recombinant from of the whole cell catalyst. Since no examples cellular uptake of NADPH could be found in literature, it is unlikely that the addition of NADPH to the biotransformation buffer would be successful.

5.6 Biotransformation - *A. calcoaceticus* homogenate

From the whole cell biotransformations it was apparent that the both 4-methyl cyclohexanone and 2-ethyl cyclohexanone were substrates for the lactone degrading pathway. As expected no lactone products could be detected during the biotransformation of 4-methyl cyclohexanone as illustrated by Figure 4.54. The requirement for NADPH addition to the reaction is clearly illustrated by Figure 4.54. There is an initial drop in the concentration of 4-methyl cyclohexanone as the NADPH present in the cell homogenate is consumed, but the lack of recycling capacity is clearly illustrated. When stoichiometric quantities of NADPH were added to the reaction the reaction proceeded as expected.

The lack of lactone products implies that the lactonase enzyme is active (Figure 1.8) and the ring has been opened. A later step in the pathway should recycle the NADPH consumed by the monooxygenase and allow the biotransformation to proceed. For this recycle to occur NAD is required and this metabolic degradation pathway does not possess an NAD recycle step. The consequences of this are that NADPH would have to be added in stoichiometric quantities or an NADPH recycle system would have to be added to the biotransformation.

As mentioned in section 4.7 the use of isatoic anhydride to inhibit the lactonase enzyme was attempted. Figure 4.55 shows a typical reaction profile for the biotransformation of 20 mM 4-methyl cyclohexanone with the addition of 1.5 mM isatoic anhydride. Isatoic anhydride was found to have a maximum solubility of 1.8 mM under the essentially aqueous biotransformation conditions. No lactone products could be detected. It is apparent however from the low levels of the unknown species produced, which as mentioned earlier is likely to be 4-methyl cyclohexanol, that the isatoic anhydride has inhibited the dehydrogenase enzyme. The difference is clearly illustrated by a comparison to Figure 4.52 where the alcohol reached a concentration of 10 mM. CHMO activity had disappeared after approximately 15 hours which is a large improvement over the activity in whole cells under similar conditions.

The stability of CHMO was examined using cyclohexanol. Unlike the case of whole cells no stability was conferred to CHMO by the presence of cyclohexanol. This is clearly illustrated by Figure 4.56. When homogenate was treated with cyclohexanol there appeared to be a small increase in CHMO stability although this could be attributed to the anti-microbial effect of cyclohexanol. The growth of bacteria could be clearly seen after some 8 hours. While the initial drop in activity is due to the inherent instability of the protein as the reaction proceeds the effect of contaminating growth increases.

Once 2-methyl cyclohexanone, a racemic substrate, could be resolved by the GC column this was used for subsequent biotransformation reactions. Figure 4.57 shows a typical reaction profile for the biotransformation of 2-methyl cyclohexanone by *A. calcoaceticus* homogenate. This reaction required stoichiometric amounts of NADPH and isatoic anhydride was added. The appearance of alcohol could not be detected, indicating that the isatoic anhydride effectively inhibited the alcohol dehydrogenase

back reaction. Due to the expected overmetabolism no lactone products could be identified. The stereoselectivity of the enzyme can however be measured by the relative disappearance of the two isomers of the ketone. The kinetic resolution of the isomers is clearly indicated by the difference in the rates of reaction of the two isomers. The configuration of the two isomers has not been established thus far.

The enantiomeric excess (e.e.) was calculated as detailed in section 3.9.2. The e.e. reaches approximately 30 % and this appears to have been maintained throughout the reaction. This is likely to be a consequence of the low concentration towards the end of the reaction producing spurious results. The rate of transformation of the most favoured isomer (believed to be the (S)-ketone, Schwab *et al.*, 1983) can be seen to slow while that for the less favoured isomer is transformed at essentially the same rate throughout the reaction. This decrease in the rate of reaction would tend to indicate that the e.e. should decrease as the concentration of the less favoured isomer increases.

5.7 Biotransformation - *E. coli* homogenate

The use of *E. coli* homogenate and 2-methyl cyclohexanone allows the separation of the two isomers of the lactone for the first time. The enzyme activity for this reaction was approximately equivalent to that for the *A. calcoaceticus* homogenate biotransformation (4.57). There are marked differences however in the profile of the reactions. In the *A. calcoaceticus* homogenate reaction, the rate of reaction of the favoured isomer decreases throughout the reaction whereas that for the *E. coli* homogenate maintains essentially the same reaction rate throughout. This led to a more rapid conversion.

It was expected that the concentration of lactone produced would closely match the starting concentration of the ketone. Figure 4.59 shows that the combined concentration of the reactants and products after 350 minutes was approximately 13 mM from an initial starting concentration of 20 mM. The lactone product was not available commercially and the response factor was therefore based upon that of caprolactone. It is unlikely however that the difference in response factor could account for discrepancy in concentration. The discrepancy must therefore be due to either a loss of ketone, lactone product or the transformation of the ketone to some other species. As discussed

previously, there is no evidence of instability of the lactone product under the biotransformation conditions. The ketone substrate is known to be stable under the reaction conditions and is not subject to significant losses due to evaporation. The most likely reason for the loss is therefore a competing biotransformation.

As expected the e.e. of the lactone decreases as the yield of lactone produced increases as would be expected from a kinetic resolution. Up to 50 % completion the data compares well with that from the *A. calcoaceticus* homogenate (Figures 4.61 and 4.62). The slowing of reaction rate of the preferred isomer is not observed with the *E. coli* homogenate. Likewise the enantiomeric excess continues to rise reaching 60 % compared to 30 % for the *A. calcoaceticus* reaction.

The fundamental difference between the two reactions is the lack of lactone product when *A. calcoaceticus* is used. This implies that the metabolites of the lactone are inhibitory to the monooxygenase enzyme.

5.8 Summary

When considering the optimum route for the production of biocatalyst the final use of the biocatalyst must be considered. The biotransformation system will define whether the requirement is for whole cells or a crude preparation.

Organism	Fermentation type	DCW g L ⁻¹	Activity U g ⁻¹	Productivity U L ⁻¹
<i>A. calcoaceticus</i>	cyclohexanol	3	25	75
	glutamate	15	25	375
<i>E. coli</i>	batch-no supplementation	5	50	250
	batch	6.5	700	4550
	controlled growth	12	400	4800
	linear feed	20	120	2400

Table 5.2: Summary of biocatalyst production

Table 5.2 illustrates very clearly the benefits of the recombinant system when producing CHMO. The specific activity per g of cells is dramatically increased from 25 to 700 units therefore increasing the productivity per unit volume of fermentation. It must be noted at this point that the cell concentration achieved during the *A. calcoaceticus* fermentation would not be possible on a larger scale without oxygen supplementation of the sparge gas. The fermentations were allowed to proceed to values of OUR (100 mmole L⁻¹ min⁻¹) that would not be achievable with a larger vessel. The use of *E. coli* also reduces the fermentation time from \approx 15 h to \approx 10 h which could result in significant savings in cost when operated at a large scale. The most important advantage of using the recombinant system is in the stability of the CHMO after induction. Once the maximum activity has been reached and the inducing cyclohexanol becomes exhausted the activity is seen to be lost. While this phenomenon can be reduced by some extent by the continual addition of cyclohexanol the process window is significantly reduced. As scale is increased this would become more of a significant problem as the time taken to process large volumes of cells to release the enzyme could be large. At full scale production, with a vessel capacity of say 1000 L the requirement for litres of flammable solvent in a process area could cause problems. In *E. coli* this phenomenon is not seen and the maximum activity is maintained once achieved.

Table 5.2 also illustrates perhaps surprisingly that the fed batch strategy to increase the productivity of the *E. coli* fermentation was not successful. While controlling the growth rate allowed an increase in dry cell weight that would not have been achievable with a batch fermentation due to oxygen transfer limitations the production of CHMO suffered as a result. Increasing the cell density has many advantages to the biocatalyst production process as a whole; reduced reactor volumes, reduced effort in upstream and downstream processing, reduced operating costs and reduced waste water. Despite these factors it is unlikely that a fed batch fermentation would be economical due to the reduction in productivity.

Many workers have proposed the control of growth rate as a means of increasing the production of recombinant proteins in *E. coli*. (Paalme *et al.*, 1990; Strandberg *et al.*, 1994). There is often a correlation between growth rate and maximum production although there is little data available for expression systems that rely on induction by additional chemicals. The increases in productivity are often attributed to a lack of

inhibitory by-products that accumulate when cells grow at their maximum growth rates (Riesenberg *et al.*, 1991) although the use of glycerol as a carbon source does limit this when compared to glucose. Growing cells at sub maximum rates has also been found to reduce the likelihood of the cells shedding their plasmid and therefore increasing the productivity. The plasmid used in this study however has proved to be very stable under the fermentation procedures used and as such reduced growth rate offers no advantage.

The phenomenon of reduced production with reduced growth rate is not unknown however. Hellmuth and co-workers (Hellmuth *et al.*, 1994) reported an optimal growth rate of 0.13 h^{-1} for their strain of *E. coli* to produce a recombinant protein. They report a decline in protein product when the growth rate was lowered to 0.11 h^{-1} and a 70% loss of production when 0.07 h^{-1} was used.

When fed batch was attempted at 0.15 h^{-1} which is approximately a third of the maximum growth rate on this medium (0.44 h^{-1}) the activity fell from 700 to 400 U g^{-1} (table 5.2). The overall productivity of the fermentation was increased marginally but the increase in productivity (due to an almost twofold increase in the dry cell weight) does not warrant the increased complexity and costs of a fed batch process.

It was possible that the rate of CHMO production could have been slower because of the reduced growth rate and the maximum activity had not been reached at the time of harvesting the fermentation. Figures 4.34 and 4.37 show that the activity had reached a maximum and that the dry cell concentration was still increasing during this time indicating that there were sufficient nutrients available and the cells were growing and should have been in a good condition for producing recombinant protein.

When the biomass was further increased without oxygen limitation by linear feeding the productivity of the fermentation was halved even though the cell concentration was approaching double that achieved with exponential feeding alone. As stated previously the data suggesting that sub maximal growth rates increase the production of recombinant proteins in *E. coli* has been based on expression systems that are growth linked (Riesenberg *et al.*, 1990) and often the productivity passes through a maximum as a function of growth rate (Riesenberg *et al.*, 1991).

The production of CHMO, in this strain, under the control of a tac promoter would appear to be dependent on the growth rate at the time of induction. Although a full range of growth rates have not been tested, to find a growth rate at which production

of CHMO is at a maximum, the data would tend to suggest that the maximum growth (0.44 h⁻¹) rate as seen in batch fermentations would produce the greatest activity.

The implication for biocatalyst production cannot be assessed without a detailed examination of the required use for the biocatalyst. The biotransformation data has shown that although the recombinant *E. coli* may be the most useful vector for producing biocatalyst on a large scale, it must be remembered that the cells produced were not capable of facilitating the reaction. In this particular case the whole cells of *A. calcoaceticus* were not a suitable biocatalyst because of overmetabolism of the required product. It is important that each substrate be examined on its own merits. While the reactants used to demonstrate the reaction in this study were found to be substrates for the lactonase enzyme it cannot be inferred that this would be true for a potential substrate for an industrial application.

The need for NADPH in these reactions makes the use of whole cells a more attractive option as the cost on a large scale would be prohibitive. As has been demonstrated however there are many problems associated with the use of whole cells. *E. coli*, as mentioned previously, is not suitable but there are other potential vectors for the CHMO gene that may prove to be useful as biocatalyst. Recent work by Stewart *et al.* (1998) has demonstrated that yeast may make a successful whole cell catalyst.

The biotransformation of the substrates chosen for this study are representative of the type of molecule that industry could utilise as chiral synthons. It is desirable to maximise the productivity of the biotransformation process when considering an increase in scale. The biotransformations described in this work involve concentrations of 20 mM (approximately 2 g L⁻¹). The most obvious way of achieving this is to increase the concentration of the reactants and hence increase the quantity of product produced per unit volume of reactor volume. The reactants and products have been found to cause enzyme inhibition at levels approaching 50 mM (Hogan, 1999) and would therefore not make increasing the productivity a trivial matter.

To overcome this inhibition and increase productivity the substrate would have to be added at a feed rate similar to the reaction rate and the product would have to be removed by some form of *in situ* product removal. The design of an *in situ* product

removal process would not be trivial however due to the similarity between the reaction components.

6 Conclusions and Further Work

6.1 Conclusion

1 The maximum cell concentration of *A. calcoaceticus* that was achieved with cyclohexanol as the sole carbon and energy source was approximately 3 g L⁻¹. This is unacceptable as viable source of biocatalyst.

2 Monosodium glutamate was found to be a good substrate for production of biocatalyst from *A. calcoaceticus*. A concentration of 14 g L⁻¹ dry cells was achieved from batch fermentation which yielded 20 U g⁻¹ CHMO activity.

3 The successful production of CHMO activity in *A. calcoaceticus* is dependent on cyclohexanol being present as a growth substrate from the beginning of the fermentation. This is most likely due to a long lag in the switch of metabolism.

4 The CHMO activity produced from *A. calcoaceticus* after induction by addition of cyclohexanol is rapidly reduced once the cyclohexanol is depleted. This has serious implications for downstream processing operations if activity is to be maintained.

5 The production of CHMO from recombinant *E. coli* JM107/pQR210 is closely associated with the growth rate at the time of induction. The maximum activity after induction with IPTG was 900 U g⁻¹ when the growth rate was at its maximum for the defined medium.

6 JM107/pQR210 required supplementation of the defined medium to maximise the production of CHMO. Without supplementation the maximum CHMO activity achieved was 58 U g⁻¹ for a batch fermentation.

7 All forms of the biocatalyst could be stored for many months at -18 °C and be used as active biocatalysts.

8 *E. coli* homogenate was the only form of CHMO that proved to be useful biocatalyst for the production of optically active lactones from the cyclic ketones chosen for study. Lactone product could not be identified with either form of *A. calcoaceticus* and the chemical inhibitor of lactonase enzyme is too toxic for routine use. *E. coli* whole cells proved unable to facilitate the reaction due most likely to an inability of the reactants to pass through the cell wall.

6.2 Further Work

The recombinant *E. coli* used in this study required the use of IPTG to induce the production of CHMO. This form of expression system is not one that could be operated on an industrial scale due to the vast cost of supplying IPTG. Other expression systems are available and one that constitutively expressed the protein throughout growth would be desirable. For ease of downstream processing it would also be advantageous to use an expression system that secreted the protein into the fermentation medium, removing the need to for cell disruption and subsequent contamination by other proteins.

Kanamycin would be preferred to ampicillin as the selection pressure applied to the recombinant *E. coli* cells. Kanamycin is both more stable during fermentation and cheaper than ampicillin due to its high efficacy at lower concentrations. Ideally the fermentation would not require antibiotic at all due to potential for operator sensitivity and adding to the environmental problems of antibiotic over usage.

Should the enzyme be required for industrial applications the effects of immobilisation need to be examined. For this to be achieved a procedure for purifying the protein will be required and the effects of protein purity on immobilisation investigated. Due to the requirement of a cofactor, the possibility of immobilising the cofactor or cofactor recycling system alongside the enzyme should be investigated.

E. coli proved to be inadequate as a whole cell catalyst but recent work has shown that the potential for using other organisms as recombinant whole cell catalysts exists (Stewart,1998). The use of a whole cell catalyst for these types of reaction is very desirable due to the previously mentioned expense and added complication of cofactors and cofactor recycling. There are numerous micro-organisms that may have potential as recombinant whole cell catalysts and these should be examined

The use of cofactors such as NADPH is not possible on a large scale due to the immense cost of such chemicals. Recycle systems are known but tend to require the use of other expensive chemicals as substrates for the second reaction. Developments in protein engineering could allow CHMO to be engineered to accept less expensive cofactors that may be more economically recycled.

The substrates chosen in this study were found to be substrates for the lactonase enzyme in *A. calcoaceticus*. It is possible that many compounds of potential interest would not be substrates and whole cells could be used as biocatalysts without degradation of the lactone product. The substrate inhibition problem encountered has very serious consequences for the operation of a large scale reaction.

As discussed earlier the development of an in situ product removal system could be vital to the future success of this enzyme as an industrial catalyst.

7 Appendices

Appendix I

Standard operating procedures were written to insure that the risks of operator exposure to *A. calcoaceticus* cells, especially in aerosol form, were reduced to a minimum. Areas where the greatest operator interaction were identified and procedures were put into place to cover these aspects of the fermentation and downstream processing. The following SOP's cover the inoculation and harvesting of the vessel as well as procedure to follow in the event of the fermenter failing.

Standard Operating Procedure

Title:

Procedure for Inoculating 2L fermenter with a class II pathogenic organism so as to minimise operator exposure and release of organism

1.0 Introduction

1.1 This document describes the inoculation of an Inceltech LH 2L fermenter from a shake flask culture so as to minimise the release and exposure of operators to a class II pathogenic organism

1.2 All culture transfers must be made in a Class II personnel protection cabinet with thorough disinfection after use.

1.3 All fermentations must be carried out in the Advanced Centre fermentation suite where all drains are fed to kill tanks and negative air pressure is maintained so as to minimise release.

1.4 Gloves must be worn during all operations inside the cabinet and hands should be washed in bactericidal soap after any culture manipulations.

2.0 Preparation for inoculation

2.1 Take sterilised acid addition cylinder and inoculum shake flask (In a suitable container) to the class II cabinet in the inocula laboratory and ensure that the cylinder, tubing and fittings are sound.

2.2 Should any spillage occur outside the cabinet refer to Fermenter Failure SOP.

2.3 Aseptically transfer inoculum from the shake flask to the cylinder taking care to replace the bungs tightly.

2.4 Should any spillage occur inside the cabinet refer to class II pathogen disinfection SOP.

2.5 Transfer cylinder to the fermenter in a suitable container.

3.0 Inoculation

3.1 Turn off to air supply to the fermenter to remove any pressure inside the vessel and connect the cylinder tubing using fittings provided ensuring a firm seal.

3.2 Remove clamp and allow the inoculum to siphon into fermenter by gravity.

3.3 Fill cylinder with acid and replace bung as quickly as possible before restoring air supply.

3.4 At the end of the fermentation the addition vessels should be chemically disinfected or autoclaved along with the fermenter vessel.

WRITTEN BY	DATE	OPERATING HEAD	DATE
S. BARCLAY	11.10.96	C. ORSBORN	12.11.96

Standard Operating Procedure

Title:

Procedure for harvesting 2L fermenter containing a Class II pathogenic organism so as to minimise operator exposure and organism release

1.0 Introduction

1.1 This document describes the harvesting procedure of an Inceltech 2L fermenter into centrifuge tubes so as to minimise release and exposure of operators to a class II pathogenic organism.

1.2 All culture transfers must be made in a Class II personnel protection cabinet with thorough disinfection after use.

1.3 Gloves must be worn during all operations inside the cabinet and hands should be washed with bactericidal soap after any culture manipulation.

2.0 Harvesting fermenter

2.1 Disconnect all lines and connections to fermenter making sure to firmly clamp addition tubes.

2.2 Take the fermenter vessel to the inocula lab (1.6) in a suitable container such as a stainless steel bucket.

2.3 In case of spillage outside the cabinet refer to Fermenter Failure SOP.

2.4 Fermenter contents can be harvested directly into centrifuge bottles by siphoning through the harvest port ancillaries.

2.5 Any spillage inside the cabinet refer to Class II pathogen disinfection SOP.

2.6 All fermenter apertures and ancillary equipment should be firmly closed and clamped before removal of vessel from cabinet and should be transported to the autoclave for sterilisation in a suitable container.

3.0 Centrifugation of culture

3.1 The rotor head of the centrifuge should be removed and transported to the Class II personnel protection cabinet.

3.2 The centrifuge bottles can then be transported to the centrifuge in the sealed rotor.

3.3 During the centrifugation procedure a sign indicating that biohazardous activities are taking place should be placed on the door of the laboratory and that only authorised personnel are permitted entry. The operator must remain in the laboratory throughout the centrifugation procedure except in the case of a fire alarm or other emergency.

3.4 When centrifugation is complete a check must be made of the bowl for released culture and the rotor must be transported back to the cabinet before opening in case of failure of the centrifuge tubes.

3.5 The rotor should be disinfected before replacing in the centrifuge, refer to class II pathogen disinfection SOP.

3.6 The supernatant and centrifuge tubes should be chemically disinfected (refer to class II pathogen disinfection SOP).

3.7 Any further manipulation of the cells should be made in the cabinet and if samples are to be stored elsewhere they should be transported in sealed bottles within a suitable container.

WRITTEN BY	DATE	OPERATING HEAD	DATE
S. BARCLAY	11.10.96	C. ORSBORN	12.11.96

Standard Operating Procedure

Title:

Procedure for disinfection and clean up following Fermenter failure leading to large scale release

1.0 Introduction

1.1 This document describes the procedure to be followed following the large scale release of a class II pathogen outside of a Class II personnel protection cabinet.

1.2 This SOP should be used in conjunction with validated experimental data to show the effectiveness of the chemical sterilant chosen in achieving sterility; in particular the length of time required for contact of the sterilising agent with the spillage.

2.0 Large scale disinfection

2.1 A sign indicating biohazardous conditions should be placed near the spill indicating that personnel should stay clear.

2.2 The operator responsible for the spillage should wear a protective face mask and gloves before attempting to deal with spillage.

2.3 Any broken glassware should be very carefully placed in a steel bucket and autoclaved to sterilise.

2.4 The spilled culture should be covered with a suitable sterilising agent such as Tego® or similar and left for the time necessary to achieve sterility as indicated by validation experiments.

2.5 The building manager or person responsible for safety should be informed of the spillage and the measures taken to deal with it.

2.6 After the specified contact time the spillage and spent culture can be mopped up and all cloths, paper towels etc. used should be discarded in a contaminated waste bin.

2.7 The spillage area should then be wiped down with a 1% solution of Tego[®] and left to dry.

2.8 After autoclaving the broken glassware should be disposed of in a waste glass bin.

WRITTEN BY	DATE	OPERATING HEAD	DATE
S. BARCLAY	11.10.96	C. ORSBORN	12.11.96

Appendix II

Figures 10.1 and 10.2 show that the best sonication regime to afford maximum CHMO activity for *A. calcoaceticus* and *E. coli* were 3×30 s and 4×10 s respectively.

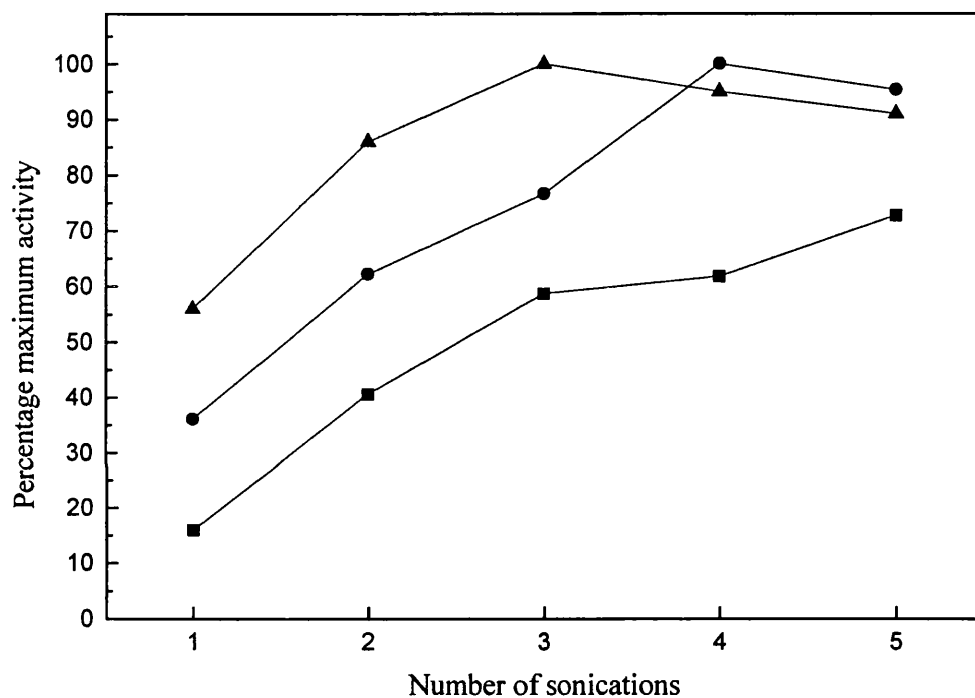


Figure 10.1 Optimum sonication conditions for the maximal release of active CHMO from *A. calcoaceticus*. This figure shows the CHMO release from cells disrupted by sonication in bursts of ten (■); twenty (●); and thirty (▲) seconds, with equal cooling time between each burst.

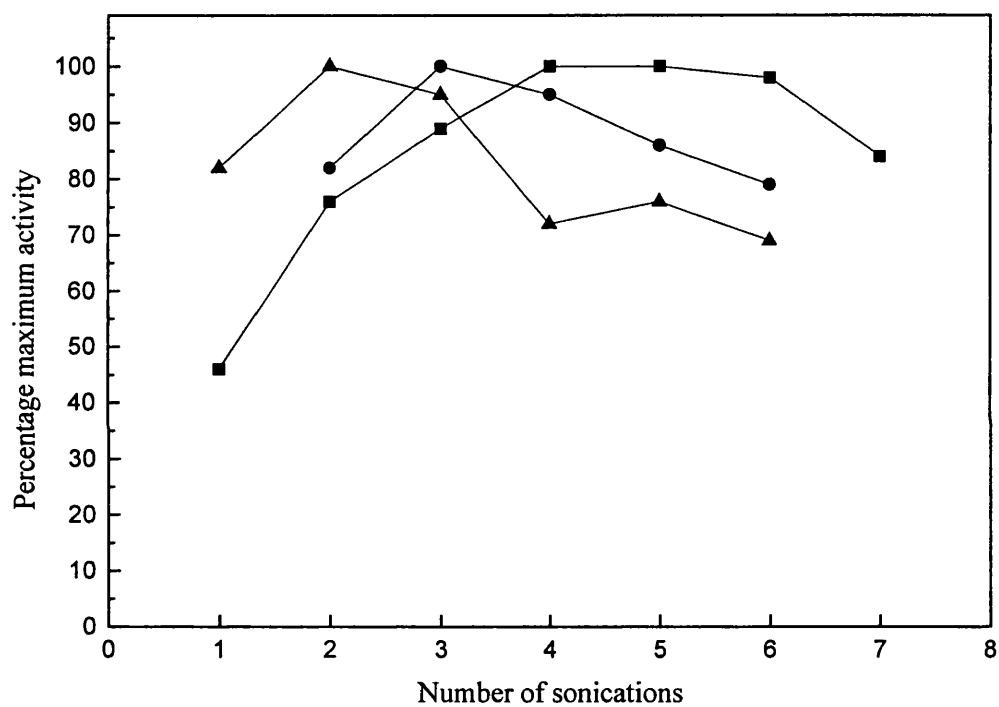
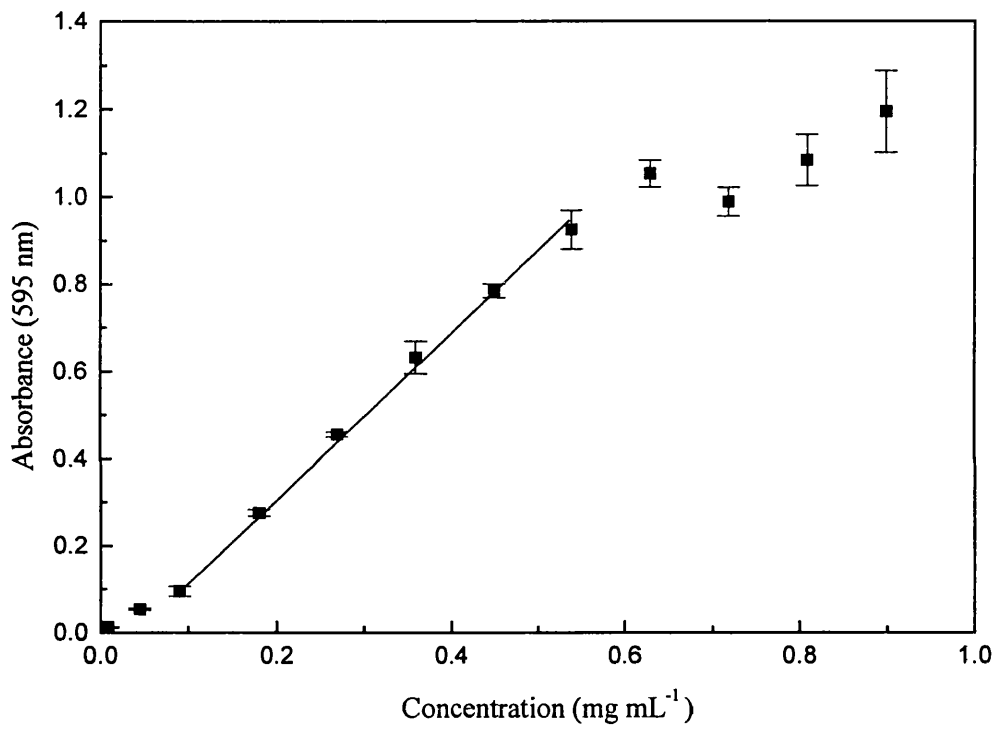


Figure 10.2: Optimum sonication conditions for the maximum release of active CHMO from *E. coli*. This figure shows the CHMO release from cells disrupted by sonication in bursts of ten (■); twenty (●); and thirty (▲) seconds, with equal cooling time between each burst.

Appendix III

Example of standard curve for Coomassie protein reagent assay using BSA (section 3.13).



8 References

Abril,O., Ryerson,C.C., Walsh,C. and Whitesides,G.M., 1989, Enzymatic Baeyer-Villiger type oxidations of ketones catalyzed by cyclohexanone oxygenase, *Bioorganic Chemistry*, 17, 41-52

Adger,B., Bes,M.T., Grogan,G., McCague,R., Pedragosa-Moreau,S., Roberts,S.M., Villa,R., Wan,P.W.H. and Willetts,A.J., 1995, Application of Enzymic Baeyer-Villiger oxidations of 2-substituted cycloalkanones to the total synthesis of (R)-(+)-Lipoic acid, *Journal of the Chemical Society: Chemical Communications*, 1563-1564.

Alphand,V., Archelas,A. and Furstoss,R., 1989, *Microbial Transformations 16: One stop synthesis of a pivotal prostaglandin chiral synthon via a highly enantioselective microbiological Baeyer-Villiger type reaction*, *Tetrahedron Letters*, 30, 3663-3664.

Alphand,V., Archelas,A. and Furstoss,R., 1990, *Microbial Transformations 13: A direct synthesis of both S and R enantiomers of 5-hexadecanolide via an enantioselective microbiological Baeyer-Villiger reaction*, *Journal of Organic Chemistry*, 55, 347-350.

Alphand,V., Archelas,A. and Furstoss,R., 1990, *Microbiological transformations 15: The enantioselective microbiological Baeyer-Villiger oxidation of alpha substituted cyclopentanones*, *Biocatalysis*, 3, 73-83.

Alphand,V. and Furstoss,R., 1992, *Microbial transformations 23: A surprising regioselectivity of microbiological Baeyer-Villiger oxidations of menthone and dihydrocarvone*, *Tetrahedron: Asymmetry*, 3, 379-382.

Amann,E., Brosius,J. and Ptashne,M., 1983, Vectors bearing a hybrid *trp-lac* promoter useful for regulated expression of cloned genes in *Escherichia coli*, *Gene*, 25, 167-178.

Atkinson,B. and Mavituna,F., in Biochemical Engineering and Biotechnology Handbook, 1983, Macmillan, Surrey, UK, p120.

Baeyer,A. and Villiger,V., 1899, Berlin Deutsche Chemie., 32, 3625.

Bhattacharya,S.K. and Dubey,A.K., 1997, Effects of dissolved oxygen and oxygen mass transfer on overexpression of target gene in recombinant *E. coli*, Enzyme and Microbial Technology, 20, 355-360.

Bolm,C., Schlinghoff,G. and Weickhardt,K., 1994, Optically active lactones from a Baeyer-Villiger-type metal-catalysed oxidation with molecular oxygen, Angewandte Chemie-International Edition, 33, 1848-1849.

Bradshaw,W., Conrad,H.,Corey,E. and Gunsalus,I., 1959, Microbiological degradation of (+)-camphor, Journal of the American Chemical Society, 81, 5507.

Branchaud,B.P. and Walsh,C.T., 1985, Functional group diversity in enzymatic oxygenation reactions catalyzed by bacterial flavin-containing cyclohexanone oxygenase, Journal of the American Chemical Society, 107, 2153-2161.

Carnell,A.J., Roberts,S.M., Sik,V. and Willetts,A.J., 1990, Enzyme-catalysed Baeyer-Villiger oxidations of some substituted bicyclo[3.2.0]heptanones, Journal of the Chemical Society: Chemical Communications, 20, 1438-1439.

Carnell,A.J., Roberts,S.M., Sik,V. and Willetts,A.J., 1991, Microbial oxidation of 7-endo-methylbicyclo[3.2.0]hept-2-en-6-one, 7,7-dimethylbicyclo[3.2.0]hept-2-en-6-one and 2-exo-bromo-3-endo-hydroxy-7,7-dimethylbicyclo[3.2.0]heptan-6-one using *A. calcoaceticus* NCIMB9871, Journal of the Chemical Society: Perkin Transactions, 1, 2385-2389.

Carnell,A. and Willetts,A., 1990, Biotransformation of cycloalkenones by fungi: Baeyer-Villiger oxidation of bicycloheptanone by dematiaceous fungi, *Biotechnology Letters*, 12, 885-890.

Carnell,A. and Willetts,A., 1992, Biotransformations by fungi: Regio- plus stereoselective Baeyer-Villiger oxidations by dematiaceous fungi, *Biotechnology Letters*, 14, 17-21.

Carrea,G., Redigolo,B., Riva,S.,Colonna,S., Gaggero,N., Battistel,E. and Bianchi,D., 1992, Effects of substrate structure on the enantioselectivity and stereochemical course of sulfoxidation catalysed by cyclohexanone monooxygenase, *Tetrahedron: Asymmetry*, 3, 1063-1068.

Chapman,P.J. and Duggleby,R.G., 1967, Dicarboxylic acid catabolism by bacteria, *Biochemical Journal*, 103, 7.

Criegee,R., 1948, *Liebigs Ann. Chem.*, 560, 127.

Davies,H.G., Green,R.H., Kelly,D.R. and Roberts,S.M., 1990, Recent advances in the generation of chiral intermediates using enzymes, *Critical Reviews in Biotechnology*, 10, 129-153.

De Boer,H.A., Comstock,L.J. and Vasser,M.,1983, The *tac* promoter: A functional hybrid derived from the *trp* and *lac* promoters, *Proceedings of the National Academy for Science, USA*, 80, 21-25.

Donoghue,N.A. and Trudgill,P.W., 1975, The metabolism of cyclohexanol by *A. Calcoaceticus* NCIB 9871, *European Journal of Biochemistry*, 60, 1-7.

Donoghue,N.A., Norris,D.B. and Trudgill, P.W., 1976, The purification and properties of cyclohexanone oxygenase from *Nocardia globerula* CL1 and *A. calcoaceticus* NCIMB 9871, *European Journal of Biochemistry*, 63, 175-192.

- Faber, K., 1992, *Biotransformations in Organic chemistry*, Springer-Verlag, New York, 1-21, 189-194.
- Gagnon, R., Grogan, G., Levitt, M.S., Roberts, S.M., Wan, P.W.H. and Willetts, A.J., 1994, Biological Baeyer-Villiger oxidation of some monocyclic and bicyclic ketones using monooxygenases from *A. calcoaceticus* NCIMB 9871 and *Pseudomonas putida* NCIMB 10007, *Journal of the Chemical Society: Perkin Transactions*, 1, 2537-2543.
- Georgiou, G., Shuler, M.L. and Wilson, D.B., 1988, Release of periplasmic enzymes and other physiological effects of β -lactamase overproduction in *Escherichia coli*, *Biotechnology and Bioengineering*, 32, 741-748.
- Gregory, M.E. and Turner, C., 1993, Open-loop control of specific growth rate in fed-batch cultures of recombinant *Escherichia coli*, *Biotechnology Letters*, 7, 889-894.
- Griffin, M. and Trudgill, P.W., 1972, The metabolism of cyclopentanol by *Pseudomonas* NCIB 9872, *Journal of Biochemistry*, 129, 595-603.
- Grogan, G., Roberts, S. and Willetts, A., 1992, Biotransformation by microbial Baeyer-Villiger monooxygenases: Stereoselective lactone formation in vitro by coupled enzyme systems, *Biotechnology Letters*, 14, 1125-1130.
- Grogan, G., Roberts, S., Wan, P. and Willetts, A., 1993, Camphor grown *Pseudomonas putida*, a multifunctional biocatalyst for undertaking Baeyer-Villiger monooxygenase-dependent biotransformations, *Biotechnology Letters*, 15, 913-918.
- Hanna, M.H., 1987, in Bungay, H.R. and Belfort, G. eds., *Advanced Biochemical Engineering*, John Wiley and Sons Inc, New York, 103-167.
- Hellmuth, K., Korz, D. J., Sanders, E. A. and Deckwer, W., D., 1994, Effect of growth rate on stability and gene expression of recombinant plasmids during continuous and high cell density cultivation of *E. coli* TG1, *Journal of Biotechnology*, 32, 289-298.

Hobbs,G.R., Mitra,R.K., Chauhan,R.P., Woodley,J.M. and Lilly,M.D., 1996, Enzyme-catalysed carbon-carbon bond formation: Large scale production of *Escherichia coli* transketolase, *Journal of Biotechnology*, 45, 173-179.

Hogan,M., 1999, PhD thesis, Department of Biochemical Engineering, University College London, UK.

Itagaki,E., 1986, Studies on steroid monooxygenase from *Cylindrocarpon raditicola* ATCC 11011. Purification and characterization, *Journal of Biochemistry*, 99, 815-824.

Jones,J.B., 1986, Enzymes in organic synthesis, *Tetrahedron*, 42, 3351-3403.

Jones,K.H., Smith,R.T. and Trudgill,P.W., 1993, Diketocamphane enantiomer-specific Baeyer-Villiger monooxygenases from camphor grown *Pseudomonas putida* ATCC17453, *Journal of General Microbiology*, 139, 797-805.

Jones,R.,1993, PhD thesis, Department of Chemical and Biochemical Engineering, University College London, UK.

Konigsberger,K., Braunegg,G., Faber,K. and Griengl,H., 1990, Baeyer-Villiger oxidation of bicyclic ketones by *Cylindrocarpon destructans* ATCC 11011, *Biotechnology Letters*, 12, 509-514.

Krow,G.R., 1981, Oxygen insertion reactions of bridged bicyclic ketones, *Tetrahedron*, 37, 2697-2724.

Latham,J.A. and Walsh,C., 1987, Mechanism based inactivation of the flavoenzyme cyclohexanone oxygenase during oxygenation of cyclic thiol ester substrates, *Journal of the American Chemical Society*, 109, 3421-3427.

- Lautrop,H., 1974, Genus IV. Acinetobacter, in Bachman,R.E. and Gibbons,N.E. eds, Bergey's manual of determinative bacteriology, Williams and Wilkins, New York, 436-438.
- Lee, S.Y., 1996, High cell-density culture of *Escherichia coli*, Topics in Biotechnology, 14, 98-105.
- Lenn,M.J. and Knowles,C.J., 1994, Production of optically active lactones using cycloalkanone oxygenases, Enzyme and Microbiology Technology, 16, 964-969.
- Levitt,M., Sandey,H. and Willetts,A., 1990, Regiospecific biotransformation of substituted norbanones by microorganisms, Biotechnology Letters, 12, 197-200.
- Lilly,M.D., 1977, A comparison of cells and enzymes as industrial catalysts. in Bohak,Z. and Sharon,N. eds., Biotechnological approaches, Academic Press Inc, New York, 127-139.
- Luli,G.W. and Strohl,W.R., 1990, Comparison of growth, acetate production and acetate inhibition of *Escherichia coli* strains in batch and fed batch fermentations, Applied and Environmental Microbiology, 56, 1004-1009.
- Magor,A.M., Warburton,J., Trower,M.K. and Griffin,M., 1986, Comparative study of the ability of 3 *Xanthobacter* species to metabolize cycloalkanes, Applied and Environmental Microbiology, 52, 665-671.
- Ohta,H., Iwabuchi,T. and Tsuchihashi,G., 1986, Stereoselective oxidation of β -methyl-sec-alcohols and α -methylketones by *Corynebacterium equi* IFO 3730, Agricultural Biological Chemistry, 50, 725-731.
- Ottolina,G., Pasta,P., Carrea,G., Colonna,S.,Dallavalle,S. and Holland,H.L., 1995, A predictive active site model for the cyclohexanone monooxygenase catalyzed oxidation of sulfides to chiral sulfoxides, Tetrahedron: Asymmetry, 6, 1375-1386.

Ouazzani-Chahdi,J., Buisson,D. and Azerad,R., 1987, Preparation of both enantiomers of a chiral lactone through combined microbiological reduction and oxidation, *Tetrahedron Letters*, 28, 1109-1112.

Ougham,H.J., Taylor,D.G. and Trudgill,P.W., 1983, Camphor revisited: Involvement of a unique monooxygenase in metabolism of 2-oxo- Δ^3 -4,5,5-trimethylcyclopentenylacetic acid by *Pseudomonas putida*, *Journal of Bacteriology*, 153, 140-152.

Paalme,T., Tiisma,K., Kahru,A., Vanatalu,K. and Vilu,R., 1990, Glucose-limited fed-batch cultivation of *Escherichia coli* with computer-controlled fixed growth rate, *Biotechnology and Bioengineering*, 35, 312-319.

Pan,J.G., Rhee,J.S. and Lebeault,J.M., 1987, Physiological constraints in increasing biomass concentration of *Escherichia coli* B in fed batch culture, *Biotechnology Letters*, 9, 89-94.

Pasta,P., Carrea,G., Holland,H.L. and Dallavalle,S., 1995, Synthesis of chiral benzyl alkyl sulfoxides by cyclohexanone monooxygenase from *A. calcoaceticus* NCIMB 9871, *Tetrahedron: Asymmetry*, 6, 933-936.

Prentis,S., 1984, *Biotechnology. A new industrial revolution*, Orbis Publishing Ltd, London, 36-62

Riesenberg,D., Schulz,V., Knorre,W.A., Pohl,H.D., Kortz,D., Sanders,E.A., Roß,A. and Deckwer, W.D., 1991, High cell density cultivation of *Escherichia coli* at controlled specific growth rate, *Journal of Biotechnology*, 20, 17-28.

Riesenberg,D., Menzel,K., Schulz,V., Schumann,K., Veith,G., Zuber,G. and Knorre,W.A., 1990, High cell density fermentation of recombinant *Escherichia coli* expressing human interferon alpha 1, *Applied Microbiology and Biotechnology*, 34, 77-82.

Roberts,S.M. and Turner,N.J., 1992, Some recent developments in the use of enzyme catalysed reactions in organic synthesis, *Journal of Biotechnology*, 22, 227-244.

Roberts,S.M. and Willetts,A., 1993, Development of the enzyme catalysed Baeyer-Villiger reaction as a useful technique in organic synthesis, *Chirality*, 5, 334-337.

Ryerson,C.C., Ballou,D.P. and Walsh,C., 1982, Mechanistic studies on cyclohexanone oxygenase, *Biochemistry*, 21, 2644-2655.

Sandey,H. and Willetts,A., 1989, Biotransformation of cycloalkanones by microorganisms, *Biotechnology Letters*, 2, 615-620.

Sandey,H., 1991, Biotransformations of bicyclic ketones to lactones by microorganisms, PhD thesis, Faculty of Science, University of Exeter.

Sandey,H. and Willetts,A., 1992, Biotransformation of cycloalkanones: controlled oxidative and reductive bioconversions by an *Acinetobacter* species, *Biotechnology Letters*, 14, 1119-1125.

Schwab,J.M., Li,W. and Thomas,L.P., 1983, Cyclohexanone oxygenase: Stereochemistry, enantioselectivity, and regioselectivity of an enzyme-catalyzed Baeyer-Villiger reaction, *Journal of the American Chemical Society*, 105, 4800-4808

Secundo,F., Carrea,G., Dallavalle,S. and Franzosi,G., 1993, Asymmetric oxidation of sulfides by cyclohexanone monooxygenase, *Tetrahedron: Asymmetry*, 4, 1981-1982.

Shipston,N.F, Lenn,M.J. and Knowles,C.J., 1992, Enantioselective whole cell and isolated enzyme catalysed Baeyer-Villiger oxidation of bicyclo[3.2.0]hept-2-en-6-one, *Journal of Microbiological Methods*, 15, 41-52.

Stewart,J.D., Reed,K.W., Martinez,C.A., Zhu,J., Chen,G. and Kayser,M.M., 1998, Recombinant Baker's yeast as a whole cell catalyst for asymmetric Baeyer-Villiger oxidations, *Journal of the American Chemical Society*, 120, 3541-3548.

Strandberg,L., Andersson,L. and Enfors,S., 1994, The use of fed batch cultivation for achieving high cell densities in the production of a recombinant protein in *Escherichia coli*, *FEMS Microbiology Reviews*, 14, 53-56.

Suzuki,M., Takeda,H. and Nayori.R., 1982, Bis(trimethylsilyl) peroxide for the Baeyer-Villiger type oxidation, *Journal of Organic Chemistry*, 47, 902-904.

Taschner,M.J. and Black,D.J., 1988, The enzymatic Baeyer-Villiger oxidation: Enantioselective synthesis of lactones from mesomeric cyclohexanones, *Journal of the American Chemical Society*, 110, 6892-6893.

Taschner,M.J. and Peddada,L., 1992, The enzymatic Baeyer-Villiger oxidation of a series of bicyclo[2.2.1]hept-2-en-7-ones, *Journal of the Chemical Society-Chemical Communications*, 19, 1384-1385.

Taschner,M.J., Peddada,L., Cyr,P., Chen,Q.Z. and Black,D.J.,1992, in *Microbial reagents in organic synthesis*, S.Servi Ed., Kluwer Academic Publisher, Dordrecht, 347.

Taschner,M.J., Black,D.J. and Chen,Q., 1993, The enzymatic Baeyer-Villiger oxidation: A study of 4-substituted cyclohexanones, *Tetrahedron-Asymmetry*, 4, 1387-1390.

Taylor,D. and Trudgill,P., 1986, Camphor revisited: Studies of 2,5-diketocamphane-1,2-monooxygenase from *Pseudomonas putida* ATCC 17453, *Journal of Bacteriology*, 165, 2, 489-497.

Trudgill,P.W., 1990, Cyclohexanone 1,2-monooxygenase from *A. calcoaceticus* NCIMB 9871, *Methods in Enzymology*, 188, 70-77.

Willetts,A.J., Knowles,C.J., Levitt,M.S., Roberts,S.M., Sandey,H. and Shipston,N.F., 1991, Biotransformation of endo-bicyclo[2.2.1]heptan-2-ols and endo-bicyclo[3.2.0]hept-2-en-6-ol into the corresponding lactones, Journal of the Chemical Society: Perkin Transactions, 1, 1608-1610.

Wright,M., Knowles,C., Petit,F. and Furstoss,R., 1994, Enantioselective inhibition studies of the cyclohexanone monooxygenase from *Acinetobacter* sp. NCIMB 9871, Biotechnology Letters, 16, 1287-1292.

Wright,M.A., Taylor,I.A., Lenn,M.J., Kelly,D.R., Mahdi,J.G. and Knowles,C.J., 1994, Baeyer-Villiger monooxygenases from microorganisms, FEMS Microbiology Letters, 116, 67-72.

Yoon, S.K. and Kang, W.K., 1994, Fed-batch operation of recombinant *Escherichia coli* containing *trp* promoter with controlled specific growth rate, Biotechnology and Bioengineering, 43, 995-999.